Agrin promotes acetylcholine receptor clustering at the mammalian neuro-muscular junction by PI3K/GSK3β-mediated regulation of +TIPs and microtubule capture

Inauguraldissertation

zur Erlangung des Würde eines Doktors der Philosophie

vorgelegt der

Philosophisch-Naturwissenschaftlichen Fakultät

der Universität Basel

von

Stefan Sladeček

aus Wien, Österreich

Basel, Januar 2013

creative commons

Namensnennung-Keine kommerzielle Nutzung-Keine Bearbeitung 2.5 Schweiz

---

Sie dürfen:

das Werk vervielfältigen, verbreiten und öffentlich zugänglich machen

Zu den folgenden Bedingungen:

Namensnennung. Sie müssen den Namen des Autors/Rechteinhabers in der von ihm festgelegten Weise nennen (wodurch aber nicht der Eindruck entstehen darf, Sie oder die Nutzung des Werkes durch Sie würden entlohnt).

Keine kommerzielle Nutzung. Dieses Werk darf nicht für kommerzielle Zwecke verwendet werden.

Keine Bearbeitung. Dieses Werk darf nicht bearbeitet oder in anderer Weise verändert werden.

- Im Falle einer Verbreitung müssen Sie anderen die Lizenzbedingungen, unter welche dieses Werk fällt, mitteilen. Am Einfachsten ist es, einen Link auf diese Seite einzubinden.
- Jede der vorgenannten Bedingungen kann aufgehoben werden, sofern Sie die Einwilligung des Rechteinhabers dazu erhalten.
- Diese Lizenz lässt die Urheberpersönlichkeitsrechte unberührt.

Quelle: http://creativecommons.org/licenses/by-nc-nd/2.5/ch/ Datum: 3.4.2009

Genehmigt von der Philosophisch-Naturwissenschaftlichen Fakultät
auf Antrag von

Prof. Dr. Markus Ruegg (Fakultätsverantwortlicher)

em. Prof. Dr. Hans-Rudolf Brenner (Dissertationsleiter)

Prof. Dr. Christoph Handschin (Koreferent)

Basel, am 11. Dezember 2012

Prof. Dr. Jörg Schibler
Dekan

Für meine Eltern, denen ich viel zu verdanken habe.

Zusammenfassung

Neurotransmission an der neuromuskulären Endplatte von Säugetieren erfolgt durch Ausschüttung von Acetylcholin (ACh) aus motorischen Nerven in den synaptischen Spalt und verursacht letztendlich Muskelkontraktion im angesteuerten Muskel. Der Signalstoff Agrin, welcher ebenfalls vom Motornerv sekretiert wird, ist hauptverantwortlich für die postsynaptische Differenzierung der Muskelfasern und bewirkt die räumliche Konzentration der Rezeptoren für den Neurotransmitter Acetylcholin (AChR) in einem kleinen - meist zentralen - Areal der Faser unterhalb des Ansatzpunkt der Motornervendigung. Nach intensiver Beforschung sind die Endeffekte von Agrin auf Muskelfasern gut dokumentiert und viele involvierte Moleküle bekannt. Trotzdem ist die Rolle des subsynaptischen Mikrotubuli-Zytoskeletts beim Transport, bei der Membraninsertion und bei der Konzentrierung von AChR-Molekülen wenig erforscht und die zugrundeliegenden molekularen Mechanismen, welche ein Mikrotubuli-Netzwerk unterhalb der Synapse etablieren, sind grossteils unbekannt. Im Zuge meiner Doktorarbeit untersuchte ich daher neue Aspekte der agrin-induzierten biochemischen Signalübertragung im Muskel und deren zellbiologischen Konsequenzen auf das Mikrotubuli-Zytoskelett.

Gerichteter intrazellulärer Vesikel-Transport erfolgt generell entlang von polaren Cytoskelettstrukturen, ein grosser Teil davon entlang von Mikrotubuli - kurzlebige Cytoskelettfilamente, deren dynamischeres „Plus-Ende" beständig zwischen Wachsen und Schrumpfen wechselt. Bestimmte Stimuli jedoch können über Signaltransduktions-kaskaden dazu führen, dass die schnell wachsenden Plus-Enden der Mikrotubuli mithilfe assoziierter Proteine (+TIP-Proteine) längerfristig an die Innenseite der Zellmembran oder an das Actinzytoskelett binden und dort verankert werden („*Microtubule Capture*"). Dieser Vorgang stabilisiert die betreffenden Mikrotubuli und verlängert ihre Halbwertszeit – die stabilisierten Microtubuli dienen der Zelle in weiterer Folge als gerichtete Transportrouten.

In meiner Doktorarbeit konnte ich zeigen, dass die Acetylcholinrezeptor-reiche postsynaptische Zentralregion der Muskelfasern von einem dichten Netzwerk von Microtubuli umgeben ist, einige dieser Microtubuli sind zudem durch post-translationale Modifikationen weiter stabilisiert. Weiters konnte ich demonstrieren, dass der Botenstoff Agrin im Muskel eine biochemische Signaltransduktions-kaskade auslöst, welche die PI3-Kinase aktiviert und an deren Ende GSK3β durch Phosphorylierung lokal inaktiviert wird.

Da viele der zuvor erwähnten +TIP-Proteine, zum Beispiel CLASP2, durch GSK3β negativ reguliert sind, ist eine lokalisierte Inaktivierung von GSK3β zentrale Voraussetzung dafür, dass +TIP-Proteine an Mikrotubuli Plus-Enden binden können und somit zur Etablierung von stabilen Mikrotubuli-Filamenten beitragen. Nach agrin-induzierter Inaktivierung von GSK3β bindet CLASP2 an Mikrotubuli Plus-Enden und befestigt diese am Zellkortex in der AChR-reichen Region von Myotuben in Wechselwirkung mit LL5β - welches von PI3K zur synaptischen Membran rekrutiert wird. Die betreffenden Mikrotubuli werden dadurch stabilisiert und können der Zelle als intrazelluläre Transportrouten für postsynaptisches Material wie etwa AChRs und Strukturproteine dienen.

Funktionsverändernde Mutationen beteiligter Moleküle sowie pharmakologische Eingriffe in den PI3K/GSK3β-Signalweg zeigten allesamt Effekte auf die lokale Konzentrierung von AChRs, die mit oben angeführter Kausalkette konsistent sind: Die Depolymerisierung von Microtubuli, die Hemmung der PI3-Kinase, der Verlust des *Clasp2*-Gens, die shRNA-vermittelte Unterdrückung der LL5β-Expression sowie die Hyperaktivierung von GSK3β führten jeweils zu reduzierter Grösse der AChR-Ansammlungen, während die Hemmung von GSK3β die Grösse der AChR-Ansammlungen erhöhte. Zusammengefasst trägt agrin-induzierte und +TIP-vermittelte Befestigung von Mikrotubuli an der subsynaptischen Membran zur fokalen Insertion und zum lokalen Konzentration von AChRs bei.

Abstract

Neurotransmission at the neuromuscular synapse of mammals occurs after secretion of acetylcholine (ACh) from the motor nerve into the synaptic cleft and ultimately results in contraction of the target muscle. The signaling molecule agrin, which is also secreted by the motoneuron, is the main organizer of postsynaptic differentiation and induces the clustering of receptors for the neurotransmitter acetylcholine (AChR) in a small – mostly central – area of the myofiber directly underneath the motoneuron terminal bouton. After intense research, the end results of agrin-induced differentiation are well documented and many involved molecules are known. Nevertheless, the role of the subsynaptic microtubule (MT) cytoskeleton in the process of AChR transport, insertion and clustering and the molecular mechanisms of the establishment of such a microtubule network are poorly defined. During my thesis, I analyzed new aspects of agrin-induced biochemical signaling and the cell biological consequences for the microtubule cytoskeleton.

Targeted intracellular transport of vesicles generally occurs along polar cytoskeletal structures, a major part along microtubules – cytoskeletal filaments that are normally short-lived with a highly dynamic "plus-end", which alternates between periods of growing and shrinking. However, certain stimuli induce signal transduction cascades which result in the "capture" of microtubule plus-ends at the cell cortex by interaction of plus-end binding proteins (+TIPS) with factors that localize to the cortex or the actin cytoskeleton. This event stabilizes microtubules and can drastically increase their lifetime – affected microtubule then serve the cell as stable, directional transport tracks.

During my thesis, I could show that the AChR-rich postsynaptic membrane encompasses a dense subsynaptic MT network, with some MTs further stabilized by post-translational modifications. In addition, I could

demonstrate that agrin induces PI3 kinase signaling in muscle, which ultimately inactivates GSK3β by phosphorylation.
Since many of the former mentioned +TIP proteins are negatively regulated by GSK3β, localized inactivation of GSK3β is crucial to enable +TIP-mediated microtubule capture and establishment of stable transport tracks at sites with elevated protein requirements such as the postsynaptic membrane. +TIP proteins, in particular Clasp2, then capture MTs at the cell cortex within AChR-rich sites by interacting with the membrane PIP_3-sensor LL5β and thus establish intracellular transport routes for focal transport of postsynaptic material like AChRs and structural proteins towards the synapse.

Mutants of involved molecules as well as pharmacologic manipulation of the PI3K/GSK3β-axis displayed effects on the clustering of AChRs, which are fully consistent with the aforementioned chain of events: Microtubule depolymerization, inhibition of PI3K, loss of the *clasp2* gene, shRNA-mediated repression of LL5β expression and hyper-activation of GSK3β lead to reduced AChR clustering, while inhibition of GSK3β elevates AChR clustering. Taken together, agrin-induced and +TIP-mediated MT capture at the subsynaptic muscle membrane contributes to focal insertion and clustering of AChRs at the neuromuscular junction.

Table of Contents

I. Introduction

I.1. The vertebrate neuromuscular junction (NMJ)

I.1.1. General introduction

Contraction of skeletal muscle enables animals any kind of body movement and contraction of the diaphragm is crucial for the ability to breathe. Voluntary control of skeletal muscle requires a highly specialized and organized physical connection between a muscle fiber and an α-motor nerve, this connection is called neuro-muscular junction (NMJ) and is the body's peripheral equivalent to synapses in the central nervous system, except that postsynaptic neurons are substituted by single muscle fibers. The NMJ is thus a chemical synapse that is anatomically and functionally differentiated for signal transmission from a motor nerve terminal to a circumscribed postsynaptic region on the muscle fiber (Engel, 2008). During development, motor nerve axons growing out of the spinal cord reach muscles and branch to contact multiple myofibers (Figure 1B). Each branch then forms several pre-synaptic terminal boutons on the muscle fiber it innervates (Figure 1A), supernumerary boutons stemming from more than one nerve branch innervating the same myofiber are later eliminated (Figure 1C).

Thus, a mature motor unit consists of one motoneuron and multiple myofibers under its control. Each presynaptic bouton is precisely positioned over postsynaptic junctional membrane folds harboring nicotinic acetylcholine receptors (AChRs; Figure 1A and Figure 2A). The presynaptic boutons contain a dense body termed the active zone where synaptic vesicles containing the neurotransmitter acetylcholine (ACh) dock and fuse to release their content into the synaptic cleft in response to an action potential. Schwann cells ensheath the motor axons and form a cap over the nerve terminal (Figure 2A). In addition, Schwann cells supply myelin, an insulating substance wrapped around the axon, which increases electric resistance in the axonal membrane underneath. Myelination of axons spares small gaps (termed rings

of Ranvier), thus enabling saltatory impulse propagation along these gaps down the axon, which drastically increases the velocity of nerve transmission. This is necessary given that some motor axons are longer than one meter in humans (Burden, 2002; Sanes and Lichtman, 2001).

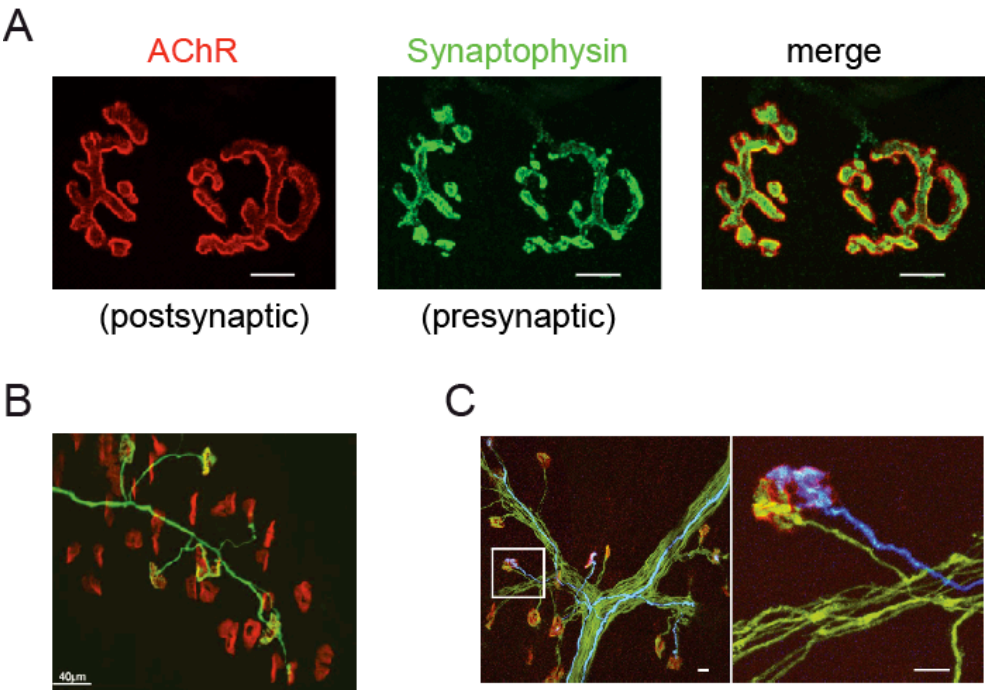

Figure 1: Synaptic morphology at the NMJ
A) Presynaptic motor nerve termini (stained for synaptophysin, green) and postsynaptic acetylcholine receptors (labeled with α-Btx-594, red) in the muscle fiber membrane are exactly juxtaposed to each other; scale bar is 10µm. **B)** P8 sternomastoid muscle from a Thy1::YFP transgenic mouse that expresses YFP (green) in only a small subset of motor axons, thus enabling visualization of single motor units (one motoneuron and the synapses controlled by it); scale bar is 40µm. **C)** Sternomastoid muscle from a P8 double transgenic mouse in which all axons express YFP (green) and a few axons express CFP (blue). AChRs are labeled with α-Btx-594 (red). At this stage, synapse elimination has not occurred yet, resulting in some double-innervated NMJs with two competing axons - one such NMJ is boxed on the left and shown at higher magnification; scale bar is 10µm. B) and C) taken from (Lichtman and Sanes, 2003).

The pre- and postsynaptic membranes of NMJs are not only separated by a synaptic cleft of 80-100nm, but also by a basal membrane, which consists of various laminins, collagens, perlecan and nidogen. The basal membrane has mechanical, organizing and inductive functions ((Sanes, 2003) & (Figure 2)), furthermore it is involved in muscle regeneration and re-innervation after injury.

The vertebrate NMJ is by far the most studied and best understood of all synapses, due to a number of advantages: its peripheral localization and its enormous size in comparison to central brain synapses make it easily accessible. Under physiologic conditions, every synapse consists of only one presynaptic input, and postsynaptic myofibers contain only a single kind of neurotransmitter receptor. These facts render the NMJ a comparatively simple system, which is ideal to study synaptic development and maintenance and to explore the functions of individual molecules in these processes.

I.1.2. Structure & development of the postsynaptic muscle membrane

The acetylcholine receptor is heteropentameric ligand-gated ion channel. The muscle form consists of 2 α1, one β, one δ and either one γ or ε subunit, depending on the developmental stage (Sine, 2012). In the course of development – after initial contact between the growth cone of the motoneuron and the muscle fiber (which occurs in mice at around day E13.5) - the heparansulfate-glycoprotein agrin is secreted by the motor nerve. Agrin is deposited in the basal lamina (the major part of the basement membrane) by binding to laminin, which is critical for its function (Burgess et al., 2000; Denzer et al., 1997).

Agrin induces in the muscle fiber the clustering of pre-expressed and evenly distributed AChRs to a small central patch of very high density (>10.000 molecules/μm^2 synaptically as compared to ~10 molecules/μm^2 extra-synaptically). Synaptic accumulation processes occur also for other synaptic signaling and structural molecules as well as for several nuclei, which become subsynaptically anchored and transcriptionally specialized (Brenner et al., 1990; Burden, 1998; Burden, 2002; Merlie and Sanes, 1985; Sanes and Lichtman, 2001; Schaeffer et al., 2001; Witzemann, 2006).

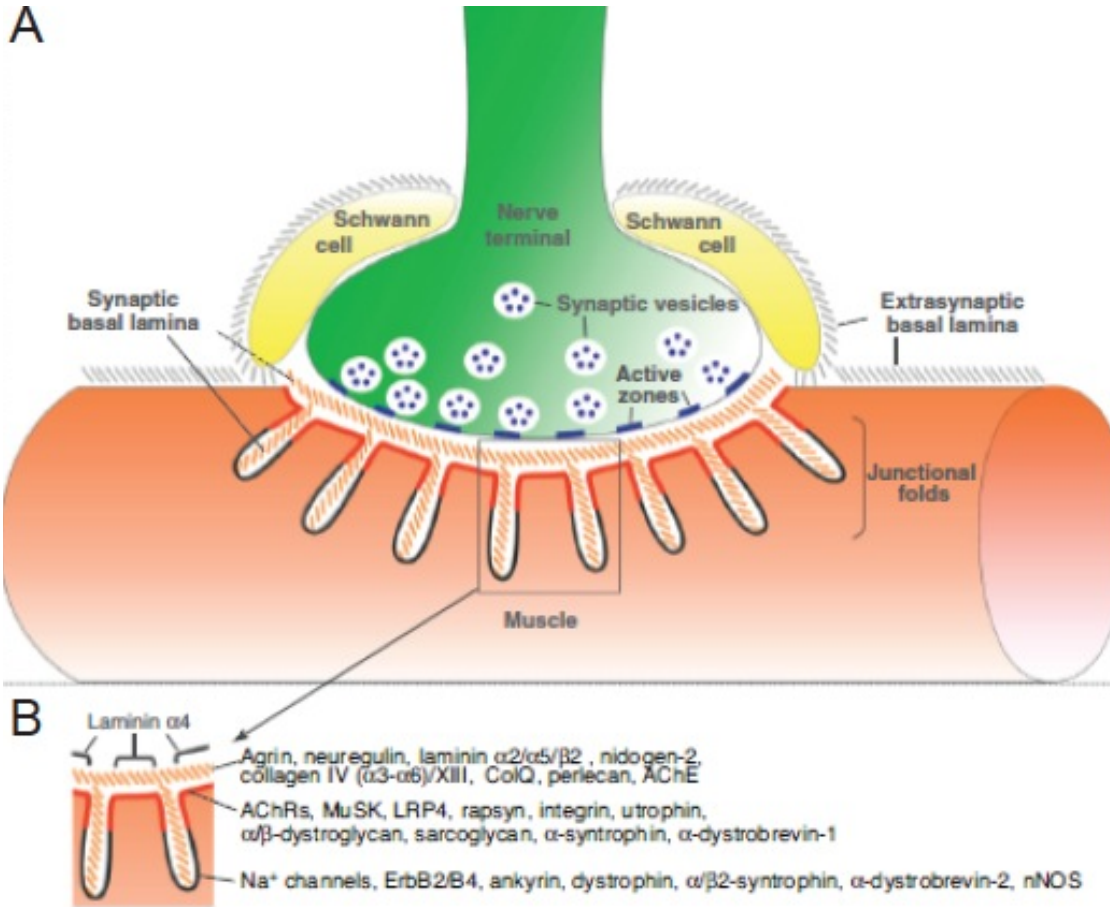

Figure 2: Structure and morphology of an adult NMJ
A) Gross anatomical structure of an adult NMJ, depicting the presynaptic motor nerve (green), nerve-capping Schwann cells (yellow), a postsynaptic myofiber (red), and the basal lamina. Note the synaptic gutter in the muscle fiber, which is referred to as primary synaptic fold and the invagination of the gutter, which are called secondary or junctional folds. **B)** Detailed structure of junctional folds indicating the precise location of key molecules. Scheme from (Shi et al., 2012).

The neuronally secreted isoform of agrin, which includes critical splice inserts, is necessary and sufficient for AChR clustering and induction of most other aspects of postsynaptic differentiation (Bezakova and Ruegg, 2003; Burgess et al., 1999; Gautam et al., 1996; Gesemann et al., 1995; Jones et al., 1997; McMahan et al., 1992; Reist et al., 1992). Even after full maturation of the NMJ, sustained agrin/MuSK signaling is needed throughout lifetime for active NMJ maintenance, as loss of agrin expression in young adult leads to drastic premature aging symptoms of the NMJ, including nerve atrophy and postsynaptic AChRs (Samuel et al., 2012).

MuSK, the muscle-specific receptor tyrosine kinase (Jennings et al., 1993; Valenzuela et al., 1995), co-localizes with AChRs in the postsynaptic membrane and acts as receptor for agrin (Glass et al., 1996) via its associated co-receptor Lrp4 (Kim et al., 2008; Zhang et al., 2008). Initially, agrin directly binds to Lrp4 by its z8 loop, which is only contained in the neural isoform, thus explaining why muscle-secreted agrin is not able to induce AChR clustering (Gesemann et al., 1996; Zong et al., 2012). Agrin and MuSK/Lrp4 orchestrate the postsynaptic NMJ development; consequently, MuSK or Lrp4 deficient mice die at birth and don't show any signs of postsynaptic differentiation or any body movement, whereas AChR genes are expressed at normal levels (DeChiara et al., 1996; Weatherbee et al., 2006).

Thus, MuSK or Lrp4 deficiency displays a phenotype even more severe than agrin knock-out, which also yields no viable offspring, but shows at least residual postsynaptic differentiation in form of aneural AChR clusters (Gautam et al., 1996). The difference of phenotype severity indicates that MuSK functions rudimentarily even in absence of its ligand by acting as a structural scaffold and/or signaling scaffold for other signaling components even in absence of its own signaling activity. Moreover, other ligands for MuSK, like certain Wnt proteins (Zhang et al., 2012) could partially compensate for agrin deficiency and thus enable AChR pre-patterning (Gautam et al., 1996).

Another crucial factor for AChR clustering downstream of MuSK signaling is the cytoplasmic protein rapsyn, which precisely co-localizes with AChRs and anchors them to the actin cytoskeleton (Apel et al., 1997; Moransard et al., 2003). Rapsyn deficient mice die within hours after birth from weak breath. They display accumulations of MuSK, but their AChRs remain unclustered and diffusely distributed (Gautam et al., 1995), moreover MuSK signaling is compromised in absence of rapsyn (Apel et al., 1997). Perinatal lethality is furthermore observed in mice with genomic deficiency of AChRα1, which

display complete absence of AChR clustering (An et al., 2010) or ChAT, the enzyme necessary to synthesize the ligand ACh (Brandon et al., 2003; Misgeld et al., 2002).

Absence of AChRε subunit (Missias et al., 1997; Witzemann et al., 1996) or AChRγ subunit (Liu et al., 2008; Takahashi et al., 2002) also causes severe neuromuscular defects, but still enables residual AChR clustering and is not perinatally lethal. Interestingly, AChRs seem to have an active role in the development of the postsynaptic apparatus: they are required for clustering of postsynaptic components (Marangi et al., 2001; Ono et al., 2001) and even the absence of only the adult AChRε subunit severely compromises the overall postsynaptic architecture (Missias et al., 1997). Moreover, AChR anchoring to the cytoskeleton via rapsyn seems to precede AChR clustering (Moransard et al., 2003), underlining the complex and interdependent molecular interactions involved in the postsynaptic assembly leading to a mature NMJ.

Development of the NMJ is furthermore not unidirectional with the motoneuron inducing postsynaptic differentiation in a "passive" muscle. Rather, full maturation of the motor endplate involves a complex mutual interaction of motor nerve and muscle fibers and a delicate balance of anterograde and retrograde signals. Muscle Lrp4 (Yumoto et al., 2012) has been shown to act as retrograde signals for full presynaptic differentiation and MuSK localization in the myofiber membrane determines the future location of motor axon ingrowth and synapse formation (Kim and Burden, 2008).

I.1.3. Contractile function of the NMJ

The main function of the neuromuscular junction is excitation-contraction coupling, a physiological process converting an electrical stimulus into a mechanical response. This process is fundamental to muscle physiology, in

which the electrical stimulus is an action potential in the motoneuron and the mechanical response is muscle contraction (Sandow, 1952). Muscle contraction involves a complex series of events, starting with an action potential originating from the central nervous system that reaches a motoneuron, which propagates it down along its axon towards the presynaptic boutons by activating voltage-gated sodium channels. When the action potential reaches the presynaptic ending, it causes a calcium ion influx through voltage-gated calcium channels. The ensuing Ca^{2+} influx causes vesicles containing the neurotransmitter acetylcholine to fuse with the plasma membrane, thus releasing acetylcholine into the synaptic cleft between the motoneuron terminal and the specialized postsynaptic area of the skeletal muscle fiber. Acetylcholine diffuses across the synaptic cleft and binds to nicotinic acetylcholine receptors on the myofiber membrane.

This event activates the nicotinic AChRs and opens their intrinsic Na^+/K^+ channels, causing sodium influx and potassium efflux. Because the channel is more permeable to sodium and because of electrochemical gradients, more Na^+ flows in than K^+ flows out. As a result, each ACh-vesicle released into the synaptic cleft generates miniature endplate potentials (MEPP) in the muscle fiber with the membrane becoming more positively charged (or less polarized, respectively). MEPPs are additive and sum up to generate an end plate potential (EPP), which triggers an action potential in the muscle as soon as the threshold for an EPP is reached. This action potential spreads through the muscle fiber's network of T-tubules, which are invaginations of the sarcolemma, thus depolarizing the inner portion of the muscle fiber. Depolarization activates L-type voltage-dependent Ca^{2+} channels (termed dihydropyridine receptors) in the T tubule membrane, which are in vicinity of Ca^{2+}-release channels (called ryanodine receptors) embedded in the membrane of the adjacent sarcoplasmic reticulum (SR), which is inside the myofiber. Final result of this signal relay is calcium release from the SR into the cytoplasm of the myofiber.

The released calcium binds to troponin, which is present on the thin actin filaments of myofibrils. Troponin then allosterically modulates tropomyosin, thereby unblocking binding sites for myosin on actin. Myosin now binds to the uncovered binding sites on the actin filaments using ATP-hydrolysis, the following release of ADP and inorganic phosphate enables sliding of myosin along actin, a process termed power stroke. This event pulls the Z-bands towards each other and the central M-line, thus shortening the sarcomere, the muscle's contraction unit. Re-association of myosin with ATP allows myosin to release actin and to return to its start conformation.

The last steps of ATP-dependent myosin binding to actin and the following ADP and P_i -release-dependent power stroke repeat as long as ATP is available and calcium is present in the thin filament. During these repetitions (which are termed contraction cycles), calcium is actively pumped back into the sarcoplasmic reticulum. When the calcium supply is exhausted in the thin filament, troponin causes tropomyosin to change back its conformation, thus blocking again myosin's binding to actin, which finally stops the contraction process (Alberts et al., 2002).

I.1.4. Biochemical and cell biological processes downstream of agrin

Agrin signaling via MuSK/Lrp4 is of overwhelming importance for development of a mature postsynaptic apparatus in myofibers as illustrated by severe defects or even complete absence of postsynaptic differentiation if components of this pathway are deficient or critically mutated. Section I.1.2. outlined the lethal neuromuscular phenotypes of mice deficient for the muscle-specific receptor-tyrosine kinase MuSK, its ligand agrin, AChR subunits, the AChR-anchoring protein rapsyn or the ACh synthesizing enzyme ChAT. Besides the aforementioned proteins, muscle fibers employ a plethora of molecular interactions and signaling pathways downstream of agrin/MuSK to establish a mature NMJ, many of which regulate the cytoskeleton, gene expression or the stability of macromolecular complexes at the postsynaptic membrane.

Dok-7 is a cytoplasmic interactor of MuSK and essential for correct MuSK localization and activation upon agrin treatment. Mice lacking Dok-7 fail to localize MuSK in the central region of muscle and form neither AChR clusters nor neuromuscular synapses (Bergamin et al., 2010; Inoue et al., 2009; Okada et al., 2006). Binding of Tid1 to activated MuSK precedes binding of Dok-7 and is prerequisite for Dok-7 binding to MuSK (Linnoila et al., 2008). Clustering of AChRs in response to agrin involves cytoskeletal rearrangements, vesicle transport along cytoskeletal tracks, propelling of membranous AChRs (Bloch, 1986; Connolly, 1984; Connolly, 1985; Connolly and Graham, 1985; Dai et al., 2000) and anchoring of postsynaptic proteins to a cytoskeletal scaffold (Apel et al., 1997; Banks et al., 2003; Moransard et al., 2003).

Reorganization of the subsynaptic cytoskeleton provides mechanic stability to the synapse as a whole and also means to ensure targeted transport of synaptic material towards the synaptic membrane plus anchoring possibilities for NMJ components. Rapsyn, for example, connects synaptic AChRs to the actin cytoskeleton (Apel et al., 1997; Borges and Ferns, 2001; Borges et al., 2008; Mohamed et al., 2001; Moransard et al., 2003), this process being dependent on agrin-induced tyrosine-phosphorylation of the AChRβ subunit by Src family kinases (Borges and Ferns, 2001; Mittaud et al., 2001; Mohamed et al., 2001), which strengthens the interaction of AChR pentamers with rapsyn (Borges et al., 2008; Moransard et al., 2003). Initial cytoskeletal modifications during AChR clustering in response to agrin are achieved by activation of several downstream pathways: MuSK activates amongst others the tyrosine kinase Abl (Finn et al., 2003) and the geranylgeranyltransferase GGT1, which subsequently helps to activate GTPases of the Rho family (Luo et al., 2003). Rho GTPases are crucial cytoskeletal regulators and have been implicated in the process of AChR clustering (Weston et al., 2003; Weston et al., 2000; Weston et al., 2007) in a manner dependent on PI3K activity (Nizhynska et al., 2007).

Furthermore, MuSK-associated Dvl activates PAK1 (Luo et al., 2002), which is involved in the regulation of actin dynamics in several ways (Chan and Manser, 2012; Wu et al., 2010). Dvl is a constituent of Wnt signaling, which has broad effects on NMJ synapse formation (Gordon et al., 2012; Henriquez and Salinas, 2012; Henriquez et al., 2008; Jing et al., 2010; Jing et al., 2009). Some Wnts are able to bind directly to MuSK/Lrp4 and to induce AChR clustering independently of agrin (Zhang et al., 2012), other Wnt proteins collaborate with the Agrin-MuSK signaling and again other Wnt family members that activate β-catenin signaling are inhibitory for post-synaptic differentiation. Moreover, Wnt proteins are implicated in AChR pre-patterning, a process in which AChRs form (mostly central) aggregates during development, before the arrival of the motoneuron (Henriquez and Salinas 2012). Besides Wnts themselves and Dvl, other members of the Wnt pathway such as APC (Wang et al., 2003) and β-catenin (Li et al., 2008; Wu et al., 2012) are also implicated into NMJ formation.

MuSK activation recruits APC, which not only functions in Wnt signaling, but is also involved into the regulation of cytoskeletal dynamics, where it can bind to either actin (Moseley et al., 2007) or microtubules (Näthke, 2004). APC is a contact point for several cytoskeletal regulators of the GTPase family or their upstream regulators such as IQGAP1 and Asef (Kawasaki et al., 2000; Watanabe et al., 2004) and is therefore a crucial component for establishing cell polarity. APC is concentrated at the synaptic muscle membrane (Wang et al., 2003), where it is implicated in the process of AChR clustering, probably by organizing cytoskeletal rearrangements.

Other cytoskeletal proteins which are enriched at the postsynaptic NMJ are LL5β (Kishi et al., 2005), a membranous PIP_3-sensor (Paranavitane et al., 2003) and binding partner for microtubules decorated with the plus-end binding protein CLASP2 (Lansbergen et al., 2006). Another cytoskeleton organizing protein, ACF7, which crosslinks actin microfilaments with microtubules, has been shown to be involved in the rapsyn-mediated

immobilization of AChRs by bridging rapsyn to the actin cytoskeleton (Antolik et al., 2007). Taken together, the presence of a whole set of different cytoskeletal proteins and their regulators at the postsynaptic muscle membrane indicates a profound physiologic need for the establishment of a stable subsynaptic cytoskeletal network that serves to confer structural stability and as stable transport tracks towards the postsynapse for protein supply.

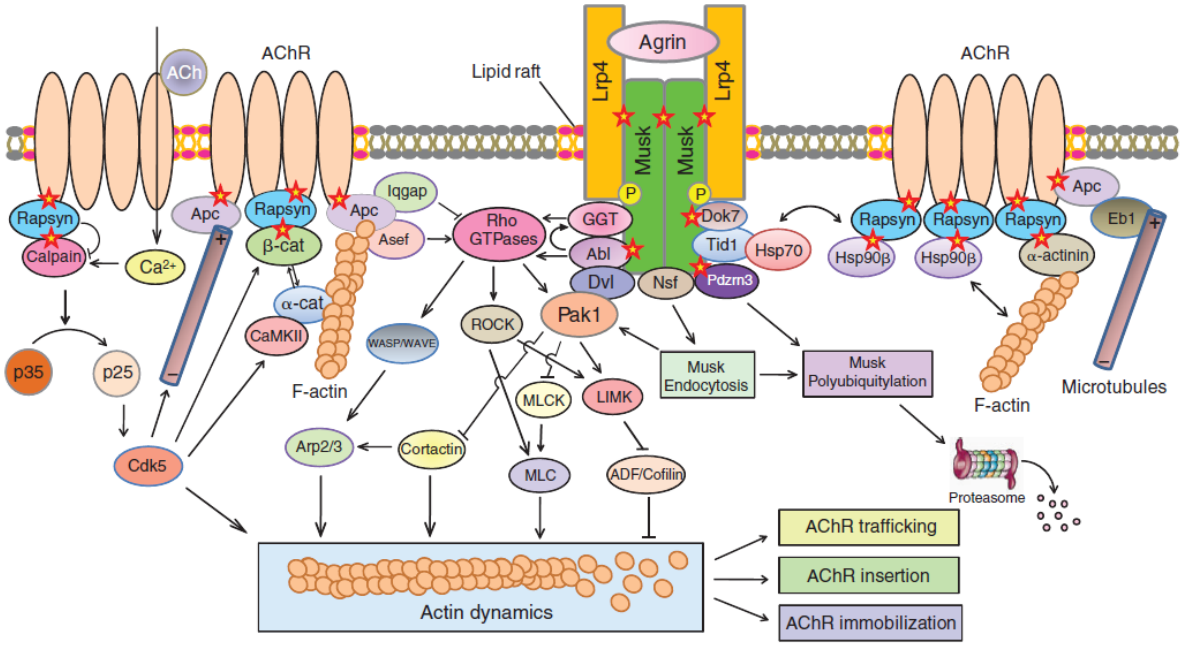

Figure 3: Intracellular pathways activated by agrin for AChR clustering
Initially, agrin interacts with Lrp4 to increase its interaction with MuSK, which dimerizes and partially activates MuSK. Subsequently, interactions between MuSK and distinct proteins like Dok7 and Tid1 are increased, which fully activates MuSK and its downstream signaling. Concomitantly, the tyrosine-kinase Abl and the geranylgeranyl transferase I are activated and facilitate downstream activation of Rho GTPases, which in turn regulate actin dynamics via multiple pathways. The actin cytoskeleton is involved in AChR transport, membrane insertion and immobilization. Agrin also stimulates the association of AChR with rapsyn and APC, which link the Ach receptors directly or indirectly to the cytoskeleton. Synaptic rapsyn is stabilized by Hsp90β and inhibits calpain, and thus antagonizes ACh-induced and Cdk5/CaMKII-mediated dispersal of AChR clusters. Active AChRs also recruit APC, a cytoskeletal organizer, which enables targeting of microtubules to the subsynaptic region. Red stars indicate protein-protein interactions that are increased by agrin. Scheme taken from (Wu et al., 2010).

MuSK activity also acts as a positive signal to counteract the cluster-dispersive effects of ACh-induced cdk5 activity (Lin et al., 2005).

Other molecules as diverse as heat-shock proteins (Luo et al., 2008), proteases (Chen et al., 2007) and transcription factors or co-activators like NF-κB (Wang et al., 2010) and PGC-1α (Handschin et al., 2007) are implicated in the process of AChR clustering too, thus underscoring the enormous breadth of molecules involved in the highly complex biological process of postsynaptic maturation. Some of the known biochemical signaling events downstream of agrin and their cell biological consequences are depicted in (Figure 3).

I.2. Microtubules (MTs)

I.2.1. The eukaryotic cytoskeleton

Every eukaryotic cell contains three types of cytoskeleton - actin filaments, microtubules and intermediate filaments. The cytoskeleton is vital for many aspects of cellular life like maintenance of cell shape, mitosis, motility and intracellular transport. Due to their many crucial functions for life, cytoskeletal proteins are implicated in a wide array of pathologies, including infection, cancer, cardiovascular diseases and neurodegenerative diseases (Akhmanova and Steinmetz, 2008a).

The assembly of cytoskeletal networks occurs by incorporation of small building blocks (actin, tubulin or intermediate filament proteins, respectively) into filamentous polymers. Intermediate filaments assemble through the association of antiparallel dimers into oligomers, which finally generate non-polar filaments. By contrast, the polymerization of actin and tubulin subunits occurs in a head-to-tail fashion and generates polar fibers with discernible ends having different biochemical and biophysical properties. Actin and tubulin subunits hydrolyze energy-rich phosphate bonds after incorporation – actin uses ATP, whereas tubulin employs GTP (Galjart, 2005). Intermediate filaments are more or less stable and mainly confer mechanical stability to cells, whereas actin filaments and microtubules are highly dynamic.

Actin filaments and MTs are constantly subjected to regulation by external and intracellular cues and thus serve to adapt cellular shape, polarization and targeted transport of organelles and other cargo such as protein-loaded vesicles. The ability to undergo fast turnover and assembly enables actin and microtubules to reorganize rapidly and locally in response to growth factors, polarity cues and other signals (Gundersen et al., 2004).

Microtubules and actin microfilaments interact heavily and these interactions underlie many fundamental processes in which cells need to establish and maintain dynamic cellular asymmetries. MTs and F-actin interact both regulatory and structural and their interactions are essential for basic biological processes such as cell motility, neuronal growth cone pathfinding, cellular wound healing, and cell division (Li and Gundersen, 2008; Rodriguez et al., 2003). Structural interaction is mediated by crosslinking proteins and certain molecular motors, while regulatory interaction involves mutual regulation of actin and MT dynamics via associated proteins such as Rho-family GTPases and other regulators (Hall and Lalli, 2010; Rodriguez et al., 2003). Regulation of MT by the actin cytoskeleton is well documented (Gundersen et al., 2004), as is regulation of F-actin by MTs (Basu and Chang, 2007).

I.2.2. General properties of microtubules

Microtubules are hollow cylinders (about 25 nm in diameter) composed of stable heterodimers of α- and β-tubulin (Ludueńa et al., 1977; Weisenberg et al., 1968) and (Figure 4A). Initially, they were described based on similarity between hollow flagellar structures and mitotic spindle fibrils (Pease, 1963). The single building blocks, tubulin, were identified by their binding to colchicine (Borisy and Taylor, 1967a; Borisy and Taylor, 1967b) and named after their function to build "tubes" (Mohri, 1968).

Microtubules are highly dynamic structures that continuously switch between phases of growth and shrinkage by addition or removal of tubulin subunits (Desai and Mitchison, 1997; Nogales and Wang, 2006). α/β-tubulin heterodimers polymerize in a head-to-tail fashion to form polar protofilaments (Amos and Klug, 1974), 13 of which form the helical microtubule wall (Evans et al., 1985; Ledbetter and Porter, 1964; Mandelkow et al., 1986), (Figure 4B).

To enable microtubule polymerization, γ-tubulin nucleates a ring structure to which protofilaments of α/β-tubulin heterodimers can bind, thus enabling microtubule polymerization start (Oakley and Oakley, 1989; Raynaud-Messina and Merdes, 2007). Both α-tubulin and β-tubulin bind GTP (Weisenberg et al., 1968) and since GTP-bound β-tubulin has high affinity for microtubule plus-ends, it drives tubulin addition onto the polymeric structure. After incorporation in the MT polymer, β-tubulin subunits hydrolyze their loaded GTP to GDP, whereas GTP on α-tubulin remains stable. GDP-bound β-tubulin is susceptible to depolymerization and thus detaches from free, uncapped MT ends. As only GTP-bound tubulin subunits bind with high affinity to the plus-end of MT, a cap of GTP-containing tubulin building blocks protects the microtubule polymer from disassembly (Desai and Mitchison, 1997), (Figure 4B and Figure 4C).

In most mammalian cells, the minus-end of microtubules is attached to an MTOC (microtubule organizing center), which is often tightly associated with the centrosome (Luders and Stearns, 2007) and the fast-growing plus-ends radiate towards the cell cortex. The MTOC prevents shrinkage from the microtubule minus-end, so dynamic instability occurs mostly at microtubule plus-ends. If the minus-end is not attached to an MTOC, dissociation of GDP-bound tubulin subunits can occur at these minus-ends. After conversion of the free tubulin dimers back to the GTP-bound form, the subunits can again be incorporated at the plus end, thus "treadmilling" through the microtubule (Galjart, 2005). Even if the minus-end is not attached, the two ends of a

microtubule show different polymerization rates; the plus-end grows and shrinks faster while the minus-end grows/shrinks slower or not at all (Allen and Borisy, 1974), (Figure 4C).

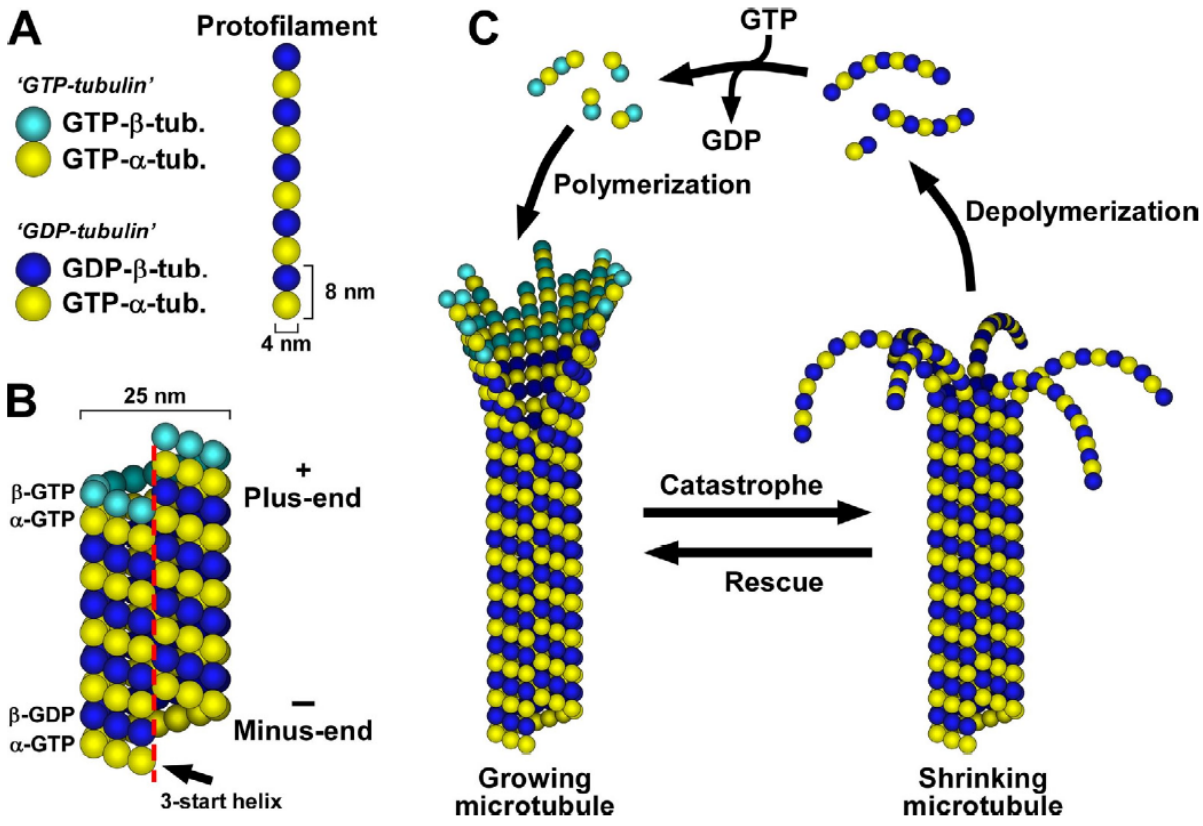

Figure 4: Microtubules – Structure and Dynamics
A) Heterodimers of α/β-tubulin are the building blocks of microtubules and align head-to-tail to form protofilaments. Both α- and β-tubulin bind one molecule of guanine nucleotide. GTP associated with β-tubulin is hydrolyzed after incorporation of the tubulin dimer. **B)** The helical microtubule wall typically consists of 13 parallel protofilaments with each turn of the helix spanning 3 tubulin monomers. This arrangement results in a lattice seam on one side of the microtubule wall (red dashed line). **C)** The structure of the microtubule is determined by the γ-tubulin ring complex (γ-TuRC) at the MTOC. Microtubules are nucleated by the binding of α/β-tubulin dimers within protofilaments to the γ-TuRC and start elongating by the addition of dimers at the plus-end. The binding, hydrolysis and exchange of GDP/GTP on the β-tubulin monomer regulates the switch between polymerization and depolymerization of microtubules, but is not required for microtubule assembly itself. Scheme adapted from (Akhmanova and Steinmetz, 2008b).

Under normal physiologic circumstances, most MT plus-ends alternate between prolonged phases of polymerization and depolymerization, a phenomenon called "dynamic instability" (Mitchison and Kirschner, 1984).

The transition from polymerization to depolymerization is referred to as catastrophe, whereas the opposite transition from depolymerization to polymerization is termed rescue (Walker et al., 1988), (Figure 4C).

I.2.3. Function and regulation of microtubules

Microtubules are functionally involved in basic processes such as intracellular transport, organelle positioning, cell shape and cell motility, and constitute complex cellular structures like centrosomes, centrioles and axonemes – the core structure of cilia and flagella. In addition, MTs form two essential structures during cell division, the mitotic spindle and the midbody. Microtubules also function as important factors for the establishment and maintenance of cell polarity. To fulfill these highly diverse functions, MTs are regulated by a plethora of microtubule-associated proteins (MAPs), which interact either with soluble tubulin building blocks or with the whole microtubule lattice or exclusively with the microtubule plus-end (Akhmanova and Steinmetz, 2008b; Cassimeris and Spittle, 2001; Galjart, 2005).

The "classical" MAPs (e.g. MAP1A/B, MAP2, tau, XMAP215, stathmin, et cetera) bind to soluble, non-polymerized subunits and along the whole length of microtubules and thereby regulate overall MT stability and interactions. Some classical MAPs stabilize microtubules by lateral binding, some by stimulating the addition of tubulin subunits to the MT polymer, some by blocking catastrophe events, or by promoting MT rescue. Stabilization is also achieved by cross-linking protofilaments or bundling of microtubules (Chapin et al., 1991). On the other hand, some classical MAPs destabilize MTs, like catastrophin, which promotes catastrophes and katanin & spastin, which sever microtubules. Stathmin sequesters single tubulin subunits, thus inhibiting rescue events (Cassimeris and Spittle, 2001; Howard and Hyman, 2007; Sharp and Ross, 2012).

Another class of MAPs, which bind along the whole microtubule, are molecular motors. The intrinsic polarity of microtubules qualifies them as tracks for directed intracellular transport. Motors of the kinesin (Verhey and Hammond, 2009; Verhey et al., 2011) and dynein (Sakakibara and Oiwa, 2011; Vallee et al., 2004) superfamilies mediate unidirectional transport of macromolecules, vesicles and organelles along MT tracks. Kinesins mediate transport towards the MT plus-end, while dyneins enable minus-end directed transport (Akhmanova and Hammer Iii, 2010; Kapitein and Hoogenraad, 2011; Karsenti et al., 2006). Furthermore, some molecular motors like MCAK and other kinesins negatively regulate overall MT stability by their MT depolymerase activity (Howard and Hyman 2007).

A third major group of MAPs associate specifically with GTP-loaded tubulin-subunits in growing MT polymers, rather than with microtubules as a whole. This protein family binds to tubulin preferentially at the more dynamic plus-end of MTs and is referred to as +TIPs, for "plus-terminal interacting proteins" (Akhmanova and Steinmetz, 2008a; Akhmanova and Steinmetz, 2010; Galjart, 2005). Since this protein family is of crucial importance for this work, it will be described in more detail in the following section.

Lastly, tubulin subunits themselves within polymeric microtubules undergo different post-translational modifications (PTMs), including detyrosination, acetylation, glutamylation, glycylation, and phosphorylation, most of which occur at the exposed C-termini of α/β-tubulin (Hammond et al., 2008; Janke and Bulinski, 2011). The wide spectrum of tubulin PTMs within microtubules broadens the functional spectrum of MT and enables functional fine-tuning of pre-existing MT polymers, as for example tubulin detyrosination is elevated in differentiated cells (Gundersen and Bulinski, 1986) and has been associated with reduced MT turnover and enhanced MT stability, respectively (Webster et al., 1987). Post-translational modifications of tubulin within MTs influence not only the stability of the affected MTs but also regulate their transporting properties (Hammond et al., 2008; Janke and Bulinski, 2011),

as for example, tubulin acetylation leads to elevated kinesin-mediated cargo transport (Cai et al., 2009; Reed et al., 2006).

I.2.4. +TIP proteins

A specialized group of MAPs are the plus-end tracking proteins (+TIPs), which are conserved in all eukaryotes and specifically accumulate at growing microtubule plus-ends. Since CLIP-170 was discovered as the first +TIP (Perez et al., 1999), this diverse protein family has continuously expanded. The +TIPs known to date can be classified into 4 different groups, based on structural elements: EB family proteins, CAP-Gly proteins, proteins containing basic and Ser-rich sequences, and HEAT/WD40-repeat proteins. Plus-end tracking proteins can contribute to the regulation of microtubule dynamics, mediate the cross-talk between microtubule ends, the actin cytoskeleton and the cell cortex, and participate in transport and positioning of structural and regulatory factors and membrane organelles (Akhmanova and Steinmetz, 2008a; Akhmanova and Steinmetz, 2010; Galjart, 2010). Due to their adjustable differential binding within cells, +TIPs are crucially implicated in cell polarization during cell migration and differentiation (Jaworski et al., 2008; Neukirchen and Bradke, 2011; Watanabe et al., 2005).

+TIP family	Members
EB family proteins	EB1, EB2, EB3
CAP-Gly proteins	CLIP-170, CLIP-115, $p150^{Glued}$
Proteins with basic and Ser-rich sequences	CLASP1/2, APC, ACF7, STIM1
HEAT- and WD40-repeat proteins	LIS1, XMAP215/ChTOG
Microtubule motor proteins	MCAK, Dynein HC, Kinesins

Table 1: Overview and classification of +TIPs

End binding (EB) proteins are the "core" +TIPs expressed in every cell and bind to MTs directly. Most (or even all) other +TIPs bind to MTs indirectly via interaction with EB proteins. EBs are small proteins composed of an N-terminus and a C-terminus - both of which are highly conserved - separated

by a linker sequence. While the N-terminus is necessary and sufficient for microtubule binding (Hayashi and Ikura, 2003), the coiled-coil region of the C-terminus mediates dimerization of EB monomers (Honnappa et al., 2005). The N-terminal calponin homology domain (CH-domain) of EBs bind to tubulin near their GTP binding site, which allows EBs to bind to growing MT ends by sensing conformational changes resulting from the microtubule nucleotide state. This connection bridges MT protofilaments and provides a stabilizing zone that protects microtubules from depolymerization (Maurer et al., 2012).

The coiled-coil region in EBs partially overlaps with the unique end binding homology (EBH) domain, which is more distal and to which many other +TIPs commonly bind through their shared SxIP sequence motif and electrostatic interactions resulting from salt bridges (Honnappa et al., 2009; Kumar and Wittmann, 2012). At the very C-terminus, EBs contain a conserved EEY/F sequence motif, which is also present at the C-terminus of α-tubulin and CLIP-170 and is a point of interaction with other CAP-Gly proteins (Akhmanova and Steinmetz, 2008a; Bu and Su, 2003). In general, EB1 and EB3 are the major EB proteins and are thought to be functionally redundant, although studies of muscle cell differentiation suggest that EB1 might be dominant in undifferentiated cells while EB3 is necessary for cell differentiation (Straube and Merdes, 2007).

CAP-Gly proteins contain N-terminal cytoskeleton-associated protein glycine-rich (CAP-Gly) domains, which are responsible for their association with MTs, EB proteins and dynactin (Bu and Su, 2003; Goodson et al., 2003; Perez et al., 1999; Schroer, 2004). The CAP-Gly domain of CLIP-170 binds to the C-terminal EEY/F sequence motif contained in both EB proteins and tubulin (Bieling et al., 2008; Slep, 2010; Steinmetz and Akhmanova, 2008), terminal detyrosination of tubulin in stabilized MTs inhibits recruitment of CLIP proteins (Peris et al., 2006). The adjacent coiled-coil region mediates the homodimerization of CLIPs. The coiled-coil region of CLIP-170 is flexible

and can fold back in an intramolecular interaction, resulting in the binding of the CAP-Gly domain to the EEY/F motif and auto-inhibition of CLIP-170 (Lansbergen et al., 2004). The cargo-binding C-terminus of CLIP-170 contains two metal-binding motifs, which are not present in the close homologue CLIP-115 (De Zeeuw et al., 1997).

Proteins containing basic and Ser-rich sequences contain stretches rich in serine and basic residues that mediate their interactions with microtubules and EB proteins. Exemplary members of this family are the adenomatous polyposis coli protein APC (Barth et al., 2008; Bienz, 2002; Nathke et al., 1996; Zumbrunn et al., 2001a), the microtubule-actin crosslinking factor MACF1, also called ACF7 (Sonnenberg and Liem, 2007; Suozzi et al., 2012; Wu et al., 2008) and CLASPs, the CLIP-associating proteins (Akhmanova et al., 2001; Galjart, 2005). As with the majority of other +TIPs, members of this family bind to MTs mostly indirectly through association with EBs via their hydrophobic SxIP sequence motif (Honnappa et al., 2009; Kumar and Wittmann, 2012) and surrounding amino acids, which provide electrostatic interaction with the C-terminus of EBs (Kumar et al., 2012).

In contrast to most other +TIPs, which bind uniformly to the growing ends of all MTs, the members of this +TIP family preferentially accumulate at MT subsets that are oriented towards polar structures such as the leading edge of migrating cells or neuronal growth cones. Furthermore, binding of APC, ACF7 and CLASPs to MTs/EBs is negatively regulated by GSK3β phosphorylation (Honnappa et al., 2009; Kumar et al., 2009; Watanabe et al., 2009; Wu et al., 2011; Zumbrunn et al., 2001c) and all these proteins are implicated in region-specific MT capture during cell polarization (see section I.2.5.).

CLASP proteins interact with EBs and regulate MT dynamics at the cell cortex (Mimori-Kiyosue et al., 2005). CLASP2 captures MTs at the cell cortex by interacting with the membrane-associated PIP_3-sensor LL5β in fibroblasts

(Lansbergen et al., 2006) or by interacting with the actin-binding protein IQGAP1 in epithelial cells (Watanabe et al., 2009). CLASP proteins are furthermore involved in directional post-Golgi trafficking of vesicles along MTs and thereby also contribute to cell polarization and mobility (Miller et al., 2009).

ACF7 interacts with EB1 and APC (Subramanian et al., 2003) and enables MT sliding along F-actin as well as MT capture to actin-rich cortical sites, hence its name ACF7 - Actin crosslinking factor 7 (Kodama et al., 2003). ACF7 allows cortical recruitment of CLASP2 (Drabek et al., 2006); targeting of ACF7 to the membrane is sufficient to enable MT capture downstream of some migratory cues (Zaoui et al., 2010). ACF7 also enables polarized MT outgrowth and directional movement of skin stem cells (Wu et al., 2011).

APC promotes directed cell extension by interacting with EB1 and regulation of microtubule dynamics and stability at the leading edge of migrating cells (Barth et al., 2008), where it also influences kinesin-mediated transport (Jimbo et al., 2002). APC can moreover interact with actin either directly or indirectly via binding to the Cdc42/Rac effector and actin-binding protein IQGAP1 (Watanabe et al., 2004).

Similar to APC, ACF7 organizes the MT cytoskeleton and thereby can polarize cells during migration or functional differentiation (Applewhite et al., 2010; Barth et al., 2008; Sanchez-Soriano et al., 2009). Furthermore, the members of this +TIP family mutually influence each other, as suggested by biochemical interaction of CLASP2 and ACF7 (Drabek et al., 2006). Loss of either APC, CLASP2 or ACF7 results in similar MT phenotypes – a decrease in MT stability, density and organization along with defects in MT targeting towards the leading edge and migration deficits (Kroboth et al., 2007; Kumar and Wittmann, 2012). Of note, the members of this +TIP-family were reported to be able to bind to MT plus-ends independently of EBs, too (Kita et al., 2006; Wittmann and Waterman-Storer, 2005; Wu et al., 2011).

HEAT- and WD40-repeat proteins contain either tumor-overexpressed gene (TOG) domains in the N-terminus, which are comprised of HEAT repeats (Al-Bassam et al., 2007; Slep and Vale, 2007) or N-terminal WD40 repeat-containing domain. While XMAP215 is an example of the former group and binds to MTs directly (Gard et al., 2004), Lis1 is an example of the latter group and associates with MT-associated CLIP-170 and dynein/dynactin rather than EBs or MTs itself (Tai et al., 2002).

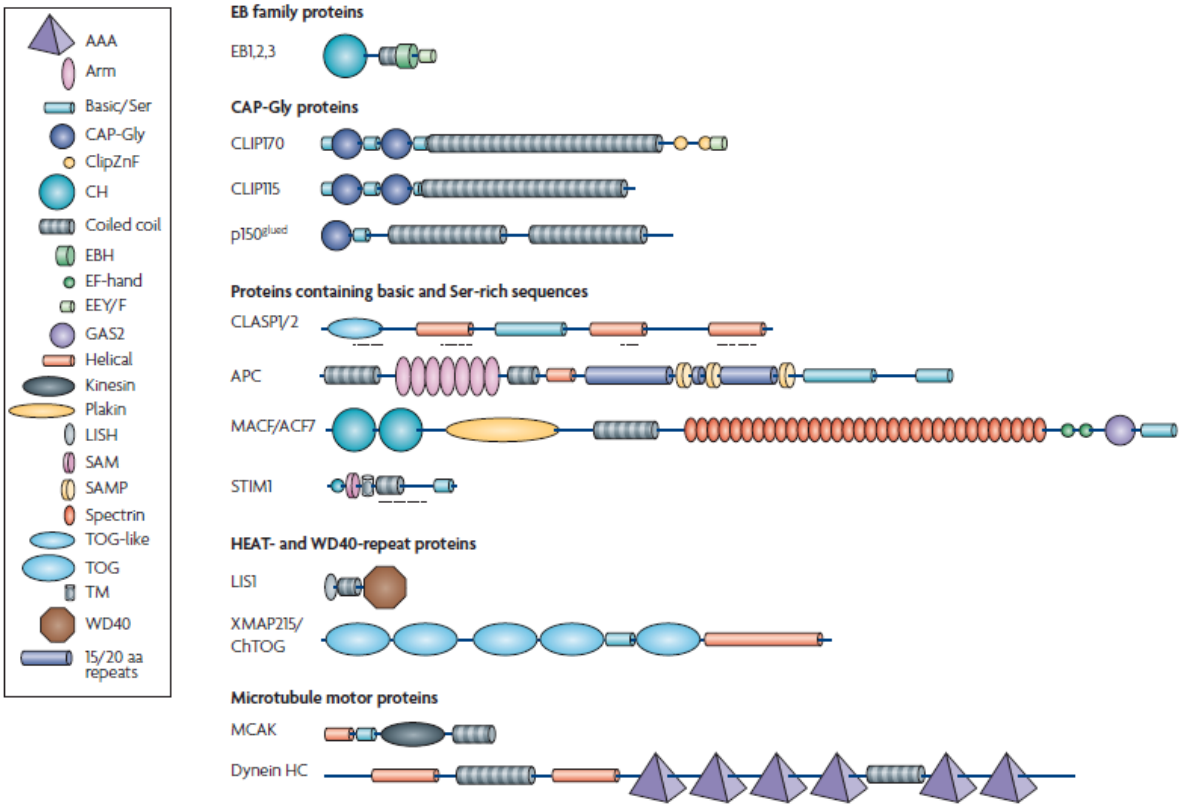

Figure 5: Structural classification of plus-end tracking proteins
The main plus-end tracking protein (+TIP) families have been grouped according to prominent structural elements that are involved in tracking the growing microtubule plus ends. AAA, ATPase family associated with various cellular activities; Arm, armadillo repeat; CAP-Gly, cytoskeleton-associated protein Gly-rich; CH, calponin homology; ClipZnF, C-terminal zinc knuckle of CLIP-170; EBH, end-binding protein homology; EF-hand, calcium-binding motif; GAS2, growth arrest-specific protein-2; LISH, LIS1 homology; SAM, sterile α motif domain; SAMP, Ser-Ala-Met-Pro repeat; TOG, tumor overexpressed gene domain; TM, transmembrane domain; WD40, motifs of ~40 amino acids, often terminating in a Trp-Asp dipeptide. Scheme taken from (Akhmanova and Steinmetz, 2008b).

I.2.5. MT capture and symmetry breaking

Under resting conditions, the highly dynamic plus-ends of microtubules permanently probe the cytosol and alternate between phases of growing, pausing and shrinking, with phase durations in the range of minutes. However, upon extracellular stimulation or intrinsic polarity cues, the growing plus-ends of MTs can be captured by factors present at the cell periphery, and stabilized. This process is of fundamental importance for symmetry breaking, cell polarization and cellular morphogenesis (Kirschner and Mitchison, 1986; Li and Gundersen, 2008). Microtubule capture involves physical interaction of two classes of proteins: proteins that are specifically associated with the plus ends of microtubules (+TIPS, see section I.2.4) and cortical capture factors, which are associated with either the cell cortex itself or the actin cytoskeleton and act as receptors for MTs or their associated +TIPs, respectively. These cortical capture factors are often regulated by RTKs, Rho GTPases, PI3K or other membrane-associated signaling factors (Gundersen, 2002; Li and Gundersen, 2008), (Figure 6 & Table 2).

Duration of MT capture depends on the involved factors and their cellular environment and can range from seconds to many hours. In the former case, microtubules just pause to either grow or shrink, whereas in the latter case, MTs are long-term capped and anchored, resulting in highly elevated MT stability, which can persist for many hours or longer. The intrinsic polar nature of microtubules qualifies them well as tracks for directed intracellular transport and is exploited by several cell types to initiate and maintain cell polarization as observed during axonal differentiation of neurons or cell migration (Gundersen, 2002; Gundersen et al., 2004; Li and Gundersen, 2008; Neukirchen and Bradke, 2011; Watanabe et al., 2005). In addition, long-term anchored microtubules (longer than 10 minutes) often become post-translationally modified, which further increases the lifetime of affected microtubules by rendering them more resistant to depolymerization and in addition enhances kinesin-dependent transport (Hammond et al., 2008; Janke and Bulinski, 2011; Li and Gundersen, 2008).

Cultured hippocampal neurons initially extend multiple morphologically indistinguishable, undifferentiated neurites. This symmetry is broken when one of the neurites (the future axon) begins to grow rapidly and acquires axonal markers (such as dephosphorylated tau), whereas the other neurites remain short. Over time, the short neurites grow and differentiate into dendrites by acquiring dendritic MT markers (such as MAP2).

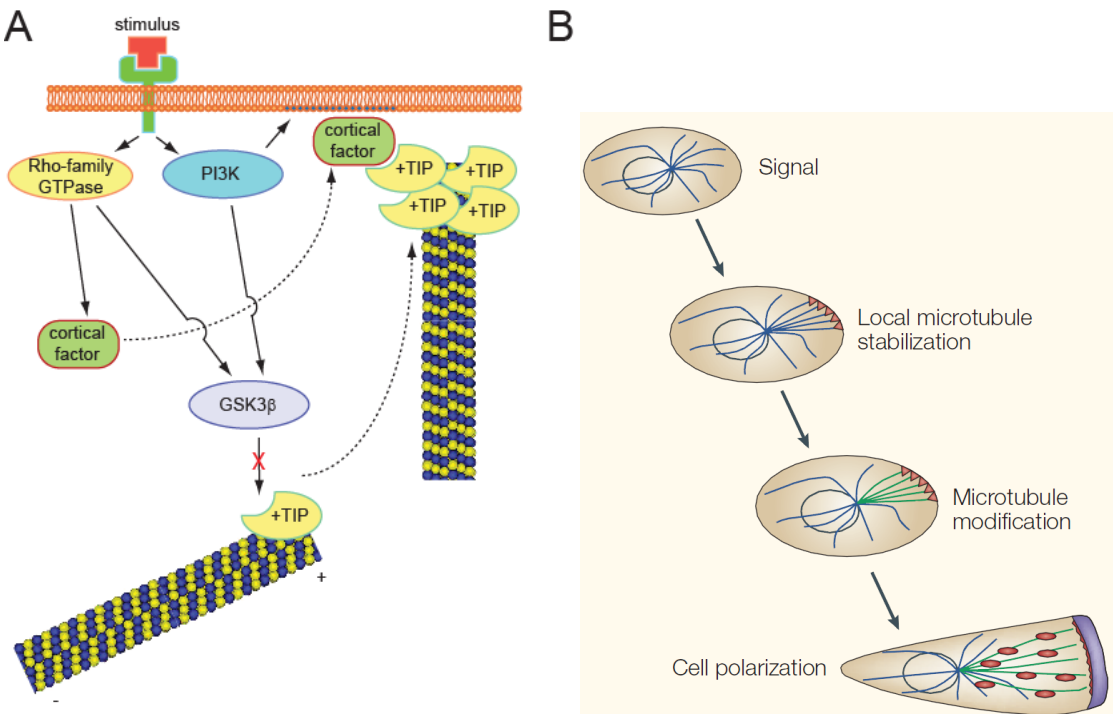

Figure 6: Molecular mechanism and cellular consequences of MT capture
A) Upon stimulation by growth factors, LPA, adhesion– and migration cues, cells engage Rho GTPases and PI3K to rearrange their cytoskeleton. In the context of MT capture, Rho GTPases and their effectors and/or PI3K and downstream molecules inactivate GSK3β by phosphorylation, which leads to a pool of hypophosphorylated +TIP protein with elevated affinity for MT plus-ends. At the same time, PI3K generates PIP_3 membrane domains (blue membrane area), to which cortical factors can bind, either just by their PH domain (which has a high affinity for PIP_3) or after activation by RhoGTPase effectors. The MT plus-ends - which are now highly decorated with +TIPs - then can bind to cortical factors, which are membrane-associated or F-actin-associated, thereby enabling MT capture. Tubulin subunits within captured MT can then be subjected to post-translational modifications, which further elevate MT stability. **B)** The event chain of local MT capture, stabilization and modification generates stable MT tracks within cells and establishes cell polarity. Scheme in B) taken from (Gundersen, 2002).

MTs in neuronal processes are more stable than the dynamic microtubules in proliferating cells, as shown by their resistance to MT-depolymerizing agents

and by their higher levels of post-translationally modified tubulin. The presence of acetylated tubulin in one cell process even precedes the axonal differentiation of this very process and thus seems to be a causative reason for axon specification. Moreover, subcellular application of taxol - a drug which stabilizes MTs - selectively to one neurite, is also sufficient to determine this neurite for axonal differentiation (Li and Gundersen, 2008).

In migrating fibroblasts, cell symmetry is broken upon migratory cues. This occurs by reorientation of the centrosome, to which MT minus-ends are anchored and more importantly, by selective MT capture and stabilization at the leading edge via interaction of +TIP proteins (e.g. EBs, APC and CLASPs) with cortical factors or the actin cytoskeleton (Li and Gundersen, 2008; Ridley et al., 2003), (Figure 6, Table 2 and section I.2.4). MT stabilization then directly enhances kinesin-based transport and maintains initial polarity in a self-reinforcing way, in both neurons and migrating fibroblasts. Taken together, selective MT stabilization is not only a consequence of cell polarization but rather permits it.

Once established, cell polarity varies in longevity, depending on the cell type. In neurons, epithelia and migrating fibroblasts, cell polarity itself is inherent to proper cell function and is thus maintained long-term in these cell types. In other cell like neutrophils during chase, polarity rather serves short-term functions allowing the cell to respond to spatial and temporal changes in external stimuli and is not maintained beyond fulfilling such a short-term function.

Interestingly, most members of the +TIP subfamily which contains basic and serine-rich sequences (CLASPs, ACF7, APC) are implicated in MT capture and regulated by GSK3β phosphorylation, which generally affects their binding to MTs and EBs negatively (Kumar et al., 2012; Kumar et al., 2009; Watanabe et al., 2009; Wu et al., 2011; Zumbrunn et al., 2001b). Consequently, MT capture occurs preferentially in subcellular localizations where PI3K activity is

high (Ridley et al., 2003) and/or where GSK3β has been rendered inactive by upstream signals such as LPA, migratory signals and growth factors, such as the leading edge of migratory cells (Sun et al., 2009; Yucel and Oro, 2011).

Cortical factor	Regulation	+TIP	Microtubule effect
IQGAP1	CDC42 and Rac	CLIP170	Transient stabilization (24–120 seconds)
mDia1	Rho	EB1 and APC	Long-term stabilization (hours)
LL5β	PI3K?	CLASP (Rac and GSK3β regulate CLASP)	Transient to long-term stabilization
PAR6	CDC42	Dynein and dynactin	Unknown
β-catenin	Unknown	Dynein	Transient stabilization (>2 minutes)

APC, adenomatous polyposis coli; CLASP, CLIP-associating protein; CLIP170, cytoplasmic linker protein-170; EB1, end-binding protein-1; GSK3β, glycogen synthase kinase-3β; IQGAP1, IQ motif-containing GTPase-activating protein-1; PAR6, partitioning defective-6; PI3K, phosphoinositide 3-kinase; +TIP, microtubule plus end-tracking protein; Tea, tip elongation aberrant protein.

Table 2: Molecular interactions in microtubule capture
Overview of known interactions between cortical factors and corresponding +TIP proteins, together with their mode of regulation and their effect on microtubules. Scheme taken from (Li and Gundersen, 2008).

I.2.6. MT organization in proliferating and differentiated cells

In most proliferating and migrating animal cells, the centrosome is the main site for microtubule nucleation and anchoring, leading to the formation of radial MT arrays with MT minus-ends anchored to the centrosome and plus-ends extending radially into the cell periphery. By contrast, in fully differentiated animal cells like neurons, epithelia and myotubes/muscle fibers as well as in most fungi and vascular plant cells, MT are often nucleated in a non-centrosomal fashion, showing parallel morphology (Bartolini and Gundersen, 2006). In differentiated myotubes, most MTs are organized parallel to the longitudinal axis of the cells, with their plus-ends being distal and their minus-ends localized near nuclei, which often cluster in the central region of myotubes (Tassin et al., 1985).

Generation of non-centrosomal MT arrays occurs as a multi-step process: the initial step involves formation of non-centrosomal MTs by either release from

the centrosome, catalyzed nucleation at non-centrosomal sites or breakage of pre-existing MTs. The second step involves transport by MT motor proteins or treadmilling to sites of assembly. In the final step, the non-centrosomal MTs are rearranged into cell type-specific arrays by bundling and/or capture at cortical sites, after which MTs often acquire long-term stability through PTMs. Despite their relative stability, the final non-centrosomal MT arrays may still exhibit dynamic properties and in many cases can be remodeled (Bartolini and Gundersen, 2006; Li and Gundersen, 2008).

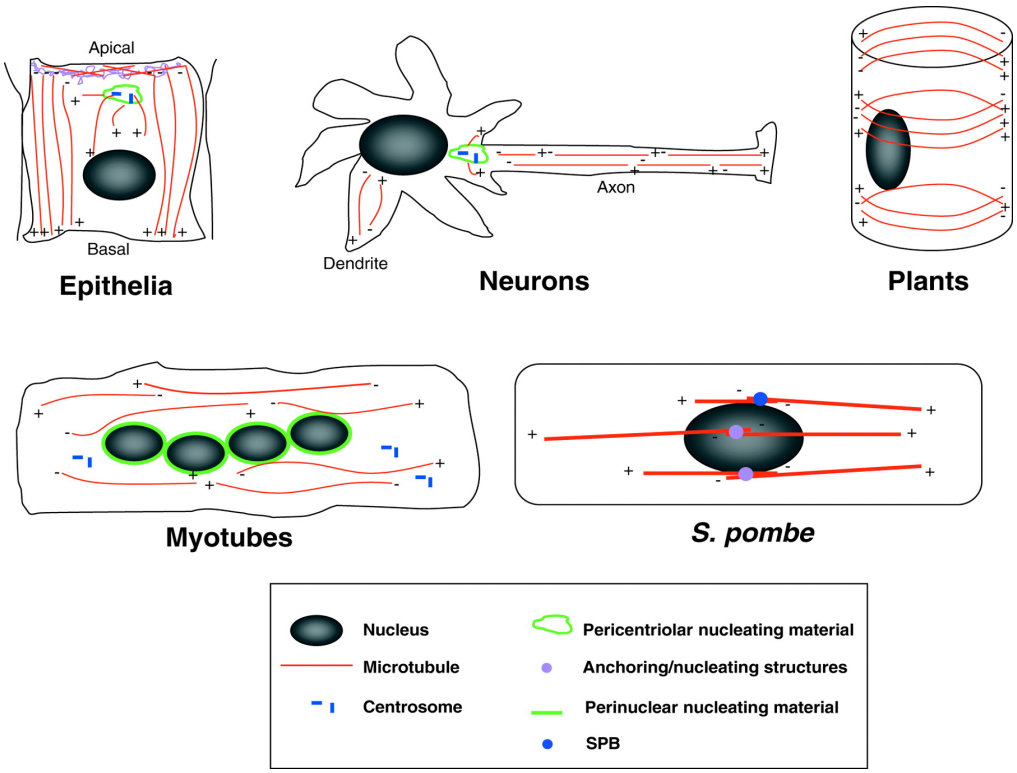

Figure 6: Microtubule organization in differentiated/polarized cell types
Various differentiated mammalian cell types, as well as yeast and plant cells, contain non-centrosomal MT array, which are generated in a multi-step process; scheme taken from (Bartolini and Gundersen, 2006).

I.2.7. MT involvement in myotube differentiation and muscle function

Skeletal muscle fibers and cultured myotubes are large multinucleated cells derived from the fusion of mononucleated myoblast into a syncytium. Elongated myoblasts display a classical radial microtubule array centered on perinuclear centrosomes, with MT minus-ends localized in perinuclear regions

and MT plus-ends being distal. After myoblast fusion, differentiated myotubes possess numerous microtubules organized in parallel along the long axis of the cells without any apparent nucleation centers (Tassin et al., 1985). Many MTs become stabilized in the course of myotube differentiation, with detyrosination occurring already at the onset of differentiation, when myoblasts elongate and align. Stabilization of MT proceeds further in fused myotubes by tubulin acetylation (Gundersen et al., 1989). Rearrangement of MT is therefore not only an effect of myotube differentiation, but rather crucially involved in the differentiation process by enabling gross morphological changes in myoblasts.

As such, microtubule dynamics and a linear, non-centrosomal array of MTs are involved in myoblast fusion, myotube differentiation and myofibrillogenesis (Antin et al., 1981; Pizon et al., 2005; Tassin et al., 1985). Moreover, MTs are implicated in the mobility of AChRs in primary cultures of chick embryonic muscle cells, suggesting an involvement of MTs in the development of neuromuscular junctions, too (Connolly, 1984; Connolly and Oldfin, 1985). MTs are also required for kinesin- and dynein-mediated movement of myonuclei (Wilson and Holzbaur, 2012) and other organelles in muscle (Elhanany-Tamir et al., 2012). Correct positioning (Metzger et al., 2012) and anchoring of myonuclei (Zhang et al., 2007) is critical for overall health, although lethality observed in mutants which fail to accumulate subsynaptic nuclei seems to be rather indirectly caused by innervation defects than by direct muscle dysfunction (Lei et al., 2009; Zhang et al., 2007).

Besides transcriptionally specialized myonuclei, the subsynaptic sarcoplasm has been shown to contain Golgi (Jasmin et al., 1989) and microtubules that are stabilized by acetylation (Jasmin et al., 1990). Taken together, the subsynaptic accumulation of cytoskeleton-anchored nuclei, a Golgi apparatus and stable microtubule transport tracks represents a sub-cellular compartment that is specialized for the transcription and post-translational

processing of postsynaptic proteins and for their targeting to the postsynaptic muscle membrane.

I.3. The role of PI3K/GSK3β in polarization and migration

I.3.1. Phosphatidylinositol-3 Kinase (PI3K)

The phosphatidylinositol 3-kinases (PI3Ks) are a conserved family of lipid kinases that phosphorylate the 3'-OH group of phosphatidylinositol-4,5-bisphosphate [$PI(4,5)P_2$] in the inner layer of the cell membrane to produce phosphatidylinositol-3,4,5-trisphosphate [$PI(3,4,5)P_3$], abbreviated as PIP_3. This reaction generates binding sites for proteins that bind to PIP_3 via their PH (pleckstrin homology) domain (DiNitto et al., 2003). A wide range of proteins with diverse functions possess a PH domain, including Akt (protein kinase B), phospholipase C (PLC), tyrosine kinases of the Btk/Tec family, insulin-receptor substrate IRS-1, RhoGEFs like Prex1 and cytoskeletal proteins such as dynamin and LL5β (DiNitto and Lambright, 2006; Paranavitane et al., 2003). All these proteins are recruited to the membrane by activated PI3K, where they in turn become activated themselves. PI3K thus induces many intracellular signaling pathways that regulate diverse functions like metabolism, survival, cell polarity and vesicle trafficking. The most ancient role for this family of enzymes is probably to mark specific cellular membranes for trafficking events, as Vps34 (vacuolar protein-sorting defective 34), the yeast homologue, performs mostly this function. Metazoans have evolved additional isoforms, which specifically serve signal transduction (Engelman et al., 2006). Signal termination occurs by degradation of PIP_3 by phosphatases like PTEN and SHIP (Cantley, 2002). In the context of cell polarization, PI3K acts as a signal amplifier by converting subtle extracellular gradients of migratory cues like chemoattractants or growth factors into steeper intracellular signaling gradients.

I.3.2. Glycogen Synthase Kinase 3

GSK3 is a highly conserved serine/threonine kinase with orthologs in plants, funghi, worms, flies and vertebrates – distant species show up to 90% sequence similarity in the kinase domain (Ali et al., 2001). GSK3 was first identified as a negative regulator of glycogen synthase and two paralogous isoenzymes with almost identical kinase domains were discovered, termed GSK3α and GSK3β. These isoenzymes differ in expression levels but have similar substrate specificity (Force and Woodgett, 2009; Woodgett, 1990). An unusual feature of GSK3 is its constitutive activity in resting and unstimulated cells, whereas cell stimulation by growth factors and other cues inhibits GSK3 by phosphorylation trough upstream kinases like Akt, S6K, PKC, PKA or p38MAPK. Besides inhibitory phosphorylation, signal-induced sequestration into protein complexes or a change of subcellular localization also serve to inhibit GSK3 activity in response to certain extracellular stimuli without phosphorylation of GSK3 (Ding et al., 2000; Kaidanovich-Beilin and Woodgett, 2011; Medina and Wandosell, 2011a; Taelman et al., 2010).

GSK3β is one of the most versatile kinases known and central in many biological processes such as endocrine signaling, immunological regulation, the regulation of proliferation through growth factor signaling and the regulation of metabolism through insulin and nutrient signaling in muscle and liver. To date, roughly 100 proteins are known to be targets of GSK3 phosphorylation (Sutherland, 2011) and due to its numerous functions, it is no surprise that GSK3 and in particular GSK3β has been associated with various pathologies, ranging from tumorigenesis over neuronal diseases like Alzheimer's disease and bi-polar disorder until metabolic disorders and immune defects (Kaidanovich-Beilin and Woodgett, 2011). GSK3 is therefore a valid therapeutic target for various diseases in the clinic. Therapeutic inhibition of GSK3 lowers blood glucose levels in type II diabetes, ameliorates neurological symptoms in Alzheimer's disease and bi-polar disorder and is under clinical testing to help cancer patients (Cohen and Goedert, 2004).

Because GSK3-mediated phosphorylation of substrates usually inhibits those substrates, the end result of GSK3 inhibition is typically functional activation of its downstream substrates. GSK3 is centrally involved in several important signal transduction pathways like Wnt, insulin and growth factor signaling and it is implicated in the biology of ES cells and progenitor cells (Force and Woodgett, 2009; Kim et al., 2009). Although GSK3α and β are entirely redundant in respect to Wnt signaling, their function differs in other cellular processes: Consequently, gene ablation of either isoenzyme yields different phenotypes: Full-body knock-out of GSK3β is lethal (Hoeflich et al., 2000), while loss of GSK3α is not (MacAulay et al., 2007), indicating non-redundant functions in some cellular functions. Tissue-specific loss of either isoenzyme also may yield different phenotypes (Patel et al., 2008), or compensatory upregulation of the remaining isoenzyme (Gillespie et al., 2011) - depending on the organ investigated. In muscle, GSK3β is ~4-fold more abundant than GSK3α (Force and Woodgett, 2009; McManus et al., 2005).

GSK3 is a master regulator of polar cytoskeletal structures (actin and MTs) and cell polarity (Sun et al., 2009). GSK3 is crucially involved in neuronal differentiation as well as migration of fibroblasts, epithel cells and stem cells (Jiang et al., 2005; Kaidanovich-Beilin et al., 2012; Kaidanovich-Beilin and Woodgett, 2011; Kim et al., 2011; Neukirchen and Bradke, 2011; Wittmann and Waterman-Storer, 2005; Wu et al., 2011). GSK3 regulates neuronal polarization by organizing the MT cytoskeleton through regulation of several classical MAPs like tau, MAP1B, MAP2 in neurons (Kaidanovich-Beilin et al., 2012) and through regulation of +TIPs like CRMP2 (Yoshimura et al., 2005), CLASP2 (Beffert et al., 2012; Hur et al., 2011) and APC (Barth et al., 2008). In addition, GSK3 is a downstream convergent point for many axon growth regulatory pathways (Kim et al., 2009; Kim et al., 2006) like PI3K, Rho-GTPases, Par3/6, TSC–mTOR and PKA (Kim et al., 2011). While regulated inhibition of both GSK3 isoenzymes is necessary for axon formation, their total loss prevents axon outgrowth (Kim et al., 2006), emphasizing the need

for tight spatial and temporal control of GSK3 activity (Hur et al., 2011; Medina and Wandosell, 2011b).

Similarly, GSK3 – with GSK3β being the far more studied isoenzyme - regulates cell polarity in migrating cells like fibroblasts, epithel cells and skin stem cells (Sun et al., 2009; Watanabe et al., 2009; Wittmann and Waterman-Storer, 2005; Wu et al., 2011; Yucel and Oro, 2011). Again here, GSK3β influences MT dynamics and cell polarity by regulation of +TIPs like ACF7 (Wu et al., 2011), CLASP2 (Kumar et al., 2009; Watanabe et al., 2009; Wittmann and Waterman-Storer, 2005), APC (Barth et al., 2008; Etienne-Manneville and Hall, 2003; Zumbrunn et al., 2001a) and molecular motors (Fumoto et al., 2006; Morfini et al., 2002; Sun et al., 2009).

Several signaling pathways like RhoGTPases, Wnt and PI3K converge on GSK3 inhibition, consequently multiple cellular inputs ultimately result in inactive GSK3 and hypophosphorylated, thus uninhibited cytoskeletal GSK3-targets, which enables them to fulfill their +TIP, MT-stabilizing and transport functions (Barth et al., 2008; Sun et al., 2009). Furthermore, GSK3 is implicated in the regulation of actin dynamics and adhesion sites (Sun et al., 2009). Similar to PI3K - one of its major upstream inactivators - GSK3 itself can be seen as a further signal amplifier by converting minute subtle extracellular signal gradients into even steeper intracellular signaling gradients.

II. Objectives

After decades of research, many general principles governing the development and maintenance of the neuromuscular junction are well established (Burden, 1998; Burden, 2002; Engel, 2008; Kummer et al., 2006; Sanes and Lichtman, 1999; Sanes and Lichtman, 2001; Shi et al., 2012; Wu et al., 2010). Agrin is established as the main organizer of postsynaptic differentiation in muscle fibers and a plethora of downstream molecules has been shown to be involved in NMJ biology on a descriptive level. However, for most of the involved molecules, defined molecular mechanisms explaining their contribution to the development of the postsynaptic apparatus is elusive. One major step in the formation of a mature NMJ is the expression of AChR molecules and their transport to the postsynaptic membrane, followed by their membrane insertion and anchoring. It is well established that the motor neuron induces gene expression of AChRs and other synaptic molecules, but little is known about mechanism responsible for the focal insertion of AChR pentamers into the postsynaptic membrane, where AChRs are clustered in the small, well circumscribed synaptic region to very high density of >10.000 molecules per μm^2 as compared to 10 molecules extra-synaptically (Sanes and Lichtman, 2001).

Focal insertion of AChR molecules requires their directed transport towards the postsynapse and likely involves the cytoskeleton, which is universally responsible for intracellular transport processes, cell polarization, structural stability, morphological adaptation and cell division (Li and Gundersen, 2008). Despite an unquestioned biological necessity for a subsynaptic cytoskeletal network, little is known about potential roles of the dynamic cytoskeleton at the postsynaptic specialization or about molecular mechanisms, which could contribute to the establishment of such a network in myofibers. Since microtubules generally confer a major proportion of intracellular transport processes, in my thesis I was interested to study the organization and regulation of subsynaptic MTs at the NMJ junction.

The behavior, stability and interactions of MTs are largely influenced by +TIP proteins, a family of proteins binding to the highly dynamic plus-ends of MTs and mediating the binding and anchoring of MT to specific subcellular structures. In various organisms and cell types, binding of +TIP proteins to MTs is regulated by signaling molecules such as PI3K, RhoGTPases, integrins, and GSK3 in response to extracellular cues as for example growth factors, lysophosphatidic acid and migratory cues. MT-bound +TIPs enable the capture of MTs at cortical sites (Akhmanova and Steinmetz, 2008a; Galjart, 2005; Galjart, 2010; Gundersen, 2002; Gundersen et al., 2004).
I therefore studied if and how agrin as the main inducer of postsynaptic differentiation governs MT behavior at the postsynaptic muscle membrane via regulation of +TIP proteins. In addition, I was interested to study agrin induced biochemical signal transduction, which could underlie the creation of a sub-cellular environment, in which +TIP-mediated MT capture can occur.

III. Results - Overview

In summary, the goal of my thesis was to investigate the molecular mechanisms underlying the induction of a subsynaptic MT network in myofibers at the mammalian neuromuscular junction *in vivo* and at acetylcholine receptors clusters in cultured myotubes *in vitro* by regulation of +TIP proteins and microtubule capture. I was also interested to find out how a subsynaptic MT network influences AChR insertion and clustering at the postsynaptic muscle membrane.

- **Part I - Manuscript I:** "Agrin regulates CLASP2-mediated capture of microtubules at the neuromuscular junction synaptic membrane"
  Schmidt N., Basu S.*, Sladecek S., Gatti S., van Haren J., Treves S., Pielage J., Galjart N. & Brenner H.-R.*

- **Part II - Manuscript II:** "Agrin-induced microtubule capture at the NMJ is mediated by GSK3β-dependent binding of CLASP2 to MT plus-ends interacting with LL5β"
  Sladecek S., Basu S.* & Brenner H.-R.*

During my thesis, I showed that a dense intracellular MT network, some of which is stabilized by post-translational modifications, surrounds the postsynaptic specialization of the mammalian NMJ. Selective microtubule capture at the postsynaptic muscle membrane *in vivo* and at AChR clusters *in vitro* occurs after agrin-induced activation of PI3K and local inactivation of GSK3β, which creates a pool of hypophosphorylated CLASP2 (and probably other +TIP) molecules, available to decorate growing MT plus-ends. In the absence of *Clasp2*, MT capture at the subsynaptic muscle membrane, AChR cluster size and density and number of synaptic myonuclei are reduced *in vivo*. In cultured myotubes, deficiency of *Clasp2* or pharmacologic inhibition of its upstream activator PI3K reduce MT capture at AChR clusters and AChR cluster size. Thus, in close collaboration with my colleagues, I established an

agrin-induced biochemical signal cascade, which regulates CLASP2-mediated MT capture at the subsynaptic muscle membrane and demonstrated its functional relevance for AChR insertion and clustering (Manuscript I – Section III.1.).

In a next step, I was interested to elucidate underlying molecular mechanism in more detail by investigating the function of membranous CLASP2 interactors and the role of CLASP2 phosphorylation in the process of MT capture. I could demonstrate that agrin-induced PI3K activity recruits LL5β to AChR clusters in cultured myotubes, which enables synaptic capture of CLASP2-decorated MT. Reduction of LL5β proteins levels via RNAi, constitutive activity of the CLASP2 kinase GSK3β or mutational pseudo-phosphorylation of CLASP2 interfere with CLASP2-mediated MT capture at agrin-induced AChR clusters in myotubes and consequently reduce AChR cluster size (Manuscript II – Section III.2.).

III.1. Manuscript I

"Agrin regulates CLASP2-mediated capture of microtubules at the neuromuscular junction synaptic membrane"

Schmidt N.[,1], Basu S.[*,1], Sladecek S.[1], Gatti S.[1], van Haren J.[2], Treves S.[3,4], Pielage J.[5], Galjart N.[2] & Brenner H.-R.[1]*

[1]Department of Biomedicine, Institute of Physiology, University of Basel, CH-4056 Basel, Switzerland
[2]Department of Cell Biology, Erasmus Medical Center, 3015 GE Rotterdam, Netherlands
[3]Department of Anesthesia and [4]Department of Biomedicine, Basel University Hospital, CH-4031 Basel, Switzerland
[5]Friedrich Miescher Institute for Biomedical Research, CH-4058 Basel, Switzerland
*equal contribution

Contribution to this manuscript: For this publication, I was involved in experimental design, conduction and analysis. I contributed the following figures: 1a, 1b, 2d, 5a, 5c, 5d and all supplementary figures.

Status of Publication: published on July 30, 2012 in the *Journal of Cell Biology*

THE JOURNAL OF CELL BIOLOGY

Published July 30, 2012

This article has original data in the JCB Data Viewer
http://jcb-dataviewer.rupress.org/jcb/browse/5556

JCB: Article

Agrin regulates CLASP2-mediated capture of microtubules at the neuromuscular junction synaptic membrane

Nadine Schmidt,[1] Sreya Basu,[1] Stefan Sladecek,[1] Sabrina Gatti,[1] Jeffrey van Haren,[2] Susan Treves,[3,4] Jan Pielage,[5] Niels Galjart,[2] and Hans Rudolf Brenner[1]

[1]Department of Biomedicine, Institute of Physiology, University of Basel, CH-4056 Basel, Switzerland
[2]Department of Cell Biology, Erasmus Medical Center, 3015 GE Rotterdam, Netherlands
[3]Department of Anesthesia and [4]Department of Biomedicine, Basel University Hospital, CH-4031 Basel, Switzerland
[5]Friedrich Miescher Institute for Biomedical Research, CH-4058 Basel, Switzerland

Agrin is the major factor mediating the neuronal regulation of postsynaptic structures at the vertebrate neuromuscular junction, but the details of how it orchestrates this unique three-dimensional structure remain unknown. Here, we show that agrin induces the formation of the dense network of microtubules in the subsynaptic cytoplasm and that this, in turn, regulates acetylcholine receptor insertion into the postsynaptic membrane. Agrin acted in part by locally activating phosphatidylinositol 3-kinase and inactivating GSK3β, which led to the local capturing of dynamic microtubules at agrin-induced acetylcholine receptor (AChR) clusters, mediated to a large extent by the microtubule plus-end tracking proteins CLASP2 and CLIP-170. Indeed, in the absence of CLASP2, microtubule plus ends at the subsynaptic muscle membrane, the density of synaptic AChRs, the size of AChR clusters, and the numbers of subsynaptic muscle nuclei with their selective gene expression programs were all reduced. Thus, the cascade linking agrin to CLASP2-mediated microtubule capturing at the synaptic membrane is essential for the maintenance of a normal neuromuscular phenotype.

Introduction

The function of the dynamic cytoskeleton in synapse formation and maintenance is poorly understood. At the neuromuscular junction (NMJ) the array of synaptic proteins such as the acetylcholine receptors (AChRs) is determined by the specific set of genes induced by the nerve selectively in the muscle nuclei underlying the synapse. However, although the nerve-induced synaptic gene expression program can explain the set of proteins expressed in the synaptic region, it does not account for their focal insertion into the postsynaptic muscle membrane where the density of, e.g., AChRs declines sharply from ~10,000/μm^2 to <5/μm^2 within a few micrometers of muscle fiber length. One possibility is a focal transport involving microtubules (MTs) oriented toward and captured at the subsynaptic muscle membrane. Indeed, the NMJ is associated with dense, subsynaptic networks of cortical actin filaments and microtubules (Jasmin et al., 1990; Ralston et al., 1999). Actin filaments are thought to be involved in anchoring AChRs along with other proteins that play a part in NMJ formation and maintenance (Dai et al., 2000; Borges and Ferns 2001), and they may be involved in MT capturing. However, the generation of the subsynaptic actin networks has not been investigated. Likewise, it is not known how MTs are organized, and whether and how they are involved in the formation of the postsynaptic membrane.

The behavior of MTs and their interactions with other intracellular components are largely regulated by MT plus-end tracking proteins (+TIPs), which specifically associate with the growing, or "plus" ends of the MTs (Galjart 2010). In motile fibroblasts, a paradigm for studying MT behavior in cultured cells (Akhmanova et al., 2001), a subset of MTs is oriented toward the leading edge and becomes selectively stabilized

N. Schmidt and S. Basu contributed equally to this paper.

Correspondence to Hans Rudolf Brenner: Hans-Rudolf.Brenner@unibas.ch; or Niels Galjart: n.galjart@erasmusmc.nl

Abbreviations used in this paper: AChR; acetylcholine receptor; GSK3, glycogen synthase kinase-3; MT, microtubule; NMJ, neuromuscular junction; PI3-K, phosphatidylinositol 3-kinase; +TIP, plus-end tracking protein.

Supplemental Material can be found at:
http://jcb.rupress.org/content/suppl/2012/07/26/jcb.201111130.DC1.html
Original image data can be found at:
http://jcb-dataviewer.rupress.org/jcb/browse/5556

The Rockefeller University Press $30.00
J. Cell Biol. Vol. 198 No. 3 421–437
www.jcb.org/cgi/doi/10.1083/jcb.201111130

(Bulinski and Gundersen 1991). Posttranslational modifications on lattice-incorporated tubulin subunits, such as de-tyrosination or acetylation, accumulate on stable MTs, allowing their recognition with specific antibodies (Bulinski and Gundersen 1991). Specific signaling pathways that are activated at the leading edge mobilize downstream effectors to recruit stable leading edge–oriented MTs. Signaling molecules include lysophosphatidic acid (LPA), which triggers a pathway dependent on the Rho-GTPase and the formin mDia (Gundersen et al., 2004), and phosphatidylinositol 3-kinase (PI3-K) acting via glycogen synthase kinase-3 (GSK3; Akhmanova et al., 2001). Several +TIPs have been implicated in selective MT capturing and stabilization, including APC, ACF7, CLIP-170, and CLASP2 (Galjart 2010). Although CLASPs were discovered (and named) through their interaction with CLIP-115 and -170, the functional significance of this interaction is still unknown, and its in vivo relevance has not yet been described.

The major factor mediating the neural regulation of postsynaptic membrane assembly at the vertebrate NMJ is agrin, a heparansulfate proteoglycan secreted from motor nerve terminals and acting through its receptor/effector, LRP4/MuSK (muscle-specific kinase; Kim et al., 2008; Zhang et al., 2008; Wu et al., 2010), in the muscle fiber membrane. Agrin on its own is sufficient to induce differentiation of functional synaptic membranes in vivo in the absence of motor nerves (Jones et al., 1997). This major organizing function makes agrin-induced AChR clustering in cultured myotubes an ideal system in which to analyze how the subsynaptic MTs come to be organized and to elucidate their roles in synapse formation in vivo.

Here, we present evidence for a novel signaling pathway downstream of agrin that allows dynamic MTs probing the interior of the muscle fiber membrane to become immobilized and captured at the synaptic membrane. Specifically, in both adult muscle and cultured myotubes, agrin triggers the activation of PI3-K, leading to the phosphorylation of GSK3β at the subsynaptic muscle membrane. This serves to cause the local capture of the plus ends of dynamic MTs at the synaptic, but not at the extrasynaptic membrane via a process involving CLASP2 and CLIP-170. Agrin/CLASP2/CLIP-170–mediated MT capturing in turn directs the focal AChR insertion into the synaptic membrane. Our data reveal, for the first time, the in vivo relevance of a CLIP-170–CLASP2 interaction in this process.

Results

The nerve terminal and agrin induce a subsynaptic network of MTs oriented toward the subsynaptic membrane

The subsynaptic muscle membrane is associated with a dense network of MTs as visualized by immunofluorescent labeling of dynamic MTs (or Tyr-tubulin; Fig. 1 a) and total MTs (or β-tubulin; Fig. 1 b). Labeling of de-tyrosinated tubulin (or Glu-tubulin) reveals an even higher enrichment of a subpopulation of stable subsynaptic MTs (Fig. 1 b). These data suggest that MTs are enriched and specifically stabilized near the NMJ and suggest the involvement of specific +TIPs in this process.

Subsynaptic MT induction can be mediated by agrin in vivo. Specifically, agrin secreted from muscle fibers upon intracellular injection of expression plasmid into nonsynaptic regions of innervated muscle fibers (Jones et al., 1997) induces ectopic AChR clusters, which have a MT network associated with them similar to that observed in vivo (Fig. 1 c). This suggests that the nerve normally induces the subsynaptic MTs, at least in part, by the secretion of agrin.

To examine the orientation of subsynaptic MTs at the NMJ, muscle fibers of knock-in mice expressing GFP-tagged CLIP-170 (Akhmanova et al., 2005) at the plus ends of the MTs were fixed in a way that preserves dynamic MTs (see Materials and methods). Labeling with an antibody against GFP showed CLIP-170 enriched at synaptic AChR clusters (Fig. 1 d). 3D reconstruction of NMJs from confocal image stacks showed that the plus ends of the MTs were preferentially colocalized with the synaptic AChR cluster. In contrast, in many instances they were completely absent from the synaptic gutter containing the nerve terminal (Fig. 1 d). These findings indicate that the plus ends of MTs probing the interior of the cell cortex become preferentially associated with synaptic AChR clusters.

In cultured cells, MT stabilization is promoted by several +TIPs, including CLASP2, which are directly or indirectly linked to the actin network (Galjart 2010). Cortical actin is highly enriched at the NMJ (Dai et al., 2000; Bruneau et al., 2008), and is thought to be involved in the anchoring of the AChRs in the subsynaptic muscle membrane. Immunolabeling of CLASP2 suggested that it was organized in a pattern similar to that of CLIP-170, with an enrichment at the crests of the synaptic folds (i.e., between troughs marked by AChR-rich lines [Fig. 2 a], as well as along the edge of the AChR cluster [Fig. 2 c]). Interestingly, the AChR cluster edge is where new AChRs are inserted into the synaptic membrane of developing NMJs (Kummer et al., 2004). Imaging NMJs after 3 d of denervation, i.e., when nerve terminals were degenerated, produced similar results (not depicted). Thus, CLIP-170 and CLASP2 immunoreactivities were postsynaptic.

Double stainings of CLIP-170 and CLASP2 at the synapse revealed significant colocalization of these proteins at the NMJ (Fig. 2 b), indicating that subsynaptic MT ends contain both +TIPs. However, MT capture and stabilization can still occur in the absence of either of these proteins as indicated by the synaptic MT networks at *Clasp2*$^{-/-}$ (Fig. 2 d) and at *Clip1*$^{-/-}$;*Clip2*$^{-/-}$ NMJs (not depicted) visualized by Tyr-tubulin and Glu-tubulin stainings. Although no impairment of stable synaptic MTs could be resolved by tubulin stainings in either of these mutants due to variable staining conditions, MT capture as revealed by CLIP-170 staining was reduced by the deletion of CLASP2 (see Fig. 4). Taken together, these findings suggest that agrin/MuSK triggers downstream signals that capture MTs at synaptic AChR clusters by a process that includes CLIP-170 and CLASP2, and that this, in turn, promotes the insertion of AChRs into the synaptic membrane.

NMJs are impaired in Clasp2$^{-/-}$ mice

To test this hypothesis, we investigated NMJs in mice in which CLASP2 had been genetically deleted. The phenotype of NMJs in adult *Clasp2*$^{-/-}$ mice was abnormal in several ways.

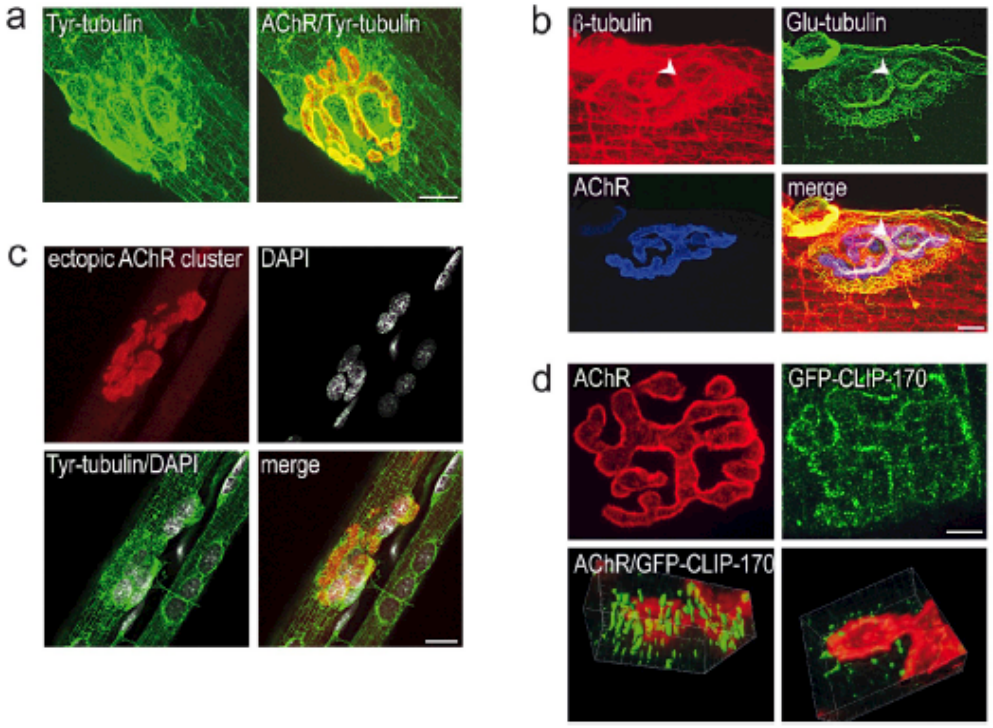

Figure 1. **The subsynaptic network of MTs at the neuromuscular junction is induced by agrin.** (a) NMJ in mouse sternomastoid muscle labeled for AChRs (red) and for Tyr-tubulin (green) reveals subsynaptic network of MTs. Bar, 10 µm. (b) MTs at the NMJ are posttranslationally modified by de-tyrosination. Labeling for β-tubulin, Glu-tubulin, and AChRs reveals synaptic and nonsynaptic MTs (red), selective de-tyrosination of subsynaptic MTs (green), and AChRs (blue). Note MTs are also present in presynaptic nerve terminal branches (arrowheads). Bar, 10 µm. (c) Network of MTs (tyr-tubulin, green) is present at nerve-free, ectopic postsynaptic membranes (marked by accumulation of AChRs [red]) induced by ectopic application of recombinant neural agrin to nonsynaptic region of adult muscle fiber. Note the accumulation of muscle nuclei, revealed by the surrounding MTs, at same site. Bar, 20 µm. (d) Tips of growing MTs are enriched at synaptic AChR clusters in epitrochleo-anconeus (ETA) muscle from *GFP-Clip-170*$^{tg/tg}$ mutant mouse. Top: en-face view of NMJ marked by AChRs (red). MT plus-ends are stained with anti-GFP antibody. Bar, 5 µm. Bottom: part of a synaptic AChR cluster (red) stained for CLIP-170 with anti-GFP antibody (green) and reconstructed in 3D from a stack of confocal images. Left, view from muscle side of AChR cluster; note the MT plus-ends approaching the synaptic AChR cluster from below the postsynaptic membrane. Right, view from presynaptic side of same AChR cluster; note absence of MT tips from primary synaptic gutter where nerve terminal was located (not stained).

Specifically, when compared with size-matched wild-type mice with similar muscle fiber diameters, the area of synaptic AChR clusters, the numbers of subsynaptic nuclei, and the density of synaptic AChRs were all reduced to ~75% of control (Fig. 3, a and b), resulting in a decline of synaptic AChR number to <60% (0.75 × 0.75). Strikingly, the rate at which AChRs were replaced was also reduced in NMJs (Fig. 3 b), suggesting a role for CLASP2 in the accumulation of this important receptor, akin to its function in polarized vesicle trafficking in motile cells (Miller et al., 2009). Although the defects in the structure of NMJs in *Clasp2*$^{-/-}$ mice would be expected to lower the safety factor for neuromuscular impulse transmission, this effect was not great enough to precipitate impairment of impulse transmission as judged from the animal's gross motor behavior.

These data indicate that CLASP2 contributes to normal synaptic function in multiple ways: by increasing synaptic AChR density through delivery of AChRs to the synaptic membrane; by increasing synaptic area and, by inference, increased quantal content of the endplate potential; and through the recruitment of subsynaptic nuclei which, through their muscle activity–resistant expression of AChR subunit and other synaptic genes, contribute to the maintenance of the NMJ.

If both CLASP2 and CLIP-170 are involved in subsynaptic MT capturing, as is also suggested by their colocalization at the NMJ (Fig. 2 b), one would expect a similar NMJ phenotype in mice lacking CLIP-170 as in the CLASP2-deficient mice. We therefore measured synaptic AChR density in CLIP-115/170–deficient mice, and found a reduction to ~80% of control (Fig. 3 c), similar to what we observed in the *Clasp2* knockouts. These results suggest that the CLASP2–CLIP-170 interaction that was documented in vitro serves to regulate synaptic function in vivo.

CLASP2 promotes attachment of MT plus-ends to synaptic membranes of mature NMJs

To test for a role of CLASP2 in MT stabilization at the NMJ, we compared the localization of MT plus-ends as visualized by

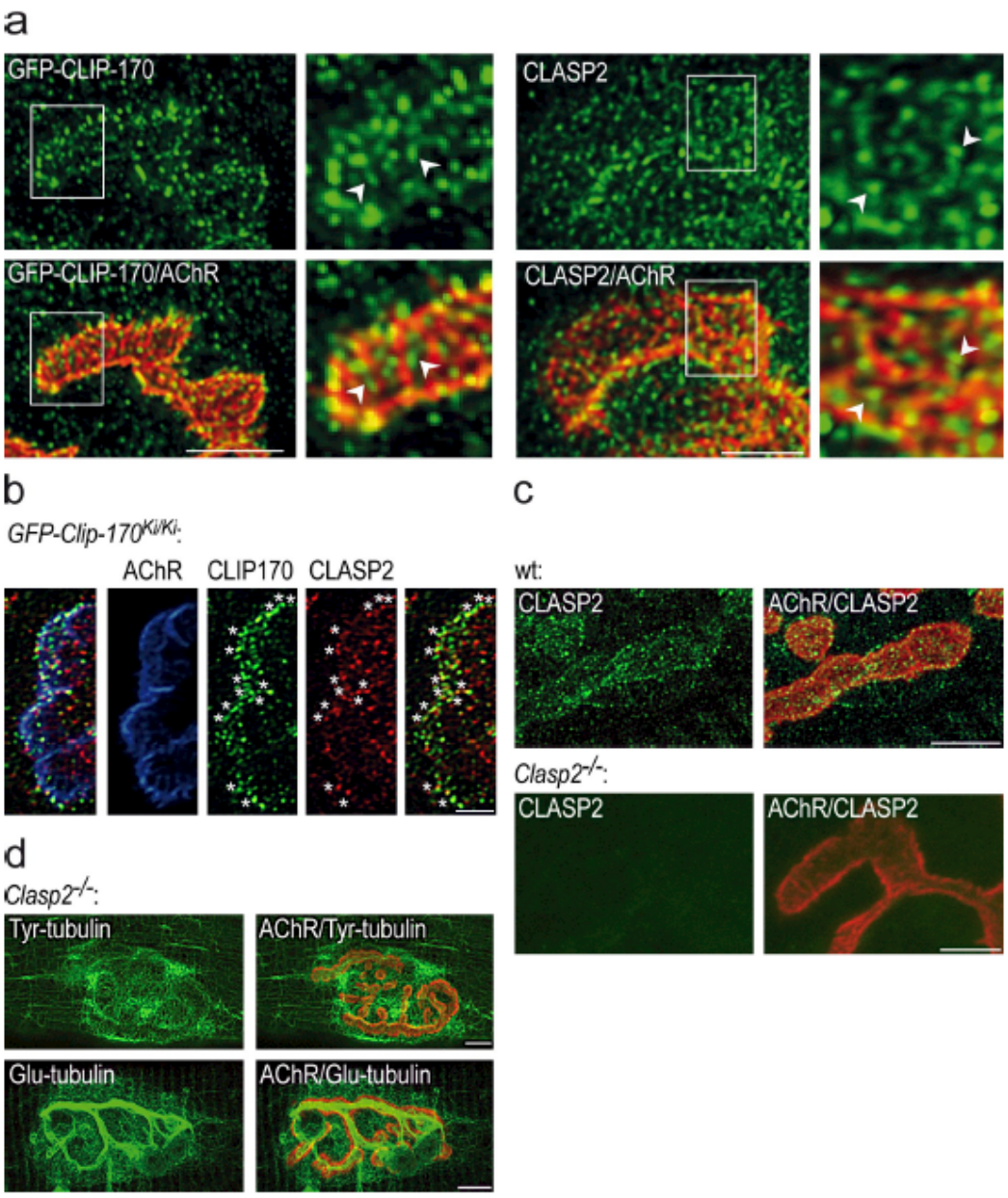

Figure 2. **Synaptic localization of CLASP2, Tyr-tubulin, and Glu-tubulin in wt and *Clasp2*$^{-/-}$ NMJs.** (a) Staining of CLIP-170 and CLASP2 at NMJ of wild-type muscle. Like CLIP-170 (left, green), CLASP2-decorated MT plus-ends (right, green) are enriched at synaptic AChR clusters primarily at their edges and at the crests of synaptic folds (arrowheads; troughs of folds marked by the AChRs). Bar, 5 µm. Note that images in panel a are from the level of the synaptic folds, i.e., deeper in the synaptic gutter; in contrast, maximum intensity projections from optical slices taken at the level of the edge of the synaptic AChR cluster and thus of the synaptic gutter (such as in Fig. 1 d, top images) reveal pronounced CLIP-170 enrichment compared with adjacent perisynaptic membrane. This explains the apparent difference in CLIP-170 intensity along the edge of the clusters in the two images (Fig. 2 a vs. 1 d). (b) Double staining of CLIP-170 and CLASP2 at NMJ of wild-type muscle. Accumulation of both +TIPs at edge of synaptic AChR cluster (blue) and overlap of the two +TIPs (marked by asterisks) is consistent with cooperation between CLIP-170 and CLASP2 at MT plus-ends. Note that some of the CLIP-170 and CLASP2 staining does not overlap, which may reflect differences in antibody accessibility and staining, or, alternatively, independent functions of these proteins in the NMJ. For localization of CLIP-170 in *Clasp2*$^{-/-}$ NMJ, see Fig. 4. Bar, 2.5 µm. (c) Top: CLASP2 is enriched at edge of synaptic AChR cluster at wild-type NMJ. Bottom: absence of CLASP2 staining of NMJ from *Clasp2*$^{-/-}$ muscle shows specificity of antibody used. Bars, 5 µm. (d) Both Tyr-tubulin (top) and Glu-tubulin (bottom) are enriched at NMJs of *Clasp2*$^{-/-}$ muscle. Bars, 10 µm.

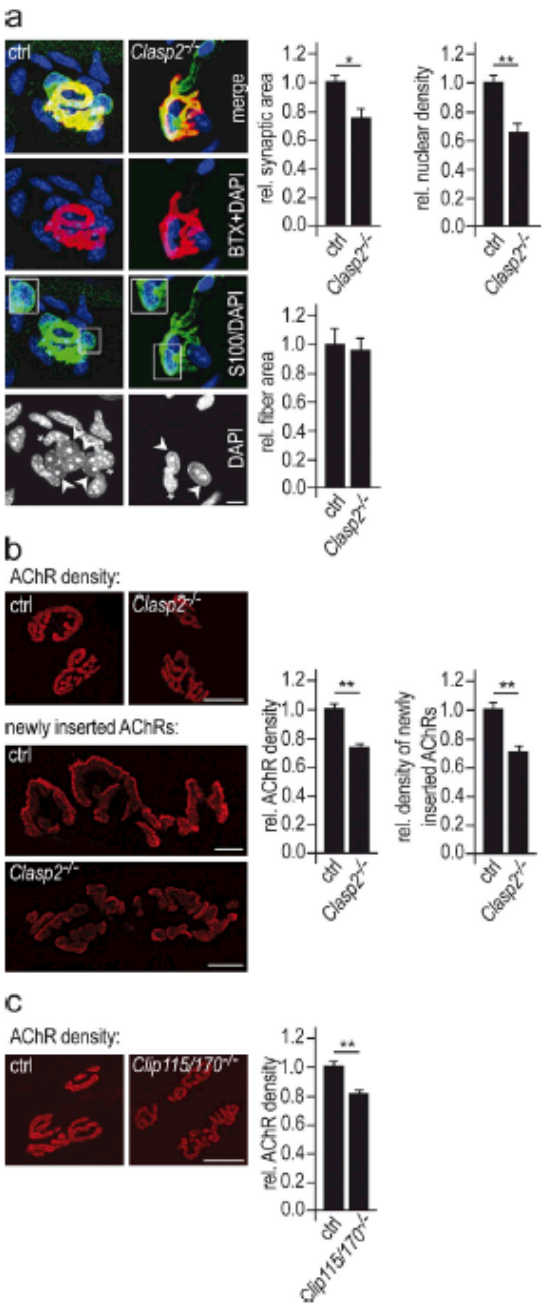

Figure 3. **Genetic deletion of CLASP2 impairs NMJs in vivo.** (a) The size of synaptic AChR clusters and the number of subsynaptic nuclei per synapse are reduced in *Clasp2*$^{-/-}$ muscle. NMJs in soleus muscles of wild-type and mutant animals of equal weights were stained for AChRs (red), the Schwann cell marker S-100 (green), and nuclei with DAPI (blue). Synaptic area was determined from AChR labeling of synapses lying en face (see Materials and methods). Nuclei surrounded by S-100 labeling were considered as terminal Schwann cells (see inset in panel labeled S100/DAPI). The number of subsynaptic muscle nuclei was estimated by subtracting the number of Schwann cell nuclei (marked by asterisks) from the number of nuclei underlying the AChR cluster (marked by arrowheads). Bar, 10 µm. Graphs show mean values of respective parameters ± SEM, $n = 47$ wild-type and 52 *Clasp2*$^{-/-}$ NMJs from 3 muscles of each genotype analyzed (*, $P < 0.05$; **, $P < 0.01$, two-sided *t* test). (b) AChR density and AChR insertion rates are reduced in *Clasp2*$^{-/-}$ muscle. To determine AChR densities sternomastoid muscles were saturated with α-BTX–Alexa 594. Bar, 25 µm. Means ± SEM, $n = 63$ and 72 NMJs from 3 wild-type and 3 *Clasp2*$^{-/-}$ muscles analyzed (*, $P < 0.05$; **, $P < 0.01$, two-sided *t* test). To estimate AChR insertion rates sternomastoid muscles were denervated to increase AChR turnover; 7 d later AChRs in superficial endplates were saturated in vivo with α-BTX–Alexa 488. After another 7 d (to allow AChR turnover), endplates were saturated with α-BTX–Alexa 594, and the average intensity of Alexa 488 fluorescence in *Clasp2*$^{-/-}$ NMJs was normalized to that in wild-type muscles. Bar, 25 µm. Means ± SEM, 28 wild-type and 25 *Clasp2*$^{-/-}$ endplates analyzed (*, $P < 0.05$; **, $P < 0.01$, two-sided *t* test). (c) AChR density is reduced in *Clip1*$^{-/-}$;*Clip2*$^{-/-}$ muscle. Analysis similar as in b. Given are means ± SEM, $n = 30$ wild-type and 31 *Clip1*$^{-/-}$;*Clip2*$^{-/-}$ (*, $P < 0.05$; **, $P < 0.01$, two-sided *t* test). Bar, 25 µm.

CLIP-170 labeling in wild-type and in *Clasp2*$^{-/-}$ mice. As described above, CLIP-170 was prominent at the edges of the synaptic AChR clusters at wild-type NMJs but was also present throughout the postsynaptic membrane in the primary synaptic fold. In *Clasp2*$^{-/-}$ mice the synaptic localization of CLIP-170 was reduced. This was most readily seen from the decrease of CLIP-170 immunoreactivity along the edges of the synaptic AChR clusters (Fig. 4 a).

Because the resolution of confocal microscopy is limited, in particular in the z-direction, some synapses were imaged by using structured illumination microscopy, which increases resolution both in x-y and in z-directions by a factor of 2 compared with conventional confocal microscopy (Gustafsson et al., 2008). In individual optical slices taken through synaptic AChR clusters oriented en face, AChR labeling appeared as contour lines following the synaptic membrane at that respective z-level. In wild-type animals, puncta of CLIP-170 immunoreactivity precisely followed these lines. This indicates that in wild-type mice the plus ends of the MTs were present exactly, within the limit of z-resolution, at the level of the synaptic membrane. In contrast, at *Clasp2*$^{-/-}$ synapses CLIP-170 puncta were largely absent from the AChR contour lines (Fig. 4 b). Thus, in the absence of CLASP2, the incidence of MT plus-ends at the level of the AChRs was markedly reduced. This observation implicates CLASP2 in the capturing of CLIP-170–labeled MT ends (and thus of MTs) at the agrin-induced AChR cluster.

Agrin phosphorylates GSK3β through PI3-K

Next we examined how agrin regulates CLASP2-mediated MT capturing. At the leading edge of motile fibroblasts CLASP2-mediated MT capturing is regulated by phosphatidylinositol 3-kinase (PI3-K) and glycogen synthase kinase-3 β (GSK3β; Akhmanova et al., 2001). In many instances, PI3-K activates AKT through its recruitment to inositol lipids and subsequent phosphorylation by PDK-1; AKT in turn phosphorylates GSK3β, which is active by default but is rendered inactive by phosphorylation on Serine 9 (Ser9). The inactivation of GSK3β triggered by PI3-K prevents phosphorylation of CLASP2 and, as a consequence, enhances its affinity to MT plus-ends (Akhmanova et al., 2005; Kumar et al., 2009; Watanabe et al., 2009). Blockade of

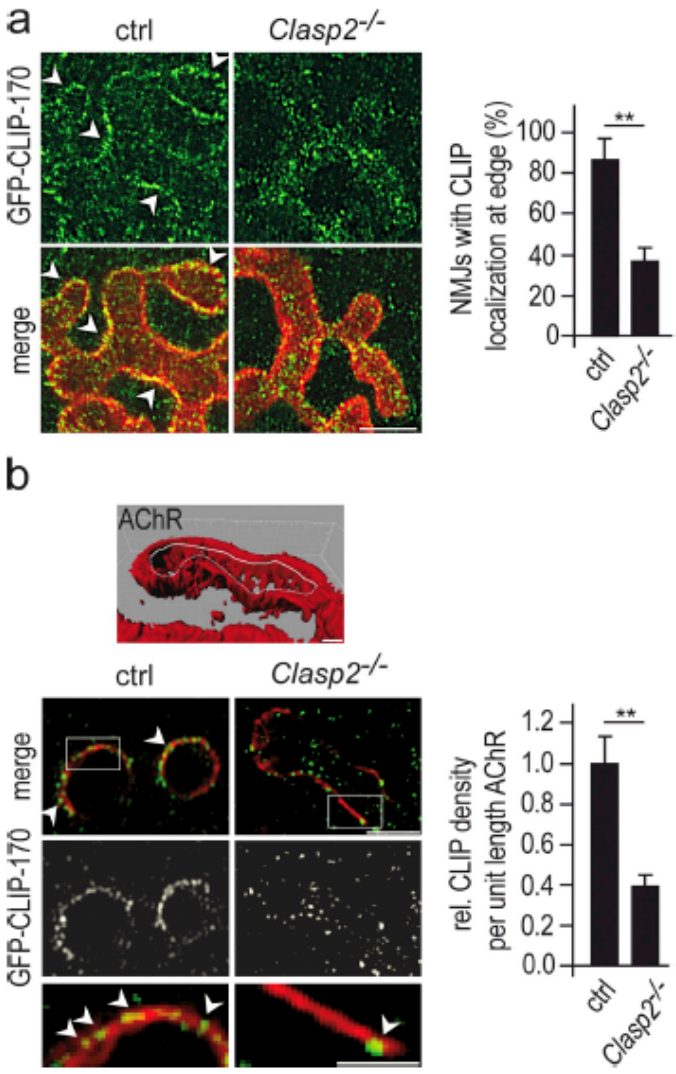

Figure 4. **Absence of CLASP2 reduces the density of GFP-CLIP-170–decorated MTs at the synaptic membrane of the NMJ in vivo.** (a) The localization of MT plus-ends (visualized by GFP labeling) at synaptic AChR clusters is reduced in *Clasp2*$^{-/-}$*;GFP-Clip170*$^{kI/kI}$ myotubes. Bar, 5 µm. Graph shows percentage of synapses with GFP-CLIP-170 enriched at the edge of the AChR cluster in wild-type and *Clasp2*$^{-/-}$ synapses (means ± SEM, n = 13 wild-type and 18 CLASP2$^{-/-}$ synapses from 3 muscles each (*, $P < 0.05$; **, $P < 0.01$, Mann Whitney U-Test). A synapse was classified "blindly" by visual inspection as enriched in CLIP-170 (arrowheads), when edges of AChR clusters were decorated with GFP puncta along >80% of their lengths. Note that further information on, e.g., number and intensity of CLIP dots cannot be extracted from these confocal images (for details, see Materials and methods). (b) Analysis by structured illumination microscopy (SIMELRYA S.1; Carl Zeiss) of the localization of GFP-CLIP-170–decorated MTs at the synaptic membrane (marked by AChRs) in wild-type and *Clasp2*$^{-/-}$*;GFP-Clip-170*$^{kI/kI}$ NMJs. NMJs stained for AChRs (red) and GFP (green). Bars, 1 µm, 3 µm, and 1.5 µm. Stacks of images of NMJs en face were taken through the entire depth of the synapse at 0.125-µm steps and processed. 10–20 µm of contour lines of AChRs (as the one illustrated by the white line in the 3D-reconstructed cluster in top panel) at each of three z-levels for each synapse were selected, and CLIP-170 puncta per length of contour line were counted (arrowheads). Bottom panels show sample AChR contour lines and CLIP-170 immunoreactivity, including enlarged insets. Graph shows combined data from three synapses each in wild-type and *Clasp2*$^{-/-}$ muscle (*, $P < 0.05$; **, $P < 0.01$, two-sided t test). Note the marked reduction in the density of CLIP-170 puncta on AChR contour lines in the absence of CLASP2.

PI3-K is known to inhibit agrin-induced AChR clustering in cultured myotubes (Nizhynska et al., 2007). We therefore tested the hypothesis that agrin, by activating PI3-K, induces phosphorylation of GSK3β at Ser9 (p-GSK3β).

To this end, C2C12 and primary wild-type myotubes were exposed to 5 nM of either agrin isoforms that are selectively expressed by motor neurons (neural agrin) or those expressed by nonneural tissues such as muscle. Of these, only neural agrin can induce synaptic membranes in muscle (Meier et al., 1998). Western blotting of lysates showed a pronounced but transient increase in both p-AKT and p-GSK3β within a few minutes in response selectively to neural, but not to nonneural agrin. Both AKT and GSK3β phosphorylation could be blocked by pretreating cells with PI3-K inhibitors (LY294002 or ZSTK474) or with AKT inhibitor (A6730; Fig. 5 a, left). Similar results were seen when myotubes were grown on a substrate impregnated with agrin, which more closely resembles physiological agrin presentation (Fig. 5 a, right; for full blots see Fig. S2). Thus agrin, by activating PI3-K and AKT, phosphorylates (i.e., inactivates) GSK3β in cultured myotubes.

We next examined whether activated PI3-K and p-GSK3β are present at the NMJ in vivo. PI3-K activity at NMJs was assessed by measuring relative synaptic GFP fluorescence levels in fibers electroporated with expression constructs encoding either a wild-type or a mutant fragment of Bruton's tyrosine kinase (BTK). Both constructs comprised a GFP tag coupled to the respective wild-type and mutant BTK pleckstrin homology domains, of which the wild type, but not the mutant, binds to PtdIns(3,4,5)P_3 formed by active PI3-K (Várnai et al., 1999). Fig. 5 b shows that the synaptic GFP fluorescence signal was greatly reduced when fibers expressed the mutant BTK-GFP construct, indicating that PI3-K is activated at the NMJ.

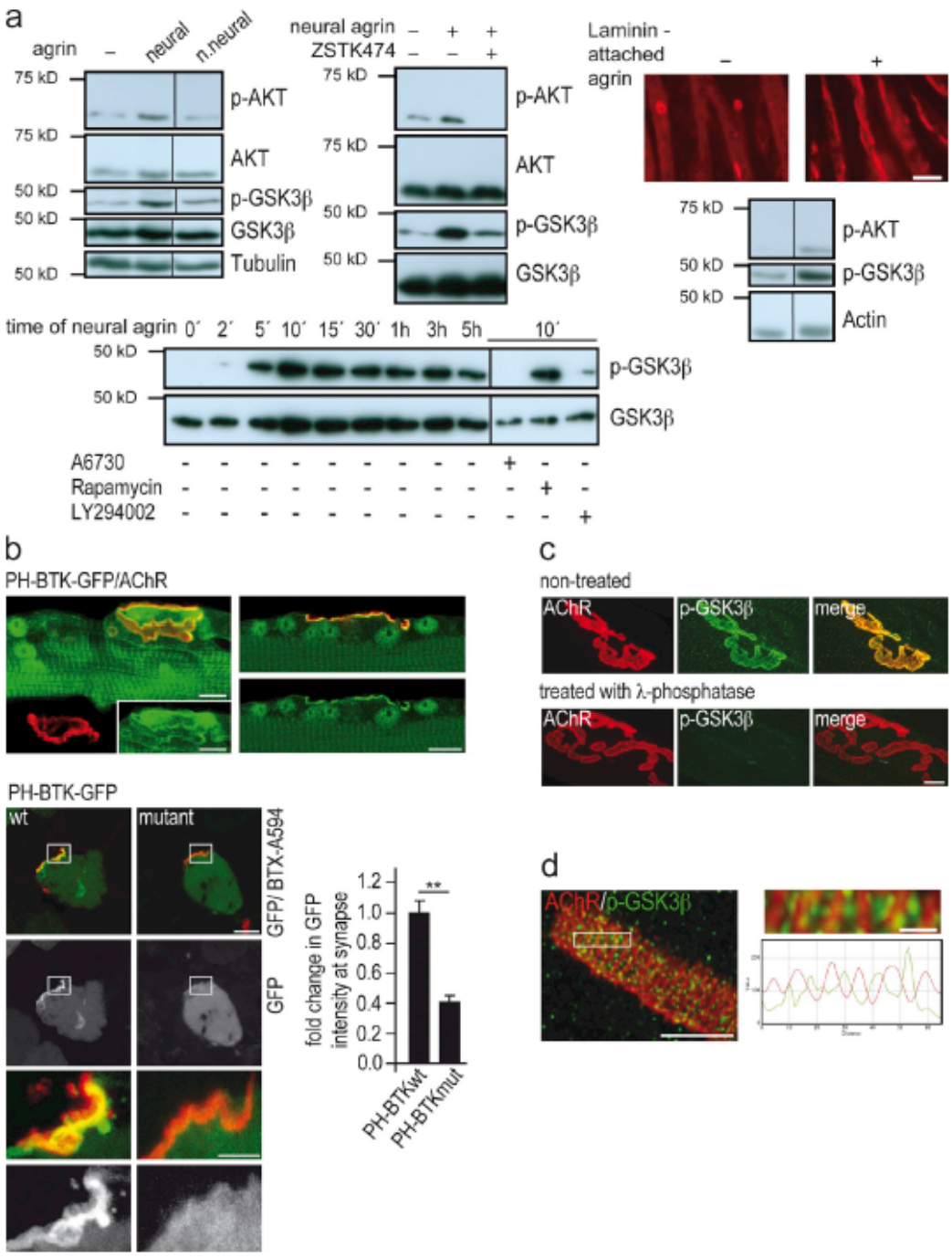

Figure 5. **Agrin phosphorylates PI3-K, AKT, and GSK3β in muscle cells.** (a) Neural, but not nonneural, agrin phosphorylates GSK3β via phosphorylation of PI3-K and AKT in cultured myotubes. Western blots of lysates from C2C12 myotubes to which soluble neural (5 nM) or nonneural (5 nM) agrin was added. Blots probed with antibodies as described in Materials and methods. Panels showing p-GSK3β and p-AKT are derived from same blot exposed for different times. Note that (1) AKT and GSK3β are not phosphorylated by nonneural agrin (top left panel, right lane); (2) their phosphorylation by neural agrin is inhibited by the PI3-K blocker LY294002 (50 μM), and the AKT inhibitor A6730 (0.5 μM, bottom left panel), respectively. Neural agrin also phosphorylates AKT and GSK3β when presented attached to culture substrate (top right panel, see Materials and methods). Full blots are shown in Fig. S1. Bar, 20 μm. (b) PI3-K is activated at the postsynaptic membrane of the NMJ. Soleus muscles of wild-type mice were electroporated with expression

Consistent with our hypothesis for the agrin-induced signaling cascade, we further observed by immunofluorescence that p-GSK3β was colocalized with the synaptic membrane of normal (Fig. 5 c; for specificity of the antibody used, see Fig. S2) and denervated NMJs (not depicted), excluding that the p-GSK3β immunoreactivity was presynaptic. p-GSK3β was not distributed evenly but appeared focally localized at the crests of the synaptic folds between the regions carrying the AChRs (Fig. 5 d), i.e., similar to CLIP-170 and CLASP2 (Fig. 2 a). When combined, these results indicate that agrin, by activating PI3-K, phosphorylates and thus inactivates GSK3β at the NMJ.

MTs are captured at agrin-induced AChR clusters by a process involving PI3-K and CLASP2

If agrin induces the trapping of plus ends of dynamic MTs at differentiating synaptic spots, it should be possible to visualize this in real time using GFP-tagged +TIPs. To mimic the stable presentation of agrin to the muscle at mature NMJs, we deposited neural agrin in small patches (20–60 µm in diameter) onto a laminin substrate. Myotubes that contact these agrin deposits form large AChR clusters that include stabilized AChRs and have associated with them a cluster of myonuclei that express the synapse-specific form of AChRs (Fig. 6 a; Jones et al., 1996). We therefore compared the dynamics of MTs in primary GFP-CLIP-170–expressing myotubes, inside and outside agrin-induced AChR clusters, using TIRF microscopy.

Analysis of individual frames of time-lapse movies (see Video 1) of wild-type myotubes suggested a much higher density of GFP-CLIP-170–labeled MT plus-ends inside the AChR clusters than outside (Fig. 6 b, center). However, maximum intensity projections (MIPs) of all 160 frames of the time-lapse imaging experiment showed that also outside the cluster many MT ends do reach the membrane (Fig. 6 b, right). The fact that inside the cluster the difference in MT plus-end density between single frames and MIPs is less pronounced than outside suggests that MT ends reaching the cell membrane inside the cluster are more likely to be captured than they are outside the cluster.

Analysis of changes in GFP-CLIP-170 labeling and distribution in distance versus time plots (so-called kymographs) revealed two types of behavior (Fig. 6 c). One type (here called type I) consisted of largely continuous movement of GFP-CLIP-170 "comets" during the time they remained within the penetration range of the evanescent wave. These comets had an average speed of 0.15 ± 0.01 µm/s (SEM, $n = 73$ tracks) and represent the continuous advance of the plus ends of growing MTs. In the other type of behavior (here called type II), the GFP-CLIP-170 fluorescence appeared stable over a period of 160 s or longer, with fluorescence flashing up at discrete spots along the track for tens of seconds before fading. Type II behavior suggests reduced freedom of GFP-CLIP-170 movement, and the capture of GFP-CLIP-170–labeled MT ends. Conspicuously, GFP-CLIP-170 dynamics was different inside and outside agrin-induced AChR clusters. Inside clusters, ∼75% of GFP-CLIP-170 tracks observed were of type II, and the remaining 25% of type I. In contrast, this ratio was reversed outside receptor clusters, where only 25% were of type II (Fig. 6 f).

As suggested above for adult NMJs, MT stabilization at agrin-induced AChR clusters in cultured myotubes was mediated by PI3-K activation and CLASP2. Specifically, when MT dynamics were examined in primary GFP-CLIP-170 myotubes treated with the PI3-K inhibitor ZSTK474 (Fig. 6 d), or in myotubes derived from *Clasp2*$^{-/-}$*;GFP-Clip-170*$^{kin/ki}$ (i.e., knockout/knock-in) mice (Fig. 6 e; see Video 2), type I and II comets were equally common in both cluster and noncluster regions (Fig. 6 f), suggesting nonspecific MT plus-end capturing both outside and inside the clusters. These experiments demonstrate that agrin enables the capture of CLIP-170–coated MT ends through a process requiring CLASP2, and that this process depends on PI3-K activation.

CLIP-170 is increased at plus ends of MTs in the proximity of agrin-induced AChR clusters

The GFP fluorescence of MT plus-ends imaged inside agrin-induced AChR clusters in control wild-type myotubes appeared brighter by eye than those in the same myotubes outside the AChR cluster. This difference could be due to MTs coming closer to the internal myotube membrane inside clusters than outside and/or to an increased load of CLIP-170 molecules on MT tips induced by agrin. To examine these possibilities, myotubes were labeled for CLIP-170 and EB3, a member of the EB1-family of "core" +TIPs that is expressed in myotubes (Fig. 7). Myotubes were then imaged by confocal microscopy, and the intensity of CLIP-170 fluorescence on MT plus-ends, identified by their EB3 immunoreactivity, was assayed inside and outside AChR clusters by line scans. At MT plus-ends inside AChR clusters in control myotubes the intensity of CLIP labeling was significantly higher than outside clusters, whereas EB3 was not changed (Fig. 7 a). This suggests that pathways activated by agrin increase the affinity of CLIP-170 for MT plus-ends.

Next, we examined whether the increase in CLIP-170 load was mediated through PI3K and CLASP2 by repeating the

constructs for PH-BTK or PH-BTKmut, i.e., pleckstrin homology domain fragments of Bruton tyrosine kinase, which specifically bind (PH-BTK-GFP) or do not bind (PH-BTK_R28C-GFP) to PIP_3, a read-out for PI3-K activity. Both constructs were tagged with eGFP (see Várnai et al., 1999; Bohnacker et al., 2009). Top: longitudinal confocal sections passing through NMJs of muscle fibers expressing elevated GFP (green) at synaptic AChR cluster (BTX594, red). Bars, 10 µm. Bottom: cross sections through fibers electroporated with the two constructs. Synaptic localization of PH-BTK-GFP is higher than that of PH-BTKmut-GFP, indicating synaptic PI3-K activity. Graph shows means ± SEM of fold change in GFP intensity at synaptic AChR clusters at 10–14 d after electroporation with PH-BTK or PH-BTKmut, respectively ($n = 20$ synapses on GFP-positive fibers per construct examined, *, $P < 0.05$; **, $P < 0.01$, two-sided *t* test). Bars, 7.5 µm and 3 µm. (c) P-GSK3β is enriched at the NMJ. Immunoreactivity is abolished by pretreatment of muscle with lambda-phosphatase. Bar, 10 µm. For specificity of antibody used, see Fig. S2. (d) High resolution confocal image of p-GSK3β immunoreactivity. GSK3β-(Ser9)P labeling was not distributed evenly. Rather, p-GSK3β labeling was preferentially located between the crests of the synaptic folds carrying the AChRs, as is the case for CLIP-170 and CLASP2 (Fig. 2 a). Enlarged inset and corresponding line profiles of AChR and GSK3β-P fluorescence are shown on the right. Bars, 3 µm and 0.5 µm.

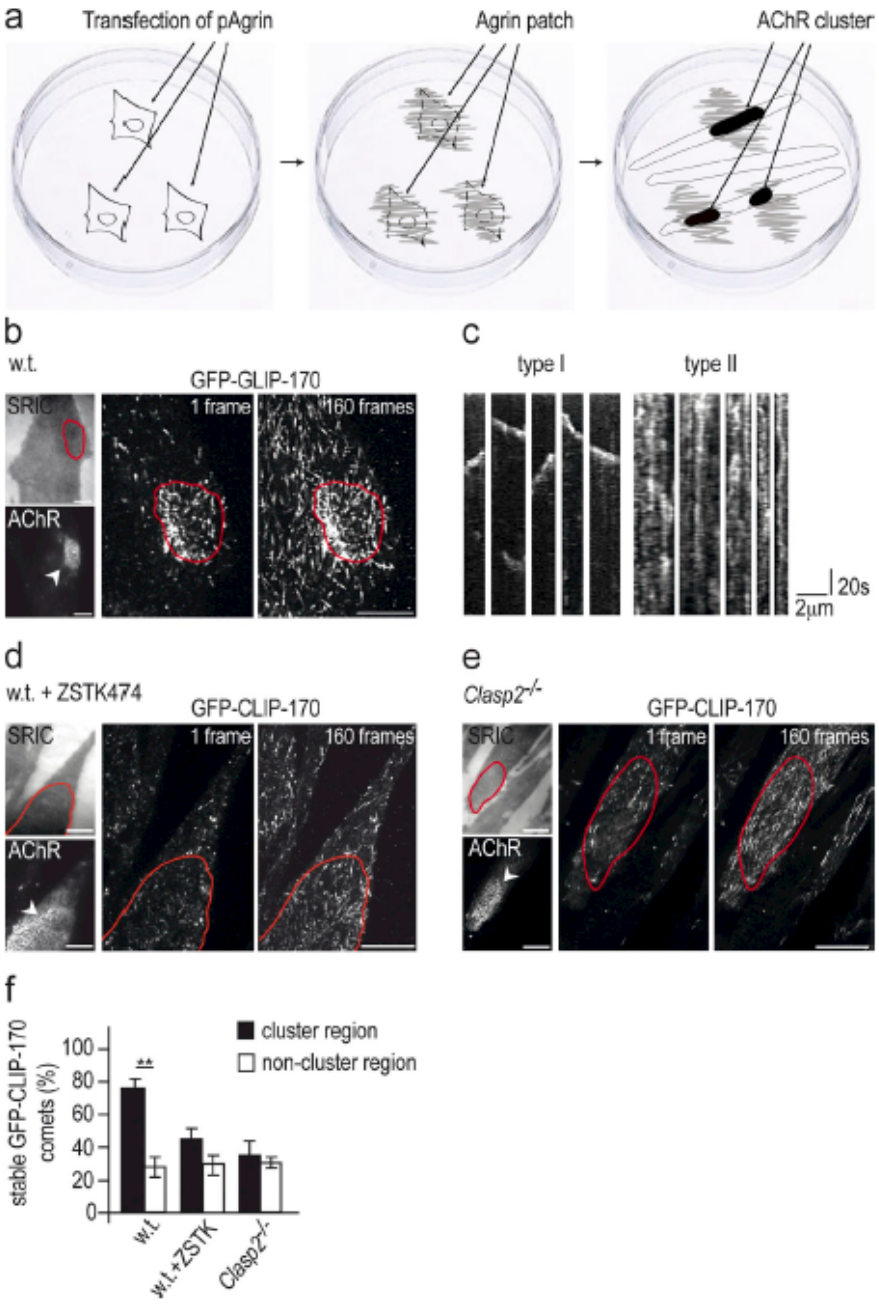

Figure 6. **Capturing of dynamic MTs at agrin-induced AChR clusters in cultured myotubes is abolished by pharmacological inhibition of PI3-K and by genetic elimination of *Clasp2*.** (a) Scheme illustrating focal impregnation of culture substrate with neural agrin. Transfected COS1 cells secrete and locally deposit neural agrin on a laminin substrate, and the cells are then lysed. Stable AChR clusters form where *GFP-Clip-170*$^{tg/tg}$ myotubes contact agrin deposits. (b) MT plus-ends decorated with GFP-CLIP-170 as observed by TIRF microscopy at 1-s intervals for 160 s. Shown are AChR cluster, surface reflective interference contrast (SRIC) image of same myotube, first frame and maximum intensity projection of all 160 images of the stack. Note higher density and brighter GFP signal at AChR cluster (marked in red). Bars, 10 µm. (c) Representative examples of kymograms of type I and type II comet behavior. See text for discussion of comet behavior and criteria for comet classification. (d) Same as in b, except that myotubes had been incubated for 90 min in ZSTK474 (5 µM) before GFP analysis. Note that "cluster"-specific comet behavior is abolished. Bars, 10 µm. (e) Same as in b, except that myotubes derived from *Clasp2*$^{-/-}$*;GFP-Clip-170*$^{tg/tg}$ mice were used. Note that "cluster"-specific comet behavior is abolished. Bars, 10 µm. (f) Quantification of comet behavior inside and outside agrin-induced AChR clusters. Comet immobilization by neural agrin is abolished by inhibition of PI3-K or the absence of CLASP2. Comets are grouped from kymograms into type I (mobile) and type II (stable) comets as described in the text, and the percentages of stable comets, both inside and outside agrin-induced AChR clusters, is given (means ± SEM, $n = 4$ myotubes for each condition; number of comets analyzed: wild type: 374; wild type, ZSTK474-treated: 342; *Clasp2*$^{-/-}$: 323; *, $P < 0.05$; **, $P < 0.01$, two-sided *t* test).

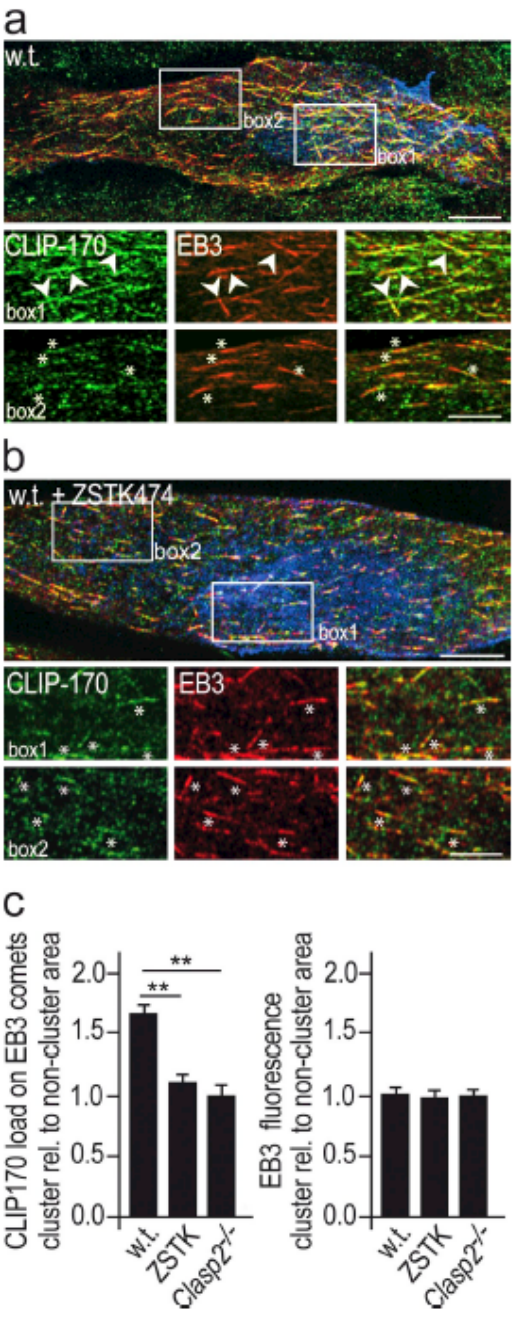

Figure 7. **The CLIP-170 load relative to EB3 at MT plus-ends is greater inside than outside AChR clusters and is reduced by PI3-K inhibition and by deletion of *Clasp2*.** (a) Comets in AChR clusters in *GFP-Clip-170$^{ki/ki}$* myotubes revealed by immunolabeling of EB3 and of GFP, to visualize CLIP-170. Regions outlined by boxes within and outside AChR cluster are shown enlarged at bottom. Agrin-induced AChR clusters in blue, GFP-CLIP-170 in green, EB3 in red. Note increased load of CLIP-170 at comets in AChR cluster (arrowheads) compared with comets outside cluster lacking increased CLIP-170 (asterisks). Bars: (top) 10 µm; (bottom) 5 µm. (b) Same as panel a but after blockade of PI3K with ZSTK474. Note reduction in CLIP-170 load in PI3-K–blocked compared with nonblocked myotubes. Bars: (top) 10 µm; (bottom) 5 µm. Asterisks same as in panel a. (c) Quantification of CLIP-170 staining on EB3-stained comets inside relative to that of comets outside AChR clusters. The elevated CLIP-170 load at agrin-induced AChR clusters observed in wild-type myotubes is abolished by PI3-K inhibition and by genetic deletion of *Clasp2*. EB3 staining is similar inside and outside AChR clusters. Percentages are means ± SEM from 84 to 245 comets analyzed in wild-type, ZSTK474-blocked, and *Clasp2*$^{-/-}$ myotubes (4 cells each). *, $P < 0.05$; **, $P < 0.01$, two-sided *t* test.

above experiment in wild-type myotubes treated with ZSTK474 (Fig. 7 b) and in *Clasp2*$^{-/-}$ mutant myotubes (not depicted). In both cases the enrichment of CLIP-170 was reduced to extrasynaptic levels (Fig. 7 c). Thus, in addition to CLASP2 deficiency, blockade of PI3-K inhibited CLIP-170 enrichment. These data strongly suggest that agrin leads to CLASP2-mediated MT capture and regulates the load of CLIP-170 at MT plus-ends, whereas EB3 remains unchanged; they provide further evidence for the in vivo relevance of a CLIP–CLASP interaction.

MTs are required for insertion of AChRs into agrin-induced AChR clusters in cultured myotubes in a manner dependent on PI3-K and CLASP2

Having found that CLASP2 deletion reduces the area and density of synaptic AChR clusters at NMJs in vivo, we examined the role of MT capturing in the maintenance of agrin-induced AChR clusters in cultured myotubes. In a first set of experiments, we asked whether MT integrity was essential for the maintenance of agrin-induced AChR clustering. Myotubes were treated with 10 µM nocodazole for 3 h, sufficient to depolymerize most MTs. At the end of the drug treatment, the AChR clusters were labeled with α-BTX, and their area measured. The clusters of AChR in nocodazole-treated myotubes were markedly (60%) smaller than those in untreated myotubes (Fig. 8 a). The density of AChRs was, however, unchanged. These data indicate that the number of AChRs in the clusters was decreased by nocodazole.

This decrease might occur through reduced AChR insertion into, or accelerated AChR removal from, the clusters. To distinguish between these possibilities the experiment was repeated, but with AChR clusters stained at the beginning of the drug incubation period. With this protocol, AChR cluster size was similar in control and in nocodazole-treated myotubes (Fig. 8 b). Thus, once AChRs had been inserted into the cluster, their removal was not affected by nocodazole. These experiments thus demonstrate that nocodazole reduces AChR cluster size by impairment of AChR insertion, and further, that in these experiments, measuring AChR cluster size can be used to differentiate between AChR insertion and removal.

Finally, we tested the effects of inhibitors of PI3-K, AKT, and GSK3β, on AChR insertion. Using the criteria just described, inhibition of PI3-K and AKT decreased and inhibition of GSK3β increased AChR insertion into AChR clusters (Fig. 8 a). Likewise, genetic deletion of *Clasp2* (using *Clasp2*$^{-/-}$ myotubes) reduced AChR insertion (Fig. 8 c). In these *Clasp2*$^{-/-}$ myotubes, in contrast to wild-type myotubes, inhibition of PI3-K

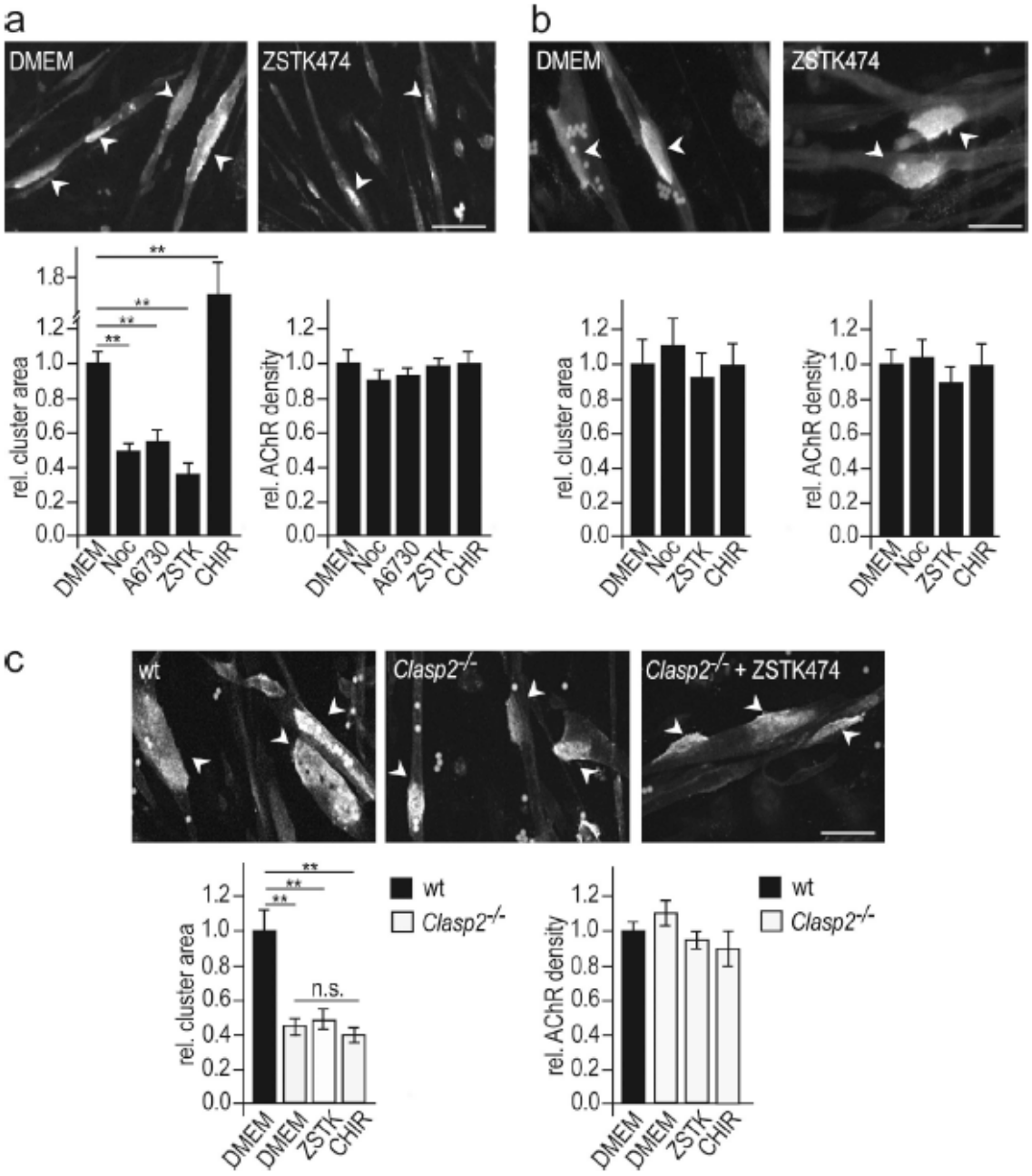

Figure 8. **Impairment of MT function by nocodazole, by inhibition of PI3-K and AKT, and by genetic deletion of CLASP2 impairs AChR insertion into agrin-induced AChR clusters in cultured myotubes.** (a) Areas of agrin-induced AChR clusters in primary myotubes appear smaller when AChRs are stained after 3 h of treatment with the following drugs: nocodazole (10 µM); inhibitors of AKT (A6730, 0.5 µM); PI3-K (ZSTK474, 5 µM; only the effect of ZSTK474 is illustrated). However, the density of AChRs in clusters remains unchanged. Conversely, inhibiting GSK3β activity (CHIR99021, 0.1 µM) increases AChR cluster size. Bar, 30 µm. Means ± SEM. Total numbers of AChR clusters analyzed in two independent experiments: Control (wild type): 78; nocodazole: 67; A6730: 68; ZSTK474: 38; CHIR99021: 54 (*, $P < 0.05$; **, $P < 0.01$, two-sided *t* test). (b) In contrast, AChR clusters appear unchanged after 3 h of drug treatment when AChRs are stained at the time of drug addition; again, AChR densities in clusters remain unchanged. Bar, 60 µm. Means ± SEM. Total numbers of AChR clusters analyzed in two independent experiments: Control (wild type): 30; nocodazole: 46; ZSTK474: 27; CHIR99021: 21 (*, $P < 0.05$; **, $P < 0.01$, two-sided *t* test). (c) AChR clusters are smaller in *Clasp2*$^{-/-}$ than in wild-type muscle, and unlike in wild-type muscle (see panel a), cluster size is not affected by ZSTK474 (5 µM) or CHIR99021 (0.1 µM). AChRs were stained after drug treatment. Bar: 30 µm. Graphs give means ± SEM, 20–78 clusters analyzed from 2 cultures for each condition (*, $P < 0.05$; **, $P < 0.01$, two-sided *t* test). AChR clusters marked by arrowheads.

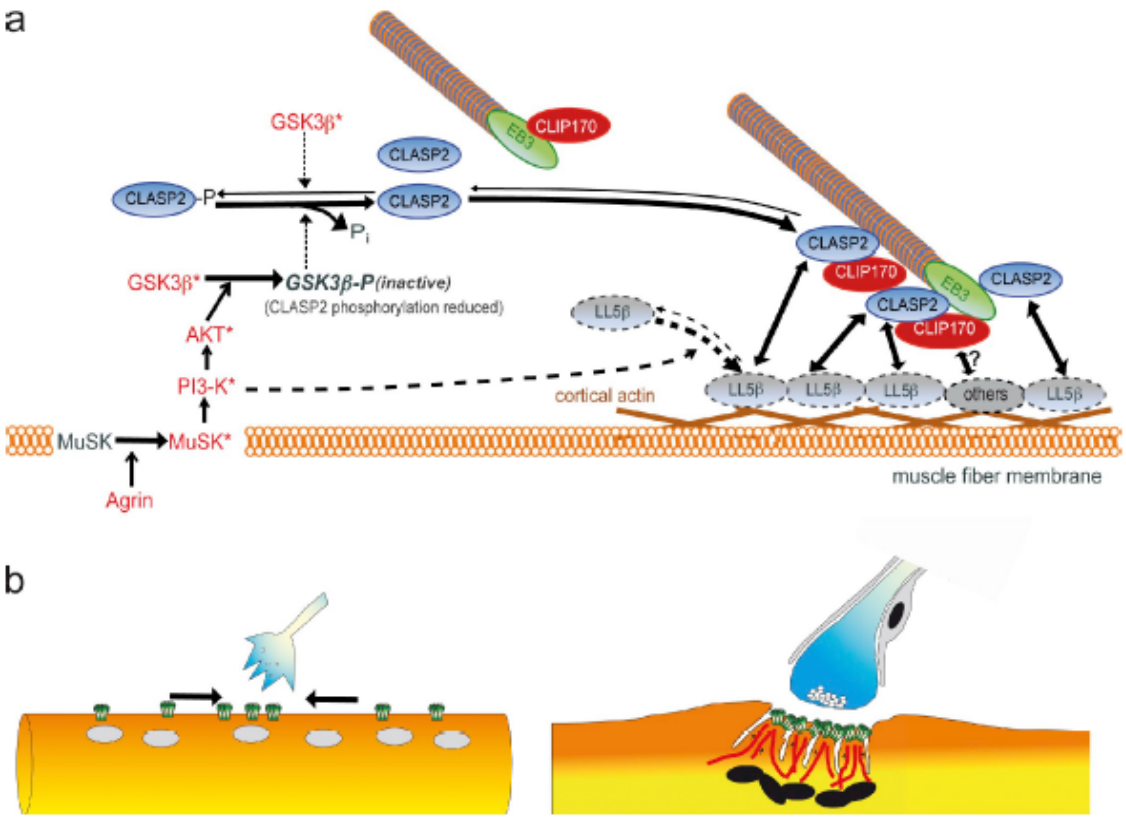

Figure 9. **Regulation and function of CLIP-170/CLASP2-dependent microtubule stabilization at the postsynaptic membrane of the neuromuscular junction.** (a) Working model summarizing the role of neural agrin to capture MTs at the postsynaptic membrane of the NMJ. Agrin-induced MT capturing at AChR clusters is regulated through: (1) local GSK3β inactivation promoting the recruitment of unphosphorylated CLASP2 to MT plus-ends and lattice; (2) recruitment of CLIP-170 through CLIP/CLASP and CLIP/MT interactions; (3) local, PI3-K–dependent recruitment and immobilization of LL5β in the synaptic membrane. Molecules and their interactions inferred from work published in other systems rather than from present data in muscle cells are marked by broken symbols. (b) At developing NMJs, constitutively expressed synaptic AChRs are delivered to synaptic membrane by lateral diffusion in the plane of the cell membrane (arrows). At adult NMJs, MTs stabilized by mechanisms outlined in panel a ensure focal delivery of synaptic AChRs to the crests of synaptic folds. Cartoon in panel b is modified from Ruegg, 2005.

(ZSTK474) did not reduce AChR insertion any further (Fig. 8 c), nor did inhibition of GSK3β with CHIR 99021 increase receptor insertion, indicating that PI3-K, p-GSK3β, and CLASP2 are part of the same signaling cascade. Taken together, these experiments are consistent with our observations at mature NMJs (Fig. 3 b) and strongly support our model (see Fig. 9) that agrin, acting through PI3-K and p-GSK3β, promotes MT capturing at the synapse (Fig. 4 b and Fig. 6), and that this enhances AChR insertion into agrin-induced AChR clusters.

Discussion

The role of dynamic MTs in synaptic function is only beginning to be understood. It has only recently been reported that dynamic MTs enter dendritic spines transiently in a way that appears to be dependent on synaptic activity and correlated with LTP (Gu et al., 2008; Hu et al., 2008; Jaworski et al., 2009). However, neither the mechanisms that regulate MT entry into spines nor their role in modulating synaptic plasticity have been established.

Here, we have used the NMJ of a GFP-CLIP-170 knock-in mouse mutant as a model for studying the role of MTs at the synapse. This model has two major advantages. First, subsynaptic differentiation and maintenance of the NMJ, including the regulation of a stable subsynaptic MT network, are controlled by one major organizer, agrin. In our in vitro paradigm, agrin was presented in a locally stable fashion, similar to that in the muscle fiber's synaptic basal lamina in vivo. Second, the use of myotubes derived from GFP-CLIP-170 knock-in mice ensures normal expression levels of this GFP-tagged +TIP, which functions in vivo like nontagged CLIP-170 (Akhmanova et al., 2005). This allows us to observe GFP-CLIP-170–decorated dynamic MTs at agrin-induced AChR clusters under completely physiological conditions.

The classical function of agrin is to cluster AChRs (and other synaptic proteins) in the subsynaptic muscle membrane. This involves the induction of a scaffold for anchoring these proteins at high density to the subsynaptic actin cytoskeleton. The present experiments, both at NMJs in vivo and in cultured

myotubes, now reveal an additional aspect of agrin function in the clustering process, i.e., in the insertion of the AChRs into the synaptic receptor cluster. AChR insertion into the synaptic muscle membrane requires MTs captured at the synaptic membrane via a pathway downstream of agrin regulating, through PI3-K and GSK3β, the CLASP2-mediated MT capture at the subsynaptic membrane. Thus, synaptic MT capturing at the NMJ might be regulated similarly as at the leading edge of migrating cells where, by inactivation of GSK3β, CLASP2 is dephosphorylated, which increases its association with MTs (Kumar et al., 2009; Watanabe et al., 2009).

MTs can be linked through nonphosphorylated CLASP2 to cortical sites in two nonmutually exclusive ways: (1) through the PIP3 sensor LL5β (Lansbergen et al., 2006; Hotta et al., 2010), and (2) through direct binding of CLASP2 to actin (Tsvetkov et al., 2007). In addition, as suggested by the increase of the CLIP load on MTs at AChR clusters, increased (de-phosphorylated) CLASP2 at the clusters might increase binding of CLIP-170 via direct CLASP2–CLIP interactions. Whether increased CLIP also participates in MT capturing at the NMJ, e.g., through the Rac effector IQGAP1 to actin (Fukata et al., 2002; Watanabe et al., 2004) or through potentiating further CLASP2 binding, is not known, but would be consistent with the reduced AChR density at *Clip115*$^{-/-}$*;Clip170*$^{-/-}$ NMJs (Fig. 3 c).

Of the potential CLASP2 interactors, LL5β is expressed in the endplate membrane and is localized at the crests between the AChR-rich regions at the mouth of the folds (Kishi et al., 2005), i.e., where p-GSK3β, CLIP-170, and CLASP2 are enriched (Figs. 1, 2, and 4). Further, its depletion inhibits AChR clustering (Kishi et al., 2005). LL5β is thus a strong candidate for mediating the GSK3-β/CLASP2–dependent MT capturing observed here. Our working model for CLASP2-mediated aspects of synaptic MT capturing is illustrated in Fig. 9.

MT capturing at the NMJ might also be mediated via the +TIPs APC (Zumbrunn et al., 2001) and ACF7 (Wu et al., 2011). Of these, APC is enriched at the NMJ, and overexpression of a dominant-negative APC truncation mutant inhibits agrin-dependent AChR clustering in cultured myotubes (Wang et al., 2003). Finally, ankyrin has been shown to be involved in the MT organization at the NMJ perhaps by acting as a membrane receptor for dynactin, with which it interacts (Ayalon et al., 2008), and which stabilizes MTs at adherens junctions (Shaw et al., 2007). Such additional mechanisms for synaptic MT capturing may account for the relatively mild phenotype at *Clasp2*$^{-/-}$ and at *Clip1*$^{-/-}$*;Clip2*$^{-/-}$ NMJs.

The 30% reduction in the number of junctional nuclei at *Clasp2*$^{-/-}$ NMJs raises the alternative possibility that reduced synapse-specific AChR gene expression might account for the reduction in synaptic size and AChR density. Although we cannot exclude this for synaptic size, AChR density is unlikely to be affected by 30% reduced AChR expression, as AChR densities are similar at NMJs of AChRε$^{+/+}$ and AChRε$^{+/-}$ synapses (Missias et al., 1997), and the amplitudes of miniature endplate currents do not change between the first and ninth postnatal weeks (Witzemann et al., 1996), when synaptic size and nuclear number increase dramatically.

The directed transport of synaptic components to the endplate membrane as proposed here for CLASP2-mediated synaptic MT capturing may be more important at mature NMJs than during early stages of their development. Early in NMJ development, muscle fibers express high levels of synaptic proteins, including AChRs, along their entire surface as part of their developmental program. This allows the recruitment of proteins to the developing synapse by lateral diffusion in the plane of the cell membrane (Anderson and Cohen 1977; Flanagan-Steet et al., 2005). In contrast, at later stages of NMJ maturation, when nerve-induced electrical muscle activity has down-regulated extrasynaptic AChR expression, the supply of synaptic molecules from nonsynaptic membrane is no longer available. This necessitates the transport of AChRs and other synaptic proteins from the TGN below the synaptic membrane where synapse-specific gene expression is maintained by the agrin-induced transcription from the fundamental muscle nuclei underlying the synapse (Brenner et al., 1990). The mechanisms described here can explain the highly focal nature of this transport to the synaptic muscle membrane through mechanisms similar to those controlling polarity and directed migration in motile cells.

Materials and methods

Animals

Generation of the *Clasp2* single knockout strain and of the *Clip1;Clip2* double knockout mouse strain will be described elsewhere. In brief, the genes encoding CLIP-170 (*Clip1* gene) and CLIP-115 (*Clip2* gene) were targeted by homologous recombination in embryonic stem (ES) cells. In the case of the *Clip1* gene we inserted a GFP-loxP-Neo-loxP casette (where Neo indicates the neomycin resistance gene) into the exon containing the ATG translation initiation codon. This yielded the *Clip1* knockout allele. Removal of the neomycin resistance gene in ES cells by Cre recombinase yielded the *GFP-Clip170* knock-in (*ki*) allele (Akhmanova et al., 2005). In the case of the *Clip2* gene we inserted a loxP-neo-loxP casette at the 5′ end of the gene and a loxP-Puro-loxP-LacZ casette (where Puro indicates the puromycin resistance gene, and LacZ the β-galactosidase gene) at the 3′ end of the gene. Cre-mediated recombination in ES cells yielded the *Clip2* knockout allele (Hoogenraad et al., 2002). Single *Clip1* and *Clip2* knockout and *GFP-Clip170*^{ki} mice were obtained by germline transmission of the modified alleles in chimeric mice, which were in turn obtained by injecting ES cells carrying the modified alleles into recipient blastocysts. The *Clip1* and *Clip2* single knockout mice were crossed to generate the double knockout line.

For electroporation and in vivo stainings, animals were anesthetized with ketamine (87 mg per kg body weight) and xylazine (13 mg per kg body weight). Postoperative analgesia was by 4 injections of buprenorphine at 12-h intervals. Mice were sacrificed with CO_2. Animal handling was approved by the Cantonal Veterinary Office of Basel-Stadt.

Depending on experimental suitability, soleus (for electroporations), epitrochleo-anconeus (ETA; for optimal preservation of dynamic microtubules) or sternomastoideus (for estimates of AChR density from whole BTX-Alexa 488–stained NMJs) muscles were used.

Chemicals and antibodies

ZSTK474 (LC Laboratories) was used at 1 or at 5 µM on cultured myotubes analyzed biochemically or by imaging, respectively. All other reagents were applied in the following concentrations: nocodazole (10 µM; Sigma-Aldrich), LY294002 (50 µM; Sigma-Aldrich), A6730 (500 nM; Sigma-Aldrich), CHIR99021 (100 nM; Axon Medchem) λ-protein phosphatase (2,000 U; New England Biolabs, Inc.), and rapamycin (100 nM; LC Laboratories). AChRs were labeled with α-BTX–Alexa 488, 594, or 647 (Invitrogen). GFP-CLIP-170 (by staining for GFP), EB1, and CLASP2 were visualized with antibodies from Invitrogen, BD, and Absea, respectively. Polyclonal rabbit antibodies against human EB3 (image clone 714028) were custom made at Absea, using a bacterially expressed and purified GST-EB3 fusion protein as antigen, as described previously (Stepanova et al., 2003). Antibodies against AKT, p-AKT (S473), GSK3β, p-GSK3β (S9; no. 9336),

and actin were purchased from Cell Signaling Technology. All other primary antibodies were obtained from Sigma-Aldrich (anti-tyrosinated α-tubulin, anti-neurofilament), Millipore (anti-detyrosinated α-tubulin), Santa Cruz Biotechnology, Inc. (anti-myc), and Dako (anti-S100; Z0311). Secondary antibodies were goat anti–rabbit, goat anti–mouse, or goat anti–rat antibodies conjugated to Alexa 488 (Invitrogen) as well as donkey anti–chicken Cy2 (Jackson ImmunoResearch Laboratories, Inc.). HRP-conjugated secondary antibodies were from Santa Cruz Biotechnology, Inc. Ringer's solution was obtained from Braun. Phosphatase inhibitors PIC1 and 2 as well as Collagenase type 1A were purchased from Sigma-Aldrich, protease inhibitors and Fugene HD from Roche, and PDGF-BB from Peprotech. Rapamycin was a gift from M.N. Hall (Biozentrum, University of Basel, Basel, Switzerland).

Estimation of synaptic PI3-K activity

40 µg of pPH-BTK-GFP or pPH-BTK R28C-GFP (Várnai et al., 1999) in 10 µl 0.9% NaCl was injected with a Hamilton syringe into the soleus muscle of anesthetized C57BL76 mice (8–10 wk old). After suturing the skin, 8 pulses (20 ms, 1 Hz, 200 V/cm) were applied to the leg using an ECM 830 electroporation system. 10–14 d later, electroporated soleus muscles were dissected, AChRs stained with 1 µg/ml α-BTX-Alexa 594 for 1 h at RT, fixed in 4% paraformaldehyde (PFA) for 2 h, placed in 30% sucrose/PBS overnight, and frozen. Muscles were then embedded and sectioned at 12-µm thickness in a cryostat (CM 1950; Leica). Sections were mounted in Citifluor and GFP and α-BTX-Alexa 594 stainings imaged using an ACS APO 63x/1.3 NA objective on an SPE confocal microscope (DMI 4000B; Leica). For the measurement of synaptic GFP intensity, the α-BTX–stained synapse of GFP-positive fibers was defined as a region of interest (ROI). Using ImageJ (National Institutes of Health), green fluorescence in this synaptic ROI was measured, the ROI moved to the extrasynaptic region of the same fiber profile, and the extrasynaptic green fluorescence was measured. Because the level of GFP expression varies across fibers within an individual muscle, the ratio of green fluorescence at the synapse to that in nonsynaptic membrane was taken as an estimate of synaptic PH-BTK-GFP or PH-BTK R28C-GFP binding, respectively.

Confocal microscopy

Muscle fibers and myotubes were imaged with an SPE confocal scanning laser microscope (DMI 4000B; Leica) at a resolution of 1024 × 1024 pixels using an HCX PL APO 100x objective (NA 1.46) or an ACS APO 63x objective (NA 1.30). Image stacks were acquired with a step size of 300 nm. For images used in 3D reconstructions, step sizes of 100 nM were used, and image stacks were deconvolved using Huygens Essential software (Scientific Volume Imaging). For comparison of different samples the same laser settings were applied. Quantitative differences potentially due to changes in the light source or camera were excluded by imaging control and mutant muscles within the same session. Nevertheless, the quality of confocal images, taken at different NMJs, was too variable to allow quantitatively precise measurements of intensity and number of GFP-CLIP-170 or CLASP2 dots or of subsynaptic MT networks visualized by Tyr-tubulin or Glu-tubulin stainings for comparison between, e.g., wild-type and mutant NMJs. This was due to unequal fixation and/or unequal penetration of antibody in different fibers (for details, see Immunocytochemistry section). Preservation of CLIP-170– and CLASP2-positive MT plus-ends in adult muscle required the use of the thin epitrochlearis-anconeus (ETA) muscle, fixed in −80°C methanol; moreover, fibers were stained in bundles, such that not all endplates within a bundle were equally exposed to antibody; finally, images needed different contrasting to optimally resolve GFP-CLIP-170 or CLASP2 dots. As a consequence, only qualitative information such as the number of endplates with clear enrichment of GFP-CLIP-170 dots along edges of synaptic AChR clusters could be extracted.

3D reconstructions (surface renderings) were performed in Imaris x64 7.4.0 on stacks acquired with a sample distance of 0.05 × 0.05 × 0.1 µm.

Preparation of primary muscle cultures

Neonatal leg muscles from wild-type and mutant neonatal muscle were minced, dissociated with collagenase type IV and dispase type II, and cells were plated on a laminin substrate in DME containing 2 mM glutamine, 20% FCS, 5 ng/ml recombinant human basic FGF, and 1% antibiotic/antimycotic solution. After 2 d, they were resuspended in PBS by brief trypsinization, treated with rat monoclonal anti–mouse α7-integrin antibody, and purified using (magnetic) Dynabeads coated with sheep anti–rat IgG and a Dynal-MPC-L magnetic particle concentrator (Blanco-Bose et al., 2001; Escher et al., 2005). C2C12 or wild-type myotubes were cultured on laminin-coated dishes locally impregnated with agrin. For the preparation of the dishes, COS-1 cells, transfected with a plasmid coding for full-length chicken agrin (Jones et al., 1996), were seeded at a density of 7–20 x 10^3 cells per 30 mm laminin-coated culture dish. After 48 h cells were extracted for 1 h in 2% Triton X-100 in PBS, followed by intensive washing (6–8x 1 h PBS) and myoblast seeding (Schmidt et al., 2011). Subsequent differentiation was in DME, 5% horse serum, and 1% antibiotic/antimycotic solution. For biochemistry, 6-well dishes were coated with 10 µg/ml laminin (Invitrogen) followed by coating with agrin solution (0.5 µg/ml, 37°C, 2 h) before cell plating (Schmidt et al., 2011). It should be noted that throughout the present paper, agrin was applied attached to the culture substrate rather than in solution to mimic the in vivo situation.

Immunocytochemistry

All immunostainings of MTs and +TIPs were done on mice epitrochlearis-anconeus (ETA) muscle, which at its thinnest part contains only ∼6 fiber layers; this makes it optimally suited for snap fixation in cold methanol, which proved crucial for preservation of +TIP-decorated MT plus-ends. ETA muscles were pinned out after excision on Sylgard supports in a culture dish, allowing medium access from both sides. To allow recovery from potential preparative stress, muscles were bathed in DME gassed with 95% CO_2/5% O_2 at 37°C for 1 h and containing 1 µg/ml fluorescent α-BTX for AChR staining. After Collagenase type 1A treatment (0.5%, 37°C, 15 min), myotube culture dishes and recovered ETA muscles were rapidly transferred to −80°C methanol for 2 h, then transferred to a 1:1 mixture of methanol and 4% PFA at −20°C for 1 h, followed by 30-min periods at 4°C and at RT. Final fixation was in 4% PFA (RT, 10 min). Teased bundles of 4–10 muscle fibers were then incubated at 4°C for 15 min in 100 mM glycine and permeabilized in 20% normal goat serum (NGS)/PBS/2% Triton X-100 at RT for 2 h. In the case of cultured myotubes, glycine treatment was followed by permeabilization in 20% NGS/PBS/0.5% Triton X-100 (RT, 1 h). Primary and secondary antibodies were diluted in 5% NGS/PBS/0.1% Triton X-100 and were applied at 4°C overnight (primaries) or at RT for 45 min (secondaries).

GSK3β phosphorylated at Ser9 was labeled in sternomastoid muscles treated with 1% Collagenase type 1A (37°C, 30 min). Muscles were fixed in 4% PFA (37°C, 20 min) and permeabilized. Teased fibers were then incubated in protein phosphatase buffer (50 mM Hepes, 100 mM NaCl, 2 mM DTT, 1 mM $MnCl_2$, and 0.01% Brij-35, pH 7.5) with or without 2,000 U λ-protein phosphatase at RT for 1 h, washed 3x with PBS, and processed as described above.

Quantification of GFP-CLIP-170 load on EB3 comets

The mean fluorescence of GFP-CLIP-170 and EB3, visualized with the respective fluorescent antibodies, was determined in ImageJ (Plugin "Measure RGB") in and outside of the AChR cluster area in nonsaturated, nonprocessed confocal images. The ratio of GFP-CLIP-170 and EB3 fluorescence served as a measure for the load of GFP-CLIP-170 on EB3 comets. For EB3 fluorescence quantitation, only the intensities of EB3 comets were taken into account.

Estimation of number of subsynaptic myonuclei

Soleus muscles from wild-type or clasp2$^{-/-}$ mice of similar weight were stained with 1 µg/ml of α-BTX–Alexa 594 in buffered L-15 medium (RT, 1 h), fixed with 4% PFA for 2 h, and individual fibers were teased and permeabilized in 20% NGS and 2% Triton X-100. Staining with S100 was performed overnight at 4°C. After incubation with secondary antibody, fibers were mounted in ProLong Gold containing DAPI. En-face synapses were imaged in 1-µm stacks using an ACS APO 63x/1.3 NA objective at the SPE confocal microscope (DMI 4000B; Leica). For synapse area measurements, synapses were outlined in the maximum intensity projection for each image manually and the area of the outlined region was calculated using ImageJ. Schwann cell nuclei marked by S100 staining were discounted from the total nuclear count as visualized by DAPI. For measurement of muscle fiber areas, muscles were treated and sectioned as described in Estimation of synaptic PI3-K activity. To delineate muscle fiber plasma membranes, cryosections were postfixed for 5 min in 2% PFA, washed, stained with Wheat Germ Agglutinin Oregon Green 488 overnight, and mounted. The analySIS software from Olympus was used to outline fiber ferrets and calculate cross-sectional area.

Structured illumination microscopy (SIM)

Fixed samples were imaged using the ELYRA S.1 structured illumination microscope (Carl Zeiss). Images were acquired using a 63x/1.40 oil Plan Apochromat objective and an EMCCD camera (iXon 885; Andor Technology). Stacks of images of NMJs en face were taken through the entire depth of the synapse at 0.125 µm. Image processing was performed using the Carl Zeiss Zen software to achieve a maximal resolution of 110 nm in

x-y and 250 nm in z-directions. For colocalization experiments, precise pixel alignment between different acquisition channels was ensured by correcting potential pixel shifts via the channel alignment function within the Zen software (Car Zeiss) using simultaneously acquired images of multispec beads (200 nm) as a reference. Image analysis was performed using Imaris software (Bitplane). Contour lines of AChRs at three z-levels for each synapse were selected, and the number of CLIP-170 puncta per length of contour line was counted.

Total internal reflection microscopy (TIRF)

Dynamics of GFP-CLIP-170 comets were measured in myotubes derived from *GFP-Clip-170$^{ki/ki}$* mice. Agrin-induced AChR clusters were stained with α-BTX–Alexa 594 (1 µg/ml, 30 min), and after washing with prewarmed DME cells were incubated at 37°C for 1 h before being mounted on a thermostat perfusion chamber. Cells were imaged at 37°C in Krebs Ringer's solution (140 mM NaCl; 5 mM KCl, 1 mM Mg^{2+}, 2 mM Ca^{2+}, 20 mM Hepes, 1 mM $NaHPO_4$, and 5.5 mM glucose) at pH 7.4. Online fluorescence images were acquired using an inverted TIRF microscope (TE2000; Nikon) equipped with an oil immersion CFI Plan Apochromat 100× TIRF objective (1.49 NA) and an electron multiplier CCD camera (C9100-13, Hamamatsu Photonics; Trewes et al., 2010). The focal plane corresponding to the coverglass/cell membrane contact was adjusted with a surface reflective interference contrast (SRIC) cube and maintained throughout the experiment with the help of a perfect focus system. GFP-CLIP-170 dynamics were imaged for 160 s with a rate of 1 frame per second (MetaMorph; Molecular Devices).

Quantitative analysis of GFP-CLIP-170 comet dynamics

Dynamics of GFP-CLIP-170 comets were analyzed inside and outside of agrin-induced AChR cluster with ImageJ (National Institutes of Health). The maxiprojection of all acquired 160 frames of the live imaging experiment was used to mark all the comet traces within the imaged area. Kymographs (time–space plots) of all the comets visualized in the TIRF plane were generated with the Kymograph plugin for ImageJ from J. Rietdorf (Friedrich Miescher Institute, Basel, Switzerland) and A. Seitz (EMBL Heidelberg, Heidelberg, Germany). To study the effect of PI3-K signaling as well as CLASP2 on GFP-CLIP-170 comet dynamics, comets from myotubes either treated with ZSTK474 (37°C, 60–80 min) or deficient in CLASP2 were used for the analysis.

Quantitative analysis of AChR cluster size

An effect of the drugs indicated or of CLASP2 deficiency on AChR cluster size was determined by incubating the cells for 3 h at 37°C in the absence or presence of pharmacological inhibitors. Cells were then fixed (4% PFA) and stained with α-BTX–Alexa 594 (1 µg/ml, 30 min) to label agrin-induced AChR clusters.

To elucidate AChR removal rates in culture, agrin-induced AChR clusters in primary cells were stained with α-BTX–Alexa 594 (1 µg/ml, 30 min) before the cells were incubated for 3 h at 37°C (to allow removal of fluorescent receptors) in the absence or presence of pharmacological inhibitors. Cells were then fixed (4% PFA) and imaged (HC Plan Apo 20x/0.70 objective; inverted microscope [DMI 6000B; Leica]; 1394 ORCA-ERA camera [Hamamatsu Photonics], Volocity 6.0.1 [PerkinElmer]). Cluster sizes after 3 h were determined by measuring the area of the remaining AChR fluorescence in ImageJ (National Institutes of Health).

Quantification of AChR density and insertion in vivo

To determine the density of AChRs in CLASP2-deficient and age-matched control littermates, the sternomastoid muscles of anaesthetized mice were exposed and bathed for 90 min in Ringer's solution containing 5 µg/ml α-BTX–Alexa 594 (a dose that has previously been demonstrated to be sufficient to saturate all receptors; Bruneau et al., 2005). Mice were sacrificed, and muscles were washed (Ringer's solution) and fixed in 4% PFA for 20 min. Dissection of the muscles was followed by mounting and imaging of superficial synapses only using confocal microscopy (63x objective, oil immersion). AChR fluorescence was measured in nonsaturated, nonprocessed images (ImageJ).

Staining of newly inserted AChRs was performed in denervated sternomastoid muscles of anaesthetized mice. Muscle denervation was followed immediately by labeling of AChRs in the synaptic as well as perisynaptic muscle membrane with a saturating dose of α-BTX–Alexa 488 (5 µg/ml, 90 min). After the removal of excess α-BTX–Alexa 488 with Ringer's solution, wounds were sutured and allowed to heal for 1 wk. Mice were re-anaesthetized, sternomastoid muscles were exposed, and newly inserted AChRs were stained with α-BTX–Alexa 594 (5 µg/ml, 90 min). Mice were then sacrificed. Fixation, mounting, image acquisition, and quantitation was done as described above.

Immunoblotting

Myotubes were lysed in 3x SDS-lysis buffer (150 mM Tris, pH 6.8, 300 mM DTT, 6% SDS, 0.2% bromophenol blue, and 30% glycerol) supplemented with phosphatase inhibitors (1:100), protease inhibitors (1/10 tablet per ml lysis buffer), and 100 mM DTT. Lysates were denatured at 95°C for 5 min and loaded on a 10% SDS-PAGE. Gels were transferred onto PVDF membranes and developed with ECL after incubation with primary and secondary antibodies.

Statistical analyses

Data are given as mean ± SEM. The Shapiro-Wilk test was used to test if datasets belong to a normally distributed population. If so, quantitative comparisons of numerical datasets were tested for statistical significance by means of the parametric, nonpaired, two-sided Student's *t* test. Otherwise the nonparametric, two-sided *U* test (Mann & Whitney) was applied. One asterisk marks P values below 5% ($P < 0.05$), whereas two asterisks correspond to P values below 1% ($P < 0.01$).

Online supplemental material

Fig. S1 shows the full blots from which Fig. 5 a was extracted. They show the effect of neural vs. nonneural agrin on phosphorylation of GSK3β and AKT and the effects of AKT, mTOR, and PI3-K inhibitors. Fig. S2 shows the tests used to demonstrate the specificity of the anti-phospho-GSK3β antibody (no. 9336; Cell Signaling Technology), using myc-tagged GSK3β wt and S9A mutant transfected into COS cells. Video 1 shows capturing of GFP-CLIP-170 comets at agrin-induced AChR clusters in primary of *GFP-CLIP-170$^{ki/ki}$* myotubes, using TIRF microscopy. Video 2 shows inhibition of capturing of GFP-CLIP-170 comets at agrin-induced AChR clusters in *Clasp2$^{-/-}$;GFP-Clip-170$^{ki/ki}$* primary myotubes, using TIRF microscopy. Online supplemental material is available at http://www.jcb.org/cgi/content/full/jcb.201111130/DC1.

We thank Dr. Matthias Wymann for suggesting the expression of PH-BTK fragments to test for PI3K activity in vivo, Michèle Courtet for technical assistance, and Dr. Clarke Slater for critical reading of the manuscript.

This work was supported by the Swiss National Science Foundation, The Swiss Foundation for Research on Muscle Diseases, The Neuromuscular Research Association Basel (NeRAB), the Netherlands Organization for Health Research and Development (ZonMW), and the Dutch Cancer Genomics Center (CGC).

Submitted: 28 November 2011
Accepted: 2 July 2012

References

Akhmanova, A., C.C. Hoogenraad, K. Drabek, T. Stepanova, B. Dortland, T. Verkerk, W. Vermeulen, B.M. Burgering, C.I. De Zeeuw, F. Grosveld, and N. Galjart. 2001. Clasps are CLIP-115 and -170 associating proteins involved in the regional regulation of microtubule dynamics in motile fibroblasts. *Cell.* 104:923–935. http://dx.doi.org/10.1016/S0092-8674(01)00288-4

Akhmanova, A., A.L. Mausset-Bonnefont, W. van Cappellen, N. Keijzer, C.C. Hoogenraad, T. Stepanova, K. Drabek, J. van der Wees, M. Mommaas, J. Onderwater, et al. 2005. The microtubule plus-end-tracking protein CLIP-170 associates with the spermatid manchette and is essential for spermatogenesis. *Genes Dev.* 19:2501–2515. http://dx.doi.org/10.1101/gad.344505

Anderson, M.J., and M.W. Cohen. 1977. Nerve-induced and spontaneous redistribution of acetylcholine receptors on cultured muscle cells. *J. Physiol.* 268:757–773.

Ayalon, G., J.Q. Davis, P.B. Scotland, and V. Bennett. 2008. An ankyrin-based mechanism for functional organization of dystrophin and dystroglycan. *Cell.* 135:1189–1200. http://dx.doi.org/10.1016/j.cell.2008.10.018

Blanco-Bose, W.E., C.C. Yao, R.H. Kramer, and H.M. Blau. 2001. Purification of mouse primary myoblasts based on alpha 7 integrin expression. *Exp. Cell Res.* 265:212–220. http://dx.doi.org/10.1006/excr.2001.5191

Bohnacker, T., R. Marone, E. Collmann, R. Calvez, E. Hirsch, and M.P. Wymann. 2009. PI3Kgamma adaptor subunits define coupling to degranulation and cell motility by distinct PtdIns(3,4,5)P_3 pools in mast cells. *Sci. Signal.* 2:ra27. http://dx.doi.org/10.1126/scisignal.2000259

Borges, L.S., and M. Ferns. 2001. Agrin-induced phosphorylation of the acetylcholine receptor regulates cytoskeletal anchoring and clustering. *J. Cell Biol.* 153:1–12. http://dx.doi.org/10.1083/jcb.153.1.1

Brenner, H.R., V. Witzemann, and B. Sakmann. 1990. Imprinting of acetylcholine receptor messenger RNA accumulation in mammalian neuromuscular synapses. *Nature.* 344:544–547. http://dx.doi.org/10.1038/344544a0

Bruneau, E., D. Sutter, R.I. Hume, and M. Akaaboune. 2005. Identification of nicotinic acetylcholine receptor recycling and its role in maintaining receptor density at the neuromuscular junction in vivo. *J. Neurosci.* 25:9949–9959. http://dx.doi.org/10.1523/JNEUROSCI.3169-05.2005

Bruneau, E.G., D.S. Brenner, J.Y. Kuwada, and M. Akaaboune. 2008. Acetylcholine receptor clustering is required for the accumulation and maintenance of scaffolding proteins. *Curr. Biol.* 18:109–115. http://dx.doi.org/10.1016/j.cub.2007.12.029

Bulinski, J.C., and G.G. Gundersen. 1991. Stabilization of post-translational modification of microtubules during cellular morphogenesis. *Bioessays.* 13:285–293. http://dx.doi.org/10.1002/bies.950130605

Dai, Z., X. Luo, H. Xie, and H.B. Peng. 2000. The actin-driven movement and formation of acetylcholine receptor clusters. *J. Cell Biol.* 150:1321–1334. http://dx.doi.org/10.1083/jcb.150.6.1321

Escher, P., E. Lacazette, M. Courtet, A. Blindenbacher, L. Landmann, G. Bezakova, K.C. Lloyd, U. Mueller, and H.R. Brenner. 2005. Synapses form in skeletal muscles lacking neuregulin receptors. *Science.* 308:1920–1923. http://dx.doi.org/10.1126/science.1108258

Flanagan-Steet, H., M.A. Fox, D. Meyer, and J.R. Sanes. 2005. Neuromuscular synapses can form in vivo by incorporation of initially aneural postsynaptic specializations. *Development.* 132:4471–4481. http://dx.doi.org/10.1242/dev.02044

Fukata, M., T. Watanabe, J. Noritake, M. Nakagawa, M. Yamaga, S. Kuroda, Y. Matsuura, A. Iwamatsu, F. Perez, and K. Kaibuchi. 2002. Rac1 and Cdc42 capture microtubules through IQGAP1 and CLIP-170. *Cell.* 109:873–885. http://dx.doi.org/10.1016/S0092-8674(02)00800-0

Galjart, N. 2010. Plus-end-tracking proteins and their interactions at microtubule ends. *Curr. Biol.* 20:R528–R537. http://dx.doi.org/10.1016/j.cub.2010.05.022

Gu, J., B.L. Firestein, and J.Q. Zheng. 2008. Microtubules in dendritic spine development. *J. Neurosci.* 28:12120–12124. http://dx.doi.org/10.1523/JNEUROSCI.2509-08.2008

Gundersen, G.G., E.R. Gomes, and Y. Wen. 2004. Cortical control of microtubule stability and polarization. *Curr. Opin. Cell Biol.* 16:106–112. http://dx.doi.org/10.1016/j.ceb.2003.11.010

Gustafsson, M.G., L. Shao, P.M. Carlton, C.J. Wang, I.N. Golubovskaya, W.Z. Cande, D.A. Agard, and J.W. Sedat. 2008. Three-dimensional resolution doubling in wide-field fluorescence microscopy by structured illumination. *Biophys. J.* 94:4957–4970. http://dx.doi.org/10.1529/biophysj.107.120345

Hoogenraad, C.C., B. Koekkoek, A. Akhmanova, H. Krugers, B. Dortland, M. Miedema, A. van Alphen, W.M. Kistler, M. Jaegle, M. Koutsourakis, et al. 2002. Targeted mutation of Cyln2 in the Williams syndrome critical region links CLIP-115 haploinsufficiency to neurodevelopmental abnormalities in mice. *Nat. Genet.* 32:116–127. http://dx.doi.org/10.1038/ng954

Hotta, A., T. Kawakatsu, T. Nakatani, T. Sato, C. Matsui, T. Sukezane, T. Akagi, T. Hamaji, I. Grigoriev, A. Akhmanova, et al. 2010. Laminin-based cell adhesion anchors microtubule plus ends to the epithelial cell basal cortex through LL5alpha/beta. *J. Cell Biol.* 189:901–917. http://dx.doi.org/10.1083/jcb.200910095

Hu, X., C. Viesselmann, S. Nam, E. Merriam, and E.W. Dent. 2008. Activity-dependent dynamic microtubule invasion of dendritic spines. *J. Neurosci.* 28:13094–13105. http://dx.doi.org/10.1523/JNEUROSCI.3074-08.2008

Jasmin, B.J., J.P. Changeux, and J. Cartaud. 1990. Compartmentalization of cold-stable and acetylated microtubules in the subsynaptic domain of chick skeletal muscle fibre. *Nature.* 344:673–675. http://dx.doi.org/10.1038/344673a0

Jaworski, J., L.C. Kapitein, S.M. Gouveia, B.R. Dortland, P.S. Wulf, I. Grigoriev, P. Camera, S.A. Spangler, P. Di Stefano, J. Demmers, et al. 2009. Dynamic microtubules regulate dendritic spine morphology and synaptic plasticity. *Neuron.* 61:85–100. http://dx.doi.org/10.1016/j.neuron.2008.11.013

Jones, G., A. Herczeg, M.A. Ruegg, M. Lichtsteiner, S. Krüger, and H.R. Brenner. 1996. Substrate-bound agrin induces expression of acetylcholine receptor epsilon-subunit gene in cultured mammalian muscle cells. *Proc. Natl. Acad. Sci. USA.* 93:5985–5990. http://dx.doi.org/10.1073/pnas.93.12.5985

Jones, G., T. Meier, M. Lichtsteiner, V. Witzemann, B. Sakmann, and H.R. Brenner. 1997. Induction by agrin of ectopic and functional postsynaptic-like membrane in innervated muscle. *Proc. Natl. Acad. Sci. USA.* 94:2654–2659. http://dx.doi.org/10.1073/pnas.94.6.2654

Kim, N., A.L. Stiegler, T.O. Cameron, P.T. Hallock, A.M. Gomez, J.H. Huang, S.R. Hubbard, M.L. Dustin, and S.J. Burden. 2008. Lrp4 is a receptor for Agrin and forms a complex with MuSK. *Cell.* 135:334–342. http://dx.doi.org/10.1016/j.cell.2008.10.002

Kishi, M., T.T. Kummer, S.J. Eglen, and J.R. Sanes. 2005. LL5beta: a regulator of postsynaptic differentiation identified in a screen for synaptically enriched transcripts at the neuromuscular junction. *J. Cell Biol.* 169:355–366. http://dx.doi.org/10.1083/jcb.200411012

Kumar, P., K.S. Lyle, S. Gierke, A. Matov, G. Danuser, and T. Wittmann. 2009. GSK3beta phosphorylation modulates CLASP-microtubule association and lamella microtubule attachment. *J. Cell Biol.* 184:895–908. http://dx.doi.org/10.1083/jcb.200901042

Kummer, T.T., T. Misgeld, J.W. Lichtman, and J.R. Sanes. 2004. Nerve-independent formation of a topologically complex postsynaptic apparatus. *J. Cell Biol.* 164:1077–1087. http://dx.doi.org/10.1083/jcb.200401115

Lansbergen, G., I. Grigoriev, Y. Mimori-Kiyosue, T. Ohtsuka, S. Higa, I. Kitajima, J. Demmers, N. Galjart, A.B. Houtsmuller, F. Grosveld, and A. Akhmanova. 2006. CLASPs attach microtubule plus ends to the cell cortex through a complex with LL5beta. *Dev. Cell.* 11:21–32. http://dx.doi.org/10.1016/j.devcel.2006.05.012

Meier, T., P.A. Marangi, J. Moll, D.M. Hauser, H.R. Brenner, and M.A. Ruegg. 1998. A minigene of neural agrin encoding the laminin-binding and acetylcholine receptor-aggregating domains is sufficient to induce postsynaptic differentiation in muscle fibres. *Eur. J. Neurosci.* 10:3141–3152. http://dx.doi.org/10.1046/j.1460-9568.1998.00320.x

Miller, P.M., A.W. Folkmann, A.R. Maia, N. Efimova, A. Efimov, and I. Kaverina. 2009. Golgi-derived CLASP-dependent microtubules control Golgi organization and polarized trafficking in motile cells. *Nat. Cell Biol.* 11:1069–1080. http://dx.doi.org/10.1038/ncb1920

Missias, A.C., J. Mudd, J.M. Cunningham, J.H. Steinbach, J.P. Merlie, and J.R. Sanes. 1997. Deficient development and maintenance of postsynaptic specializations in mutant mice lacking an 'adult' acetylcholine receptor subunit. *Development.* 124:5075–5086.

Nizhynska, V., R. Neumueller, and R. Herbst. 2007. Phosphoinositide 3-kinase acts through RAC and Cdc42 during agrin-induced acetylcholine receptor clustering. *Dev. Neurobiol.* 67:1047–1058. http://dx.doi.org/10.1002/dneu.20371

Ralston, E., Z. Lu, and T. Ploug. 1999. The organization of the Golgi complex and microtubules in skeletal muscle is fiber type-dependent. *J. Neurosci.* 19:10694–10705.

Ruegg, M.A. 2005. Organization of synaptic myonuclei by Syne proteins and their role during the formation of the nerve-muscle synapse. *Proc. Natl. Acad. Sci. USA.* 102:5643–5644. http://dx.doi.org/10.1073/pnas.0501516102

Schmidt, N., M. Akaaboune, N. Gajendran, I. Martinez-Pena y Valenzuela, S. Wakefield, R. Thurnheer, and H.R. Brenner. 2011. Neuregulin/ErbB regulate neuromuscular junction development by phosphorylation of α-dystrobrevin. *J. Cell Biol.* 195:1171–1184. http://dx.doi.org/10.1083/jcb.201107083

Shaw, R.M., A.J. Fay, M.A. Puthenveedu, M. von Zastrow, Y.N. Jan, and L.Y. Jan. 2007. Microtubule plus-end-tracking proteins target gap junctions directly from the cell interior to adherens junctions. *Cell.* 128:547–560. http://dx.doi.org/10.1016/j.cell.2006.12.037

Stepanova, T., J. Slemmer, C.C. Hoogenraad, G. Lansbergen, B. Dortland, C.I. De Zeeuw, F. Grosveld, G. van Cappellen, A. Akhmanova, and N. Galjart. 2003. Visualization of microtubule growth in cultured neurons via the use of EB3-GFP (end-binding protein 3-green fluorescent protein). *J. Neurosci.* 23:2655–2664.

Treves, S., M. Vukcevic, J. Griesser, C.F. Armstrong, M.X. Zhu, and F. Zorzato. 2010. Agonist-activated Ca2+ influx occurs at stable plasma membrane and endoplasmic reticulum junctions. *J. Cell Sci.* 123:4170–4181. http://dx.doi.org/10.1242/jcs.068387

Tsvetkov, A.S., A. Samsonov, A. Akhmanova, N. Galjart, and S.V. Popov. 2007. Microtubule-binding proteins CLASP1 and CLASP2 interact with actin filaments. *Cell Motil. Cytoskeleton.* 64:519–530. http://dx.doi.org/10.1002/cm.20201

Várnai, P., K.I. Rother, and T. Balla. 1999. Phosphatidylinositol 3-kinase-dependent membrane association of the Bruton's tyrosine kinase pleckstrin homology domain visualized in single living cells. *J. Biol. Chem.* 274:10983–10989. http://dx.doi.org/10.1074/jbc.274.16.10983

Wang, J., Z. Jing, L. Zhang, G. Zhou, J. Braun, Y. Yao, and Z.Z. Wang. 2003. Regulation of acetylcholine receptor clustering by the tumor suppressor APC. *Nat. Neurosci.* 6:1017–1018. http://dx.doi.org/10.1038/nn1128

Watanabe, T., S. Wang, J. Noritake, K. Sato, M. Fukata, M. Takefuji, M. Nakagawa, N. Izumi, T. Akiyama, and K. Kaibuchi. 2004. Interaction with IQGAP1 links APC to Rac1, Cdc42, and actin filaments during cell polarization and migration. *Dev. Cell.* 7:871–883. http://dx.doi.org/10.1016/j.devcel.2004.10.017

Watanabe, T., J. Noritake, M. Kakeno, T. Matsui, T. Harada, S. Wang, N. Itoh, K. Sato, K. Matsuzawa, A. Iwamatsu, et al. 2009. Phosphorylation of CLASP2 by GSK-3beta regulates its interaction with IQGAP1, EB1 and microtubules. *J. Cell Sci.* 122:2969–2979. http://dx.doi.org/10.1242/jcs.046649

Witzemann, V., H. Schwarz, M. Koenen, C. Berberich, A. Villarroel, A. Wernig, H.R. Brenner, and B. Sakmann. 1996. Acetylcholine receptor epsilon-subunit deletion causes muscle weakness and atrophy in juvenile and adult mice. *Proc. Natl. Acad. Sci. USA.* 93:13286–13291. http://dx.doi.org/10.1073/pnas.93.23.13286

Wu, H., W.C. Xiong, and L. Mei. 2010. To build a synapse: signaling pathways in neuromuscular junction assembly. *Development*. 137:1017–1033. http://dx.doi.org/10.1242/dev.038711

Wu, X., Q.T. Shen, D.S. Oristian, C.P. Lu, Q. Zheng, H.W. Wang, and E. Fuchs. 2011. Skin stem cells orchestrate directional migration by regulating microtubule-ACF7 connections through GSK3β. *Cell*. 144:341–352. http://dx.doi.org/10.1016/j.cell.2010.12.033

Zhang, B., S. Luo, Q. Wang, T. Suzuki, W.C. Xiong, and L. Mei. 2008. LRP4 serves as a coreceptor of agrin. *Neuron*. 60:285–297. http://dx.doi.org/10.1016/j.neuron.2008.10.006

Zumbrunn, J., K. Kinoshita, A.A. Hyman, and I.S. Näthke. 2001. Binding of the adenomatous polyposis coli protein to microtubules increases microtubule stability and is regulated by GSK3 beta phosphorylation. *Curr. Biol.* 11:44–49. http://dx.doi.org/10.1016/S0960-9822(01)00002-1

Schmidt et al., http://www.jcb.org/cgi/content/full/jcb.201111130/DC1

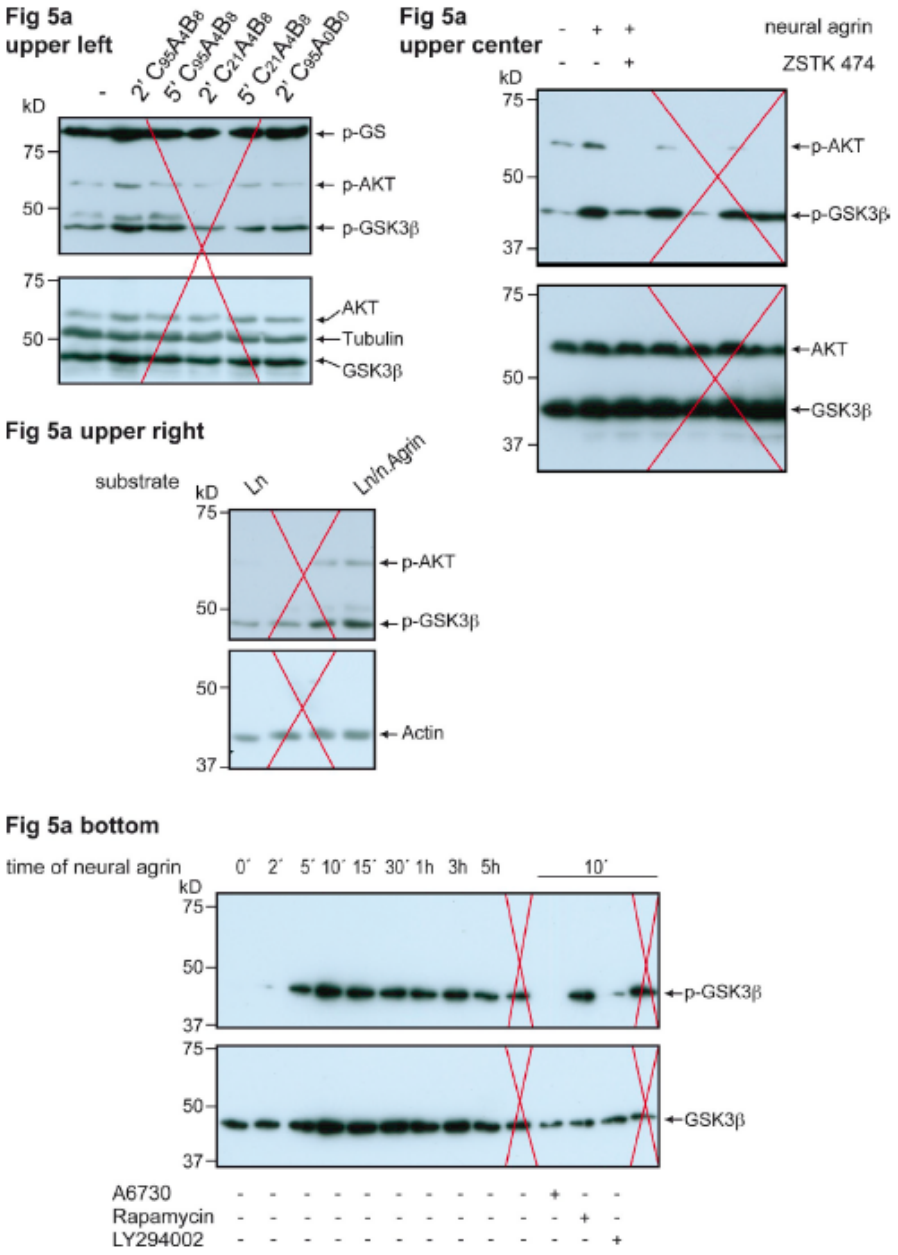

Figure S1. **Full scans of blots shown in Fig. 5 a.** Sections irrelevant for the images shown in the figure are crossed out.

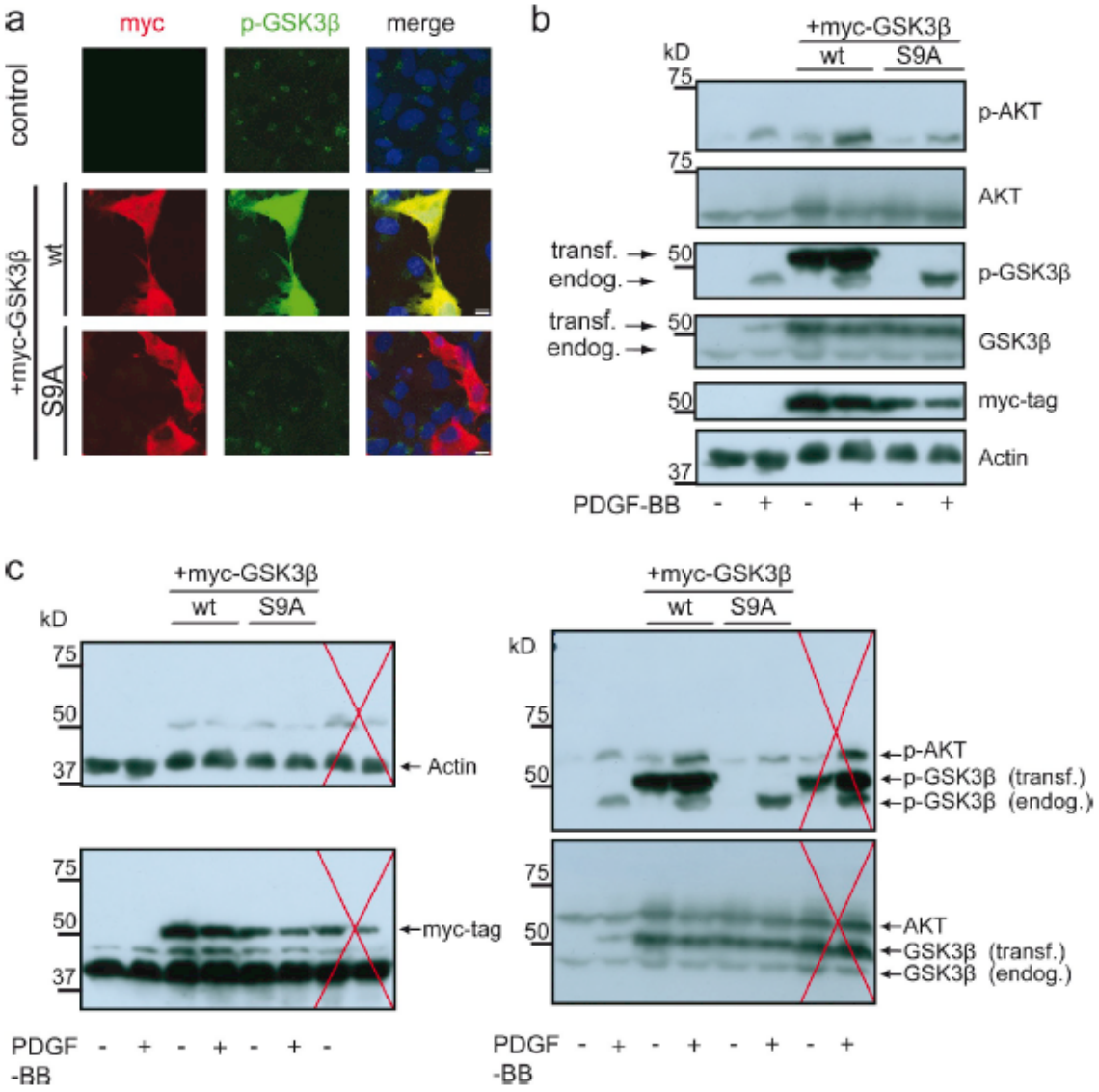

Figure S2. **Antibody no. 9336 (Cell Signaling Technology) specifically detects GSK3β-(Ser9)P.** (a) Parallel Cos1 cell cultures were left untransfected or they were transfected with expression constructs coding for myc-GSK3β-Ser9 (wt) or for myc-GSK3β-Ser9Ala (S9A). Cultures were either stained with DAPI and anti-myc or anti-GSK3β-(Ser9)P (a), or lysates were subject to WB (b) with same antibodies and those indicated in (c). In untransfected control cultures both immunofluorescence and WB show minor myc-GSK3β-(Ser9)P immunoreactivity (green) localized in the Golgi adjacent to the nuclei (blue). Transfected cells visualized by myc immunoreactivity (red) show strong myc-GSK3β-(Ser9)P immunoreactivity (green), but only when transfected with constructs for myc-GSK3β-Ser9 (wt, due to autophosphorylation), but not with myc-GSK3β-Ser9Ala (S9A). Bars, 20 μm. (c) Full scans of blots shown in b. Sections irrelevant for the images shown in the figure are crossed out.

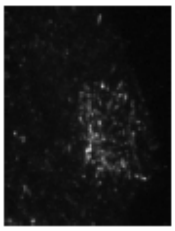

Video 1. **GFP-CLIP-170 comets are captured at agrin-induced AChR clusters.** Dynamics of GFP-CLIP-170 decorated MT plus ends in a myotube derived from a *GFP-Clip-170*$^{ki/ki}$ mouse. Note the immobilization and increased CLIP-170 loads within compared with outside of the agrin-induced AChR cluster (marked in Fig. 6 b). Frames are acquired over a period of 160 s (1 frame per second) in the TIRF plane (inverted TIRF microscope [TE2000; Nikon] equipped with an oil immersion HCX PL APO 100x TIRF objective [NA = 1.49]).

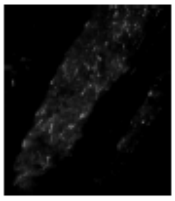

Video 2. **Deletion of CLASP2 impairs capturing of GFP-CLIP-170 comets at agrin-induced AChR clusters.** Dynamics of GFP-CLIP-170 decorated MT plus ends in a myotube derived from a *GFP-Clip-170*$^{ki/ki}$ mouse deficient in CLASP2. Note that deletion of CLASP2 abolishes the difference in MT plus-end dynamics within and outside the agrin-induced AChR cluster (marked in Fig. 6 e). Image acquisition as in Video 1.

III.2. Manuscript II

"Agrin-induced microtubule capture at the NMJ is mediated by GSK3β-dependent binding of CLASP2 to MT plus-ends interacting with LL5β"

Sladecek S.[*,1], *Basu S.*[*,1] *& Brenner H.-R.*[1]

[1]Department of Biomedicine, Institute of Physiology, University of Basel, CH-4056 Basel, Switzerland

*equal contribution

Contribution to this manuscript: For this publication, I was involved in experimental design, conduction and analysis. I contributed Figure 1, Figure 5 and was responsible for the cloning of RNAi-constructs, which were used to generate Figure 6.

Status of Publication: ready to submit

Agrin-induced microtubule capture at the NMJ is mediated by GSK3β-dependent binding of CLASP2 to MT plus-ends interacting with LL5β

by

Stefan Sladecek*, Sreya Basu* and Hans Rudolf Brenner

Institute of Physiology, Department of Biomedicine,
University of Basel

*equal contribution

Abstract

One way for neural agrin to regulate the clustering of acetylcholine receptors (AChR) at the neuromuscular junction is by locally stabilizing microtubules at the synaptic membrane through the plus-end tracking protein CLASP2. Here we investigate the molecular mechanism involved in this process. We show that constitutively active GSK3β inhibits agrin-induced AChR clustering in cultured myotubes, and that this inhibition is rescued by forced expression of a non-phoshorylatable CLASP2 mutant, but not by wt CLASP2. This indicates that the inhibitory effect of GSK3β on AChR clustering is caused at least partly by phosphorylation of CLASP2, thus interfering with CLASP2 binding to microtubule plus-ends and microtubule capture. Consistent with this, we observe that agrin-induced MT plus-end capture is inhibited by expression of phospho-mimetic CLASP2. These findings are in agreement with the idea that active GSK3β phosphorylates CLASP2, thus lowering its binding to MT plus-ends and, consequently, CLASP2-mediated MT capturing. One candidate for mediating CLASP2-dependent MT capture at the synapse is LL5β. Indeed, LL5β accumulates at synaptic membranes of the NMJ via a process involving its PH domain, suggesting recruitment of LL5β by local PI3K activation. At agrin-induced AChR clusters in cultured myotubes, LL5β is co-localized with increased density of MT plus-ends. Conversely, RNAi-mediated knock-down of LL5β expression in myotubes abolishes the increase in MT plus-end density normally observed at agrin-induced AChR clusters. Our experiments combined strongly suggest that agrin-induced MT capturing is mediated by 1.) local inactivation of GSK3β, thus, locally increasing CLASP2 binding to MT plus-ends, 2.) recruitment of LL5β to the synaptic membrane via local activation or PI3K, and 3.) local CLASP2/LL5β interaction.

Introduction

The density of neurotransmitter receptors in the postsynaptic membranes of synapses is determined by the rate of their insertion into, their stability at, as well as by their removal from the postsynaptic membrane. In turn, these parameters are regulated by signals from the presynaptic nerve terminal and by the impulse traffic at the synapse. At central synapses, the mechanisms by which they regulate postsynaptic receptor numbers are poorly understood. At the best-investigated synapse, the NMJ in the peripheral nervous system, the major presynaptic organizer of postsynaptic receptor density is agrin (Ngo et al., 2007; Wang et al., 2006; Wu et al., 2010), a heparansulfate proteoglycan secreted from the motor nerve terminal and acting through its receptor/effector LRP4/MuSK, in the muscle fiber membrane. Agrin on its own is sufficient to induce differentiation of functional synaptic membranes *in vivo* in the absence of motor nerves (Jones et al., 1997).

Postsynaptic muscle differentiation by agrin involves the induction of genes in the muscle nuclei underlying the synapse coding for both AChRs as well as for components of the subsynaptic apparatus, respectively (Brenner et al., 1990; Jones et al., 1997). The latter serve to mediate impulse-independent signaling between pre- and postsynaptic structures, such as agrin/LRP4/MuSK and neuregulin/ErbBs, as well as for the anchoring of the AChRs to the postsynaptic cytoskeleton through components such as rapsyn, utrophin, dystroglycan, and alpha-dystrobrevin (Banks et al., 2003; Moransard et al., 2003; Schmidt et al., 2011; Wu et al., 2010). In turn, the function of the postsynaptic apparatus appears to be regulated by the electrical impulse traffic at the synapse, as action potential activity in the muscle fiber regulates synaptic AChR stability through unknown mechanisms involving Ca^{++} (Caroni et al., 1993; Fumagalli et al., 1990; Megeath et al., 2003; Rotzler and Brenner, 1990).

Whereas the importance of the postsynaptic apparatus for synaptic AChR density has been established on a descriptive level (Kummer et al., 2006;

Sanes and Lichtman, 2001), the molecular mechanisms by which AChR insertion, stability and/or removal are regulated, have remained largely obscure. Recently, we have identified agrin-dependent capturing of microtubules at the synaptic muscle membrane as one mechanism promoting synaptic AChR insertion. Specifically, we proposed that agrin through activation of PI3K and inactivation of GSK3β, leads to the local capture of the plus-ends of dynamic MTs at the synaptic membrane via a process involving the MT plus-end proteins (+TIPS) CLASP2 and CLIP-170 (Schmidt et al., 2012). Agrin/CLASP2/CLIP-170-mediated MT capturing in turn directs the focal AChR insertion into the synaptic membrane, presumably through vesicle transport along microtubules. However, the mechanisms linking synaptic GSK3β inactivation to CLASP2-dependent synaptic MT capturing remained open. Here, using cultured primary myotubes, we present evidence that CLASP2 is locally dephosphorylated at the synapse, thus increasing its affinity to MT plus-ends, which are then captured to the synaptic membrane by interacting with synaptic LL5β, which is recruited to the synapse via active PI3K downstream of agrin.

Results

At the NMJ, capturing of CLIP-170 tagged microtubules and the insertion of AChRs into the synaptic muscle membrane depends on the presence of the microtubule plus-end protein (+TIP) CLASP2 (Schmidt et al., 2012). Given the reduction of CLASP2 binding to EB proteins/MT plus-ends by GSK3β-induced phosphorylation of CLASP2 in fibroblasts (Akhmanova et al., 2001; Kumar et al., 2009; Watanabe et al., 2009), and inactivation of GSK3β through phosphorylation downstream of agrin in cultured myotubes (Schmidt et al., 2012), we proposed that CLASP2-dependent synaptic MT capturing is mediated through CLASP2 de-phosphorylation induced by agrin, thus promoting CLASP2 binding to MT plus-ends (Schmidt et al., 2012). In our previous work, however, the roles of GSK3β inactivation through phosphorylation in synaptic AChR clustering, and of the phosphorylation state

of CLASP2 for synaptic MT capturing were not examined, nor was the interaction partner of CLASP2 in synaptic MT capturing identified.

Active GSK3β inhibits agrin-induced AChR clustering

To test for an effect of GSK3β activity on AChR cluster formation, primary myotubes were grown on a substrate of laminin which had been impregnated with chicken NtAcAgrin748, a fusion of the laminin-binding domain (NtA) and of cAgrinA_4B_8 (Denzer et al., 1997; Denzer et al., 1995), the C-terminal half of neural agrin comprising 4aa and 8aa splice inserts associated with agrin effectivity, to induce AChR clusters in myotubes (Gesemann et al., 1995; Ruegg et al., 1992). When agrin was used on untreated myotubes, numerous AChR clusters formed. In contrast, when myotubes were infected with an adenoviral expression construct for non-phosphorylatable and, thus, constitutively active GSK3β-S9A, the number of agrin-induced AChR clusters was strongly reduced (Fig. 1a). This suggests that active GSK3β may inhibit AChR cluster formation through phosphorylation of CLASP2.

AChR cluster formation and synaptic MT capture depends on non-phosphorylated CLASP2

If so, then inhibition of AChR cluster formation by GSK3β-S9A should be relieved by expression of a non-phosphorylatable CLASP2 construct GFP-CLASP2-9xS/A (Kumar et al., 2009). In this construct, all 9 serine residues normally phosphorylated by GSK3β are rendered non-phosphorylatable by substitution with alanine, thus promoting unrestricted CLASP2 binding to EBs at MT plus-ends (Kumar et al., 2009; Watanabe et al., 2009). Indeed, even in the presence of GSK3β-S9A, adenoviral infection of myotubes grown on laminin/agrin with GFP-CLASP2-9xS/A strongly promoted agrin-induced AChR clustering; in contrast, expression of wild type GFP-tagged CLASP2 did not rescue AChR clustering (Fig. 1b).

Next, we examined, whether MT capturing at agrin-induced AChR clusters was dependent on the phosphorylation of CLASP2. To this end, wild type

myotubes grown on laminin with patches of agrin attached (20-60 µm in diameter) were infected with expression constructs coding for either GFP-tagged CLASP2-9xS/A (phosphorylation-resistant) or GFP-tagged CLASP2-8xS/D (phospho-mimetic), respectively. CLASP2-8xS/D mimics GSK3β phosphorylation at 8 out of these 9 serine residues, thus reducing CLASP2 binding to MT plus-ends (Kumar et al., 2009). AChR clusters were stained with α-Btx-Alexa-594, and the dynamics of MT plus-ends decorated with GFP-CLASP2 fluorescence were observed by TIRF microscopy.

As expected from (Kumar et al., 2009), the difference in affinity of CLASP2-8xS/D vs. CLASP2-9xS/A to MT plus-ends was readily seen from comets outside the AChR clusters in myotubes expressing the respective CLASP2 mutants. In myotubes expressing phospho-mimetic CLASP2, comets could barely or not at all be resolved against the background of overexpressed mutant (Fig. 2a,b). In contrast, in myotubes expressing CLASP2-9xS/A examined at identical laser power and gain, comets appeared much brighter, consistent with high affinity of this CLASP2 mutant for EBs/MT plus-ends in cultured fibroblasts (Fig. 2c,d). Inside the agrin-induced AChR clusters, the appearance of GFP fluorescence was very bright, and it appeared either striped and immobile (Fig. 2a,c) or unstructured (Fig. 2b,d). This pattern was observed both in myotubes expressing GFP-CLASP2-9xS/A and those expressing GFP-CLASP2-8xS/D. Examination of GFP stripes for dynamic activity with kymograms confirmed that the vast majority of MT plus-ends was completely immobile (Fig. 2a,c,e). This was in contrast to the GFP signals from immobile comets in GFP-CLIP-170-KI mice, where GFP fluorescence along a kymogram varied in in time, location and intensity (Fig. 2e, right). We attribute the striped and unstructured GFP fluorescence at AChR clusters to binding of free GFP-CLASP2 mutant to LL5β, such that capturing of MT-bound CLASP2 by LL5β would be partially inhibited, as well as to obscuring the comets at the AChR cluster by this LL5β-bound, but 'MT-free' GFP-CLASP2.

According to our hypothesis, +TIP comets should be enriched at AChR clusters in myotubes expressing CLASP2-9xS/A, but not in myotubes expressing GFP-CLASP2-8xS/D. However, for the reasons explained above, the dynamic behavior of GFP-CLASP2-tagged comets inside the AChR clusters could not be observed. To circumvent these problems, we visualized dynamic MTs independently of their CLASP2 binding in fixed myotubes by staining MT plus-ends with an antibody to EB3, a core +TIP expressed in cultured myotubes (Schmidt et al., 2012; Straube and Merdes, 2007). Indeed, enrichment of EB3-decorated comets was seen at agrin-induced AChR clusters upon infection with GFP-CLASP2-9xS/A, but not with GFP-CLASP2-8xS/D (Fig. 3). Combined, these data suggest strongly that agrin mediates synaptic MT capturing by lowering the level of CLASP2 phosphorylation at the synapse, thus promoting its binding to MT plus-ends to allow their capture to the synaptic membrane.

CLASP2-dependent, synaptic MT capture is mediated by LL5β

The experiments described above indicate that MT capturing at agrin-induced AChR clusters is mediated by regulation of CLASP2 binding to MT plus-ends. In fibroblasts, LL5β can mediate the CLASP2-dependent attachment of MT plus-ends to the cell cortex (Lansbergen et al., 2006). LL5β is highly enriched in the subsynaptic membrane of the NMJ (Kishi et al., 2005), both through increased expression of the *Phldb2* gene selectively by the subsynaptic myonuclei and through recruitment of its protein product LL5β via a PH domain (Kishi et al., 2005), which is known to bind to PIP_3 (Paranavitane et al., 2003). Given the local activation of PI3K by agrin (Schmidt et al., 2012), LL5β is thus a prime candidate to mediate CLASP2-dependent MT capture to the subsynaptic muscle membrane. To test this hypothesis, we first examined, whether LL5β was recruited to the synaptic membrane in a manner depending of the PIP_3-binding function of its PH domain. To this end, expression constructs coding for GFP-LL5β or for GFP-LL5β-mut, in which two point mutations in its PH domain abolish LL5β binding to PIP_3 (Paranavitane et al., 2003), were electroporated into mouse soleus muscle. Two to three

weeks later, the intensities of GFP fluorescence at the synaptic relative to that in extra-synaptic membrane were compared (Fig. 4). In fibers expressing GFP-LL5β-mut, this ratio was about five times lower than in fibers expressing wild type GFP-LL5β, consistent with the recruitment of LL5β to PIP_3 in the synaptic membrane via its PH domain.

Next we examined whether LL5β is recruited to the synaptic membrane by agrin. To this end, myotubes grown on laminin-attached agrin patches were stained for AChRs and LL5β. Consistent with recruitment by agrin, LL5β was elevated at agrin-induced AChR clusters (Fig. 5); however, the distribution over the cluster area was uneven: in some regions of the AChR cluster, patches of well circumscribed, elevated levels of LL5β were seen that co-localized with elevated AChR levels (Fig. 5a); in other regions of the same cluster, levels were lower, but above those in areas outside the cluster. Patches of elevated LL5β appeared usually unstructured, but in some, LL5β was patterned in stripes (Fig. 5a) reminiscent of the stripes of GFP fluorescence seen at clusters in myotubes expressing GFP-CLASP2-8xS/D or 9xS/A (see Fig. 2). Unlike in laminin-induced AChR clusters, however, we did not observe complementary distribution of AChRs and LL5β, nor was LL5β preferentially located along the edge of the agrin-induced AChR clusters, as described before (Kishi et al., 2005).

If CLASP2-dependent MT capturing at AChR clusters is mediated by LL5β, CLASP2-decorated MTs will be enriched at patches of elevated LL5β, and knock-down of LL5β by RNAi will abolish such an enrichment. Indeed, in myotubes expressing wild type GFP-CLASP2 and stained for GFP, LL5β and AChRs, the density of GFP-positive comets was significantly higher inside than outside AChR cluster, and was particularly increased at patches of enriched LL5β (Figure 5b, bar graph).

Conversely, knocking down endogenous LL5β expression level by RNAi abolished the concentration of comets at AChR clusters. Cultured myotubes

grown on agrin patches were infected with either of two different lentiviruses expressing shRNA targeting LL5β, or for scrambled shRNA, respectively. To exclude potential interference of overexpressed GFP-CLASP2 in these experiments, MT plus-ends were visualized by immunofluorescence staining for EB3 (Fig. 6a) to study the effect of LL5β knock-down on MT plus-end density inside vs. outside AChR clusters, EB3-positive plus-ends were about twice as numerous at agrin-induced AChR clusters in myotubes expressing a scrambled construct than in myotubes expressing a shRNA construct that effectively knocked down endogenous levels of LL5β protein (Fig. 6a-c). Similarly, in the latter, the size of agrin-induced AChR clusters was significantly reduced (Fig. 6d).

Taken together, these experiments indicate that CLASP2-dependent MT capture at agrin-induced AChR clusters is mediated by the interaction of CLASP2 with LL5β recruited to the synaptic membrane via agrin-dependent activation of PI3K.

Discussion

Our results support a mechanism for MT capture at the synaptic muscle membrane that shares similarities with one first proposed for MT capturing at the leading edge of migrating cells (Akhmanova et al., 2001; Wittmann and Waterman-Storer, 2005). Specifically, our previous (Schmidt et al., 2012) and present data combined suggest that local inactivation of GSK3β at the synaptic membrane by nerve-derived agrin keeps CLASP2 at the synapse in a de-phosphorylated state, thus locally enhancing its affinity for MT plus-ends. MT plus-end-bound CLASP2 then interacts with LL5β, which is enriched at the synaptic membrane by elevated expression of its gene *Phldb2* from the subsynaptic nuclei and by recruitment of the protein product to the synaptic membrane through local activation of PI3K (Kishi et al., 2005).

Two lines of evidence support the involvement of focal GSK3 inactivation and, as a consequence, of local dephosphorylation of CLASP2 in synaptic MT

capturing: first, the inhibition of AChR clustering by constitutively active GSK3β (GSK3β-S9A) and its rescue by non-phosphorylatable GFP-CLASP2-9xS/A, and second, the enrichment of EB3 comets at AChR clusters in myotubes expressing wt or non-phosphorylatable GFP-CLASP2-9xS/A, but not by phospho-mimetic GFP-CLASP2-8xS/D. These CLASP2 mutants comprise serines that are physiological targets of GSK3β phosphorylation and are within the CLASP2 domain required for binding to EB proteins and MT plus-end tracking (Kumar et al., 2012; Kumar et al., 2009; Watanabe et al., 2009).

In contrast to migrating epithelial cells, however, where stabilization of lamella MT is mediated by non-phosphorylated CLASP2 bound and interacting with the cell cortex along the MT lattice (Kumar et al., 2009), MT capturing at agrin-induced AChR clusters in the myotubes appears to be initiated by the highly dynamic plus-ends. This is suggested by differences in MT dynamics and staining at AChR clusters of myotubes (this study and (Schmidt et al., 2012)) vs. the lamellae of migrating cells (Wittmann and Waterman-Storer, 2005). First, CLASP2 distribution is restricted to MT plus-ends comets at agrin-induced AChR clusters, whereas at lamella MTs, GFP-CLASP2 binds heavily also along the lattice of MTs (Wittmann and Waterman-Storer, 2005). Second, at AChR clusters, EB3 comet density is higher than outside, and the dynamics of the CLIP-170 comets are strongly reduced; in contrast, the dynamics of EB3 and of CLIP-170 comets are not altered as they enter the lamellae of migrating cells (Wittmann and Waterman-Storer, 2005).

A plausible explanation for these differences could be the geometries of the muscle cell around the AChR clusters vs. that of the lamella of migrating cells: in muscle cells, inactive phospho-GSK3β is highly enriched at the synaptic membrane (Schmidt et al., 2012), suggesting that it declines sharply with distance into the myoplasm where GSK3β is active. If so, CLASP2 binding to MT plus-ends would increase to interact with the cell cortex only as the dynamic MT reach the immediate vicinity of the synaptic

membrane. In contrast, in the large flat region of the lamellae of migrating cells, CLASP2 binds heavily to lattice MTs to interact with the cell cortex. The pronounced decrease of their density in cells expressing constitutively active GSK3β-S9A suggests that inactive phospho-GSK3β is ubiquitous in the lamellae, thus favoring unphosphorylated CLASP2 and, consequently its binding to MTs (including lattice) over large distances.

A likely interaction partner of MT plus-end-bound CLASP2 mediating MT capturing at the cell cortex is LL5β (Drabek et al., 2006; Lansbergen et al., 2006). LL5β is expressed by subsynaptic nuclei and recruited to the synaptic membrane of the NMJ ((Kishi et al., 2005) and Fig. 4) by agrin though PI3K activation; it is also elevated at agrin-induced AChR clusters in cultured myotubes (Fig. 5). However, unlike at the NMJ (Kishi et al., 2005), the distribution of LL5β is not uniform across the AChR clusters, but is higher in certain regions than in others, and at some of these sites, is arranged in stripes. The reasons for this LL5β distribution pattern are not clear. However, it can explain the GFP staining frequently observed in myotubes expressing wild type GFP-CLASP2 and the phosphorylation-resistant and phospho-mimetic mutants, respectively. As illustrated in Fig. 2, in some myotubes expressing GFP-CLASP2 mutants and observed with TIRF microscopy, GFP fluorescence at AChR clusters was organized in stripes reminiscent of LL5β stripes, even though, in the case of the phospho-mimetic mutant, CLASP2-8xS/D-decorated comets, due to low CLASP affinity for MTs, could not or only barely be resolved. This suggests that the striped and unstructured GFP signal observed in these myotubes represents overexpressed GFP-CLASP2 (wt or mutant) bound to agrin-induced LL5β, but not to MTs. Indeed, the association of CLASP2 with the cell cortex is MT independent (Mimori-Kiyosue et al., 2005).

Most importantly, however, the density of MTs decorated with wt GFP-CLASP2 was higher inside the AChR clusters than outside, and it was highest within the clusters where LL5β was most prominent (Fig. 5b). Conversely, in

myotubes in which LL5β expression was knocked-down by RNAi, the increase in the density of comets at AChR clusters was abolished. Combined, these experiments strongly suggest that synaptic MT capturing is mediated by the interaction of MT plus-end-bound CLASP2 and LL5β at the synaptic membrane. Both, CLASP2 binding to MT plus-ends and LL5β relocation to the synaptic membrane occur downstream of agrin-induced PI3K activation.

Methods

Animals

For electroporation, C57BL/6 mice, 8-12 weeks of age, were anesthetized with ketamine (87 mg per kg body weight) and xylazine (13 mg per kg body weight). Postoperative analgesia was by 4 injections of buprenorphine at 12-h intervals. Mice were sacrificed with CO_2. Animal handling was approved by the Cantonal Veterinary Office of Basel-Stadt.
Depending on experimental suitability, soleus (for electroporations), or sternomastoid muscles (for immunofluorescence stainings of teased muscle fibers) were used.

Constructs

To suppress expression of endogenous LL5β, two siRNA sequences were selected and modified for expression as shRNA and transduced into myotubes by lentiviral infection: One was sequence No. 2 from (Kishi et al., 2005), another (No. 4) was designed using the siRNA Selection Server at the Whitehead Institute at the Massachusetts Institute of Technology (http://jura.wi.mit.edu/siRNAext/), see (Yuan et al., 2004). The mouse genome was searched with selected sequences to ensure their specificity. DNA oligos were designed based on chosen targeting sequences according to the guidelines of the shRNA expression vector pLKO.1 (Sigma) and purchased from Microsynth (Balgach, Switzerland). After annealing, oligonucleotides were ligated into AgeI/EcoRI-digested pLKO.1, expanded,

checked by restriction digest and sequenced. After sequence verification, lentiviral particles were produced in 293T cells by co-transfection of pLKO.1 with pMD2-G and pPAX2, which together encode all necessary lentiviral proteins. Targeting sequences cloned into pLKO.1 were shLL5β No. 2: AAGCCTAAGACAGTCGTCAGA; shLL5β No. 4: AATGGTAGCTTAGAGGAAGGA; shLL5β scrambled: AACGTAATCGCGTACGACGAA; all sequences are denoted in sense orientation. To allow visualization of single shRNA infected cells, pLKO.1 including a targeting shRNA sequence was modified by replacing the puromycin selection cassette between the BamHI and NsiI sites with cDNA of Histone2B–mRFP (a gift of E.Fuchs, Rockefeller University) amplified by PCR using BglII- and NsiI-flanked primers, analogous to a strategy described in (Beronja et al., 2010).

Adenoviral mRFP-GSK3β-S9A expression construct as well as adenoviral wild type and mutant GFP-CLASP2 expression constructs (all covered aa340-1362 of hCLASP2), were a kind gift of T. Wittmann, UCSF and described elsewhere (Kumar et al., 2009; Wittmann and Waterman-Storer, 2005). GFP-tagged wild type and mutant LL5β were a gift from Len Stephens, Brabham Institute and described elsewhere (Paranavitane et al., 2003).

Antibodies and chemicals

LL5β antibody was a gift from Joshua Sanes, Harvard University and described elsewhere (Kishi et al., 2005). All other antibodies were commercial products: anti-GFP (from chicken) was from Invitrogen, polyclonal rabbit anti-hEB3 was from Absea and anti-β-Tubulin was from BD Bioscience. Secondary antibodies were Alexa-conjugated goat anti–rabbit, goat anti–mouse, or goat anti–rat antibodies (Invitrogen) as well as donkey anti–chicken Cy2 (Jackson ImmunoResearch). HRP-conjugated secondary antibodies were from Santa Cruz. AChRs were labeled with α-BTX–Alexa 488, 594, or 647 (Invitrogen). Ringer's solution was obtained from Braun. Phosphatase inhibitors PIC1 and 2 were purchased from Sigma-Aldrich, Complete protease inhibitors from Roche and transfection reagent Fugene HD

from Promega. Antibiotic/antimycotic solution was purchased from Gibco; basic FGF was purchased from Invitrogen.

Generation of adenoviral and lentiviral particles

To generate adenoviral particles for protein expression in myotubes, adenoviral vectors were linearized by PacI digest to expose the viral ITR, precipitated, washed, resuspended and transfected into the adenovirus-producing 293Ad cells. On the next day, the medium was exchanged and cells were allowed to accumulate adenoviral particles intracellularly for 10-14 days, until visible regions of cytopathic effect (CPE) were observed. Cells were then scraped off, centrifuged, the pellet was resuspended in PBS and subjected to four consecutive freeze/thaw cycles using MeOH at -80°C and cell thawing at 37°C to release adenoviral particles into solution. Cell debris was collected by centrifugation at 3 krpm for 15 minutes at RT. The supernatant containing viral particles was used to infect 293Ad cells, in order to amplify the viral stock to high titer. After 3-5 days, when visible regions of cytopathic effect were observed, cells were harvested and processed as described above. Finally, viral supernatants were aliquoted and stored at -80°C. In some cases, we were provided with ready-made adenoviral particles, which were either used directly or amplified in 293Ad cells as described above.

To generate lentiviral particles for RNAi-mediated gene silencing in myotubes, the lentiviral vector pLKO.1 (Invitrogen) containing the respective targeting sequences was co-transfected with pPAX2 and pMD2.G, which together encode all necessary lentiviral proteins. Vectors were used in molar ratio 3:2:1. On the next day, medium was changed; 48 hours later, viral supernatant was collected and concentrated 100x by using Lenti-X concentrator (Clontech). Finally, viral suspensions in PBS were aliquoted and stored at -80°C.

Cell culture

C2C12 myoblasts were expanded on dishes pre-coated with 0.2% gelatin in DMEM containing 20% FCS, 1% antibiotic/antimycotic solution and 20mM HEPES. For experiments, cells were seeded on laminin-coated dishes containing patches of either painted neural agrin or neural agrin deposited by transfected Cos cells (see next section for details). When cells reached confluency, cultures were switched to DMEM containing 2% horse serum, 1% antibiotic/antimycotic solution and 20mM HEPES to induce fusion. Cultured myotubes were either stained live with 1μg/ml fluorophore-conjugated α-BTX for 30 minutes and then fixed, permeabilized, and stained or, staining with α-BTX occurred along with the secondary antibodies after fixation/permeabilization.

For gene delivery using conventional transfection, myoblasts were transfected at confluency, immediately before switching to fusion medium using FuGENE6 (Roche). For adenoviral and lentiviral transduction, cells were infected after formation of myotubes.

Preparation of primary muscle cultures

Neonatal leg muscles from wild-type muscle were minced, dissociated with collagenase type IV and dispase type II, and cells were plated on a laminin substrate in DMEM containing 2 mM glutamine, 20% FCS, 5 ng/ml recombinant human basic FGF, and 1% antibiotic/ antimycotic solution. After 2 d, cells were resuspended in PBS by brief trypsinization, treated with rat monoclonal anti–mouse α7-integrin antibody, and purified using (magnetic) Dynabeads coated with sheep anti–rat IgG and a Dynal-MPC-L magnetic particle concentrator (Blanco-Bose et al., 2001; Escher et al., 2005). Myotubes were cultured on laminin-coated dishes focally impregnated with agrin. For the preparation of the dishes, COS-1 cells, transfected with a plasmid coding for full-length chicken agrin (Jones et al., 1996), were seeded at a density of 7–20 x 10^3 cells per 30 mm laminin-coated culture dish. After 48 h cells were extracted for 1 h in 2% Triton X-100 in PBS, followed by intense washing (6–8x 1 h PBS) and myoblast seeding (Schmidt et al.,

2011). Subsequent differentiation was in DMEM, 5% horse serum, and 1% antibiotic/antimycotic solution. For biochemistry, 6-well dishes were coated with 10 µg/ml laminin (Invitrogen) followed by coating with agrin solution (0.5 µg/ml, 37°C, 2 h) before cell plating (Schmidt et al., 2011). It should be noted that throughout the present paper, agrin was applied attached to the culture substrate rather than in solution to mimic the in vivo situation.

Confocal microscopy

Confocal microscopy was performed as described before (Schmidt et al., 2012). Briefly, myotubes were imaged with an SPE confocal scanning laser microscope (DMI 4000B; Leica) at a resolution of 1024 × 1024 pixels using an HCX PL APO 100x objective (NA 1.46) or an ACS APO 63x objective (NA 1.30). Image stacks were acquired with a step size of 300 nm. For comparison of different samples the same laser settings were applied. Quantitative differences potentially due to changes in the light source or camera were excluded by imaging control and treated cells within the same session.

Immunofluorescence

To stain +TIPs and other proteins, myotube culture dishes were dropped into -80°C methanol for 15 minutes, then transferred to a 1:1 mixture of methanol and 4% PFA at -20°C for 15 minutes, followed by 10 minutes in 4% PFA at RT and 10 minutes in 100 mM glycine. After permeabilization in PBS/0.5% Triton X-100 (RT, 30 minutes), cells were blocked in PBS/0.5% Triton X-100/5% BSA. Primary and secondary antibodies were diluted in blocking solution and were applied at 4°C overnight (primary Abs) or at RT for 45 min (secondary Abs).

Quantification of CLASP2 comets in LL5β patches at agrin-induced AChR cluster

Myotubes were infected with GFP-CLASP2 adenovirus and 48-72 hours later fixed and processed for immunofluorescence as described above. Staining was performed using antibodies for LL5β and GFP and using fluorophore-

conjugated α-BTX to visualize AChR. Confocal images were taken and analyzed by counting GFP-CLASP2 comets. A total of 10 cells was analyzed, all of which showed enrichment of CLASP2-comets at AChR clusters and further enrichment inside LL5β patches within AChR clusters. To ensure reliable quantification and to exclude variations stemming from small overall number of comets within a cell, only cells with a total amount of >10 CLASP2 comets were included into the quantification (6 cells out of 10). Significance was tested using the two-sided student t-test.

Total internal reflection microscopy

Dynamics of GFP-CLASP2 comets were measured in primary myotubes derived from C57BL/6 mice infected with GFP-CLASP2 constructs as indicated, 48 hours post infection. Agrin-induced AChR clusters were stained with α-BTX–Alexa 594 (1 µg/ml, 30 min), and after washing with pre-warmed DMEM, cells were incubated at 37°C for 1 h prior to imaging. Cells were imaged at 37°C in Krebs Ringer´s solution (140 mM NaCl; 5 mM KCl, 1 mM Mg^{2+}, 2 mM Ca^{2+}, 20 mM Hepes, 1 mM $NaHPO_4$, and 5.5 mM glucose) at pH 7.4. Online fluorescence images were acquired using an inverted TIRF microscope (TE2000; Nikon) equipped with an oil immersion CFI Plan Apochromat 100× TIRF objective (1.49 NA) and an electron multiplier CCD camera (C9100-13, Hamamatsu Photonics; (Treves et al., 2010). The focus was maintained throughout the experiment with the help of a perfect focus system. GFP-CLASP2 dynamics were imaged for between 160-180 s with a rate of 1 frame per second (MetaMorph; Molecular Devices).

Quantitative analysis of +TIP comet dynamics

Dynamics of CLASP2 comets inside and outside agrin-induced AChR clusters were analyzed using Image J (National Institutes of Health). The maximum intensity projection of 180 frames was first used to outline comet traces within the imaged area, and kymographs were generated for selected traces using the Kymograph plugin for Image J from J. Rietdorf (Friedrich Miescher Institute, Basel, Switzerland), and A. Seitz (EMBL, Heidelberg, Germany).

Quantitative analysis of +TIP comets in fixed cells

Immunostaining was performed as described previously in cultured myotubes (Schmidt et al., 2012). The AChR cluster was defined as a region of interest (ROI) and total number of EB3 comets were counted using ImageJ. A similar ROI was selected outside the cluster for each cell, and EB3 comets were counted within this as well. The number of comets per unit area was then calculated in and outside of clusters to obtain EB3 comet density.

Analysis of LL5β localization in muscle fibers

40 µg of pGFP-LL5β or pGFP-LL5β-mut (Paranavitane et al., 2003) in 10 µl 0.9% NaCl was injected with a Hamilton syringe into the soleus muscle of anesthetized C57BL76 mice (8–10 wk old). After suturing the skin, 8 pulses (20 ms, 1 Hz, 200 V/cm) were applied to the leg using an ECM 830 electroporation system. 10–14 d later, electroporated soleus muscles were dissected, AChRs stained with 1 µg/ml α-BTX-Alexa 594 for 1 h at RT, fixed in 4% paraformaldehyde (PFA) for 2 h, placed in 30% sucrose/PBS overnight, and frozen. Muscles were then embedded and sectioned at 12-µm thickness in a cryostat (CM 1950; Leica). Sections were mounted in Citifluor and imaged using an ACS APO 63x/1.3 NA objective on an SPE confocal microscope (DMI 4000B; Leica).

For the measurement of synaptic GFP intensity, the α-BTX–stained synapse of GFP-positive fibers was defined as a region of interest (ROI). Using ImageJ (National Institutes of Health), green fluorescence in this synaptic ROI was measured, the ROI moved to the extra-synaptic region of the same fiber profile, and the extra-synaptic green fluorescence was measured. Because the level of GFP expression varies across fibers within an individual muscle, the ratio of green fluorescence at the synapse versus extra-synaptic regions was calculated individually for every fiber.

Quantitative analysis of AChR cluster size upon expression of constitutively active GSK3β alone or in combination with GFP-CLASP2 constructs

To analyze the effect of constitutive GSK3β on AChR clustering, myotubes were transduced with adenoviral particles encoding mRFP-GSK3β-S9A and 48-72 hours later fixed in 4% PFA for 5 minutes. Cells were stained for AChR clusters using fluorophore-conjugated α-BTX, while mRFP signal was imaged unstained, using intrinsic protein fluorescence.
Images were taken at low magnification (HC Plan Apo 20x/0.70 objective; inverted microscope [DMI 6000B; Leica]; 1394 ORCA-ERA camera [Hamamatsu Photonics], Volocity 6.0.1 [PerkinElmer]) and AChR cluster area was quantified using ImageJ (National Institutes of Health).

To analyze the effect of constitutive GSK3β on AChR clustering in combination with CLASP2 mutants, myotubes were transduced with the indicated adenoviral constructs and 48-72 hours later fixed in 4% PFA for 5 minutes. Cells were stained for AChR clusters using fluorophore-conjugated α-BTX. GFP and mRFP signals (from GFP-CLASP2 and mRFP-GSK3β-S9A, respectively) were imaged unstained, using intrinsic protein fluorescence. Images were taken at low magnification using a confocal microscope SPE confocal scanning laser microscope (DMI 4000B; Leica) at a resolution of 1024 × 1024 pixels and 20x magnification. AChR cluster area was quantified using ImageJ.

Immunoblotting

Myotubes were lysed in 3x SDS-lysis buffer (150 mM Tris, pH 6.8, 300 mM DTT, 6% SDS, 0.2% bromophenol blue, and 30% glycerol) supplemented with phosphatase inhibitors (1:100), protease inhibitors (1/10 tablet per ml lysis buffer), and 100 mM DTT. Lysates were denatured at 95°C for 5 min and separated by SDS-PAGE. Gels were electro-transferred onto PVDF membranes and developed with ECL after incubation with primary and secondary antibodies.

Literature

Akhmanova, A., C.C. Hoogenraad, K. Drabek, T. Stepanova, B. Dortland, T. Verkerk, W. Vermeulen, B.M. Burgering, C.I. De Zeeuw, F. Grosveld, and N. Galjart. 2001. CLASPs Are CLIP-115 and -170 Associating Proteins Involved in the Regional Regulation of Microtubule Dynamics in Motile Fibroblasts. *Cell*. 104:923-935.

Banks, G.B., C. Fuhrer, M.E. Adams, and S.C. Froehner. 2003. The postsynaptic submembrane machinery at the neuromuscular junction: requirement for rapsyn and the utrophin/dystrophin-associated complex. *J Neurocytol*. 32:709-726.

Beronja, S., G. Livshits, S. Williams, and E. Fuchs. 2010. Rapid functional dissection of genetic networks via tissue-specific transduction and RNAi in mouse embryos. *Nature medicine*. 16:821-827.

Blanco-Bose, W.E., C.C. Yao, R.H. Kramer, and H.M. Blau. 2001. Purification of mouse primary myoblasts based on alpha 7 integrin expression. *Experimental cell research*. 265:212-220.

Brenner, H.R., V. Witzemann, and B. Sakmann. 1990. Imprinting of acetylcholine receptor messenger RNA accumulation in mammalian neuromuscular synapses. *Nature*. 344:544-547.

Caroni, P., S. Rotzler, J.C. Britt, and H.R. Brenner. 1993. Calcium influx and protein phosphorylation mediate the metabolic stabilization of synaptic acetylcholine receptors in muscle. *The Journal of neuroscience : the official journal of the Society for Neuroscience*. 13:1315-1325.

Denzer, A.J., R. Brandenberger, M. Gesemann, M. Chiquet, and M.A. Ruegg. 1997. Agrin binds to the nerve-muscle basal lamina via laminin. *J Cell Biol*. 137:671-683.

Denzer, A.J., M. Gesemann, B. Schumacher, and M.A. Ruegg. 1995. An amino-terminal extension is required for the secretion of chick agrin and its binding to extracellular matrix. *J Cell Biol*. 131:1547-1560.

Drabek, K., M. van Ham, T. Stepanova, K. Draegestein, R. van Horssen, C.L. Sayas, A. Akhmanova, T. ten Hagen, R. Smits, R. Fodde, F. Grosveld, and N. Galjart. 2006. Role of CLASP2 in Microtubule Stabilization and the Regulation of Persistent Motility. *Current Biology*. 16:2259-2264.

Escher, P., E. Lacazette, M. Courtet, A. Blindenbacher, L. Landmann, G. Bezakova, K.C. Lloyd, U. Mueller, and H.R. Brenner. 2005. Synapses form in skeletal muscles lacking neuregulin receptors. *Science*. 308:1920-1923.

Fumagalli, G., S. Balbi, A. Cangiano, and T. Lomo. 1990. Regulation of turnover and number of acetylcholine receptors at neuromuscular junctions. *Neuron*. 4:563-569.

Gensler, S., A. Sander, A. Korngreen, G. Traina, G. Giese, and V. Witzemann. 2001. Assembly and clustering of acetylcholine receptors containing GFP-tagged epsilon or gamma subunits: selective targeting to the neuromuscular junction in vivo. *European journal of biochemistry / FEBS*. 268:2209-2217.

Gesemann, M., A.J. Denzer, and M.A. Ruegg. 1995. Acetylcholine receptor-aggregating activity of agrin isoforms and mapping of the active site. *The Journal of Cell Biology*. 128:625-636.

Jones, G., A. Herczeg, M.A. Ruegg, M. Lichtsteiner, S. Kroger, and H.R. Brenner. 1996. Substrate-bound agrin induces expression of acetylcholine receptor epsilon-subunit gene in cultured mammalian muscle cells. *Proceedings of the National Academy of Sciences of the United States of America*. 93:5985-5990.

Jones, G., T. Meier, M. Lichtsteiner, V. Witzemann, B. Sakmann, and H.R. Brenner. 1997. Induction by agrin of ectopic and functional postsynaptic-like membrane in innervated muscle. *Proceedings of the National Academy of Sciences of the United States of America*. 94:2654-2659.

Kishi, M., T.T. Kummer, S.J. Eglen, and J.R. Sanes. 2005. LL5β. *The Journal of Cell Biology*. 169:355-366.

Kumar, P., M.S. Chimenti, H. Pemble, A. Schönichen, O. Thompson, M.P. Jacobson, and T. Wittmann. 2012. Multisite Phosphorylation Disrupts Arginine-Glutamate Salt Bridge Networks Required for Binding of Cytoplasmic Linker-associated Protein 2 (CLASP2) to End-binding Protein 1 (EB1). *Journal of Biological Chemistry*. 287:17050-17064.

Kumar, P., K.S. Lyle, S. Gierke, A. Matov, G. Danuser, and T. Wittmann. 2009. GSK3β phosphorylation modulates CLASP–microtubule association and lamella microtubule attachment. *The Journal of Cell Biology*. 184:895-908.

Kummer, T.T., T. Misgeld, and J.R. Sanes. 2006. Assembly of the postsynaptic membrane at the neuromuscular junction: paradigm lost. *Current Opinion in Neurobiology*. 16:74-82.

Lansbergen, G., I. Grigoriev, Y. Mimori-Kiyosue, T. Ohtsuka, S. Higa, I. Kitajima, J. Demmers, N. Galjart, A.B. Houtsmuller, F. Grosveld, and A. Akhmanova. 2006. CLASPs Attach Microtubule Plus Ends to the Cell Cortex through a Complex with LL5β. *Developmental Cell*. 11:21-32.

Megeath, L.J., M.T. Kirber, C. Hopf, W. Hoch, and J.R. Fallon. 2003. Calcium-dependent maintenance of agrin-induced postsynaptic specializations. *Neuroscience*. 122:659-668.

Mimori-Kiyosue, Y., I. Grigoriev, G. Lansbergen, H. Sasaki, C. Matsui, F. Severin, N. Galjart, F. Grosveld, I. Vorobjev, S. Tsukita, and A. Akhmanova. 2005. CLASP1 and CLASP2 bind to EB1 and regulate microtubule plus-end dynamics at the cell cortex. *The Journal of Cell Biology*. 168:141-153.

Moransard, M., L.S. Borges, R. Willmann, P.A. Marangi, H.R. Brenner, M.J. Ferns, and C. Fuhrer. 2003. Agrin Regulates Rapsyn Interaction with Surface Acetylcholine Receptors, and This Underlies Cytoskeletal Anchoring and Clustering. *Journal of Biological Chemistry*. 278:7350-7359.

Ngo, S.T., P.G. Noakes, and W.D. Phillips. 2007. Neural agrin: a synaptic stabiliser. *The international journal of biochemistry & cell biology*. 39:863-867.

Paranavitane, V., W.J. Coadwell, A. Eguinoa, P.T. Hawkins, and L. Stephens. 2003. LL5beta is a phosphatidylinositol (3,4,5)-trisphosphate sensor that can bind the cytoskeletal adaptor, gamma-filamin. *The Journal of biological chemistry*. 278:1328-1335.

Rotzler, S., and H.R. Brenner. 1990. Metabolic stabilization of acetylcholine receptors in vertebrate neuromuscular junction by muscle activity. *J Cell Biol*. 111:655-661.

Ruegg, M.A., K.W. Tsim, S.E. Horton, S. Kroger, G. Escher, E.M. Gensch, and U.J. McMahan. 1992. The agrin gene codes for a family of basal lamina proteins that differ in function and distribution. *Neuron*. 8:691-699.

Sanes, J.R., and J.W. Lichtman. 2001. Induction, assembly, maturation and maintenance of a postsynaptic apparatus. *Nat Rev Neurosci*. 2:791-805.

Schmidt, N., M. Akaaboune, N. Gajendran, I. Martinez-Pena y Valenzuela, S. Wakefield, R. Thurnheer, and H.R. Brenner. 2011. Neuregulin/ErbB regulate neuromuscular junction development by phosphorylation of alpha-dystrobrevin. *J Cell Biol*. 195:1171-1184.

Schmidt, N., S. Basu, S. Sladecek, S. Gatti, J. van Haren, S. Treves, J. Pielage, N. Galjart, and H.R. Brenner. 2012. Agrin regulates CLASP2-mediated capture of microtubules at the neuromuscular junction synaptic membrane. *J Cell Biol*. 198:421-437.

Straube, A., and A. Merdes. 2007. EB3 regulates microtubule dynamics at the cell cortex and is required for myoblast elongation and fusion. *Current biology : CB*. 17:1318-1325.

Treves, S., M. Vukcevic, J. Griesser, C.F. Armstrong, M.X. Zhu, and F. Zorzato. 2010. Agonist-activated Ca2+ influx occurs at stable plasma membrane and endoplasmic reticulum junctions. *J Cell Sci*. 123:4170-4181.

Wang, Q., B. Zhang, W.C. Xiong, and L. Mei. 2006. MuSK signaling at the neuromuscular junction. *Journal of molecular neuroscience : MN*. 30:223-226.

Watanabe, T., J. Noritake, M. Kakeno, T. Matsui, T. Harada, S. Wang, N. Itoh, K. Sato, K. Matsuzawa, A. Iwamatsu, N. Galjart, and K. Kaibuchi. 2009. Phosphorylation of CLASP2 by GSK-3β regulates its interaction with IQGAP1, EB1 and microtubules. *Journal of Cell Science*. 122:2969-2979.

Wittmann, T., and C.M. Waterman-Storer. 2005. Spatial regulation of CLASP affinity for microtubules by Rac1 and GSK3β in migrating epithelial cells. *The Journal of Cell Biology*. 169:929-939.

Wu, H., W.C. Xiong, and L. Mei. 2010. To build a synapse: signaling pathways in neuromuscular junction assembly. *Development*. 137:1017-1033.

Yuan, B., R. Latek, M. Hossbach, T. Tuschl, and F. Lewitter. 2004. siRNA Selection Server: an automated siRNA oligonucleotide prediction server. *Nucleic acids research*. 32:W130-134.

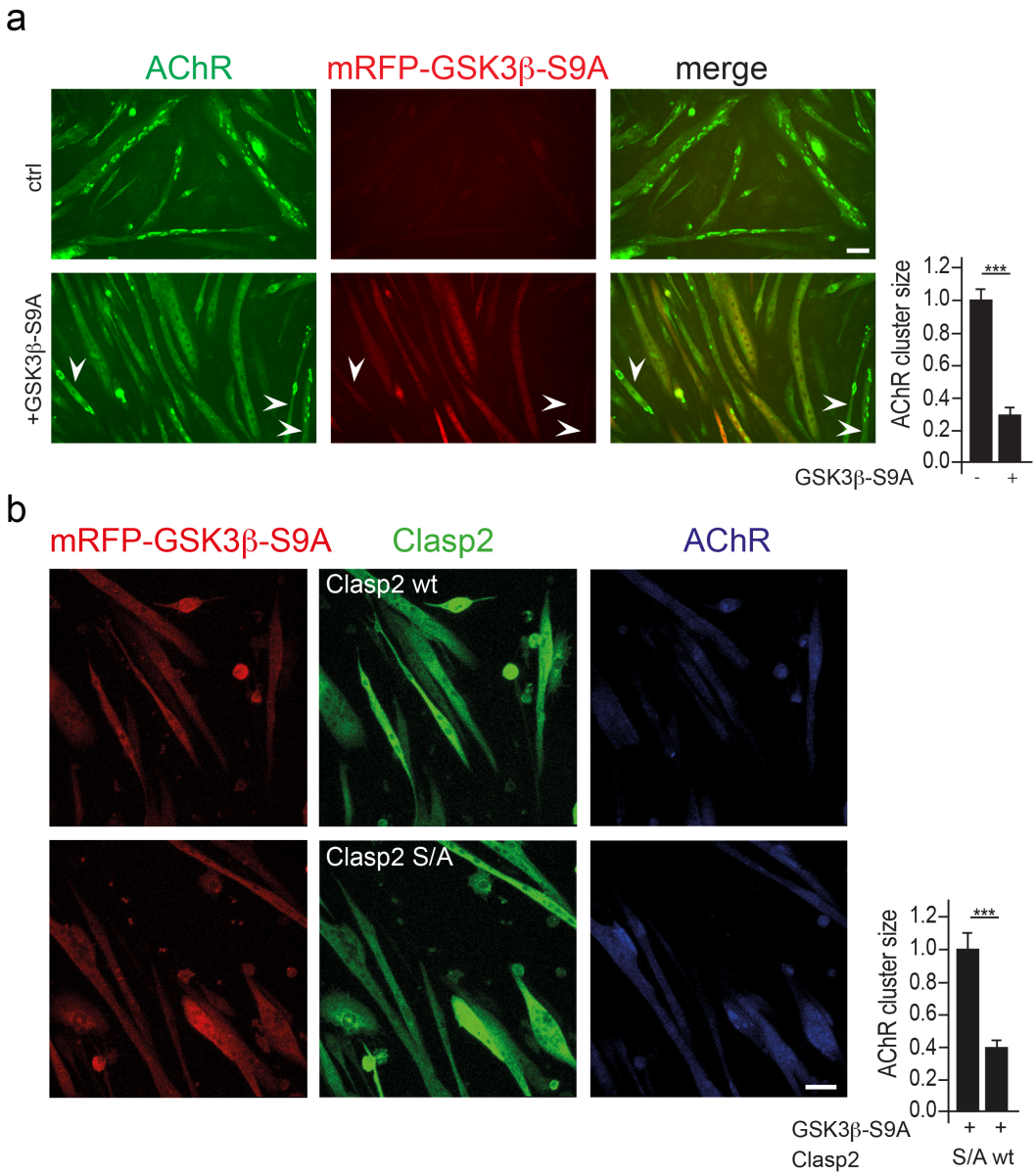

Figure 1: Agrin-induced AChR clustering in myotubes is inhibited by forced expression of constitutively active GSK3β (mRFP-GSK3β-S9A) and is rescued by expression of phosphorylation-resistant CLASP2.
(a) Myotubes differentiated on neural agrin ($NtAcAgrinA_4B_8$) immobilized on a laminin-substrate were infected with adenoviral vectors coding for mRFP-GSK3β-S9A. Two days later, myotubes were fixed in PFA and stained for AChRs with fluorophore-coupled α-BTX. Note marked reduction of AChR clusters in the majority of cells expressing constitutively active GSK3β, while the few uninfected cells (lower row, marked by asterisks) still display AChR clusters. Graphs showing mean ± s.e.m.; *** = $p<0.001$; two-sided t-test, n (ctrl) = 73, n (GSK3β-S9A infected) = 69; scale bar = 20 mm. (b) Myotubes differentiated on a laminin-attached agrin substrate were infected with a combination of adenoviral vectors coding for mRFP-GSK3β-S9A and either GFP-CLASP2 wt or non-phosphorylatable GFP-CLASP2-9xS/A. Two days later, myotubes were fixed in PFA and stained for AChRs with fluorophore-coupled α-BTX. Note that AChR cluster defects upon expression of constitutively active GSK3β are partly rescued by phosphorylation-resistant CLASP2-9xS/A. Graphs showing mean ± s.e.m.; *** = $p<0.001$; two-sided t-test, n (CLASP2-9xS/A) = 157, n (CLASP2 wt) = 165; scale bar = 20 mm.

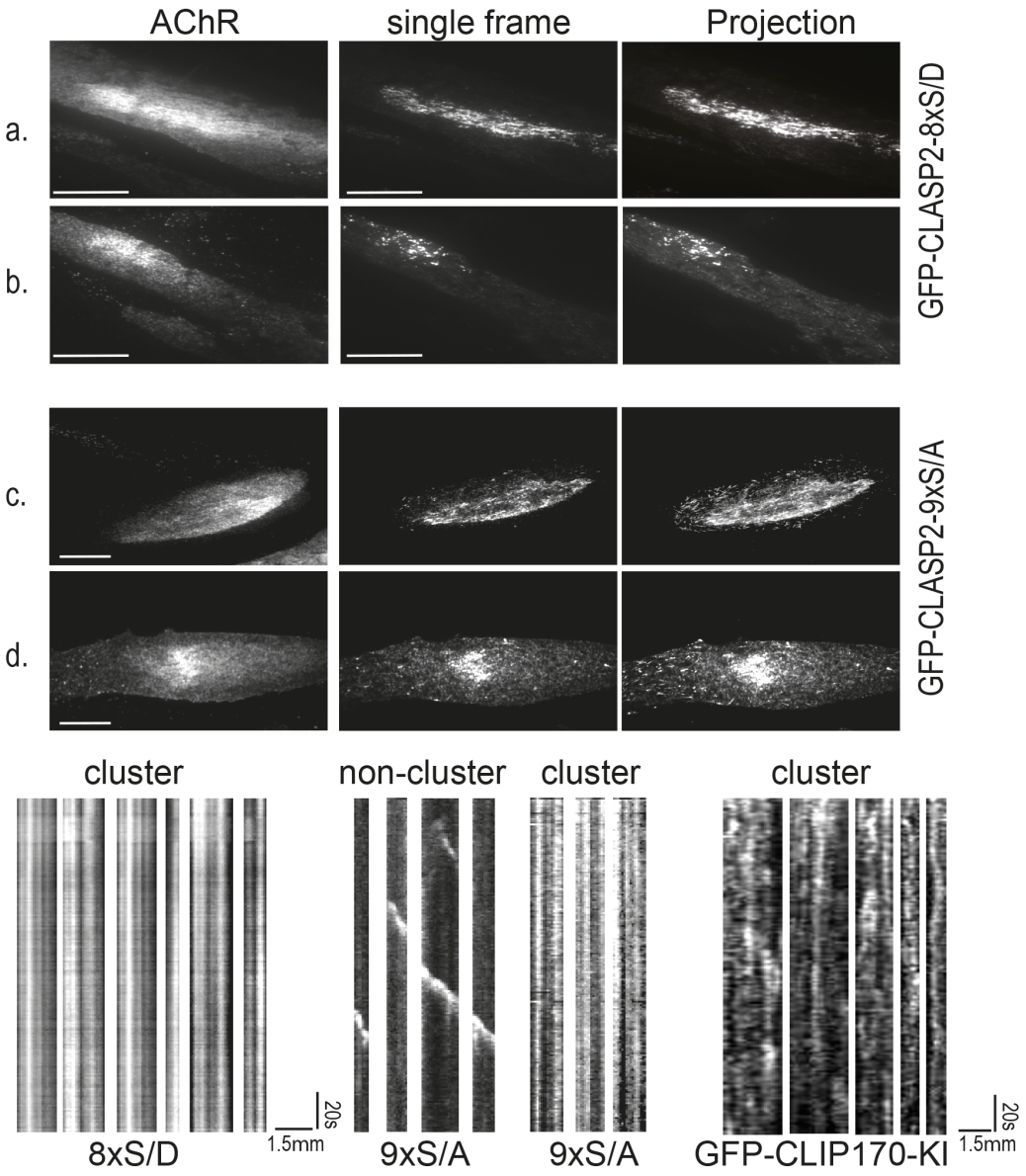

Figure 2: Both phospho-mimetic and phosphorylation-resistant CLASP2 accumulate at agrin-induced AChR clusters.
Myotubes differentiated on neural agrin immobilized on a laminin-substrate were infected with adenoviral vectors coding for GFP-tagged either phospho-mimetic CLASP2 (CLASP-8xS/D; a,b) or phosphorylation-resistant CLASP2 (CLASP2-9xS/A; c,d). Fluorescence signals may appear striped (upper rows; a,c) or unstructured (lower rows; b,d). Middle column shows single frames, right column represents maximum intensity projections of 160 to 180 frames taken in TIRF microscopy at 1 frame per second. Note that in myotubes expressing GFP-CLASP-8xS/D (a,b), comets cannot be resolved outside the AChR clusters - in contrast to myotubes expressing GFP-CLASP2-9xS/A (c,d). This is consistent with high affinity of phosphorylation-resistant CLASP2 for microtubule plus-ends (Kumar et al., 2009). Inside clusters, the striped GFP fluorescence signals show no dynamics as indicated by in kymograms shown in (e). Kymograms of GFP-CLIP-170-decorated microtubules within AChR clusters in myotubes are shown for comparison; scale bars= 10 μm.

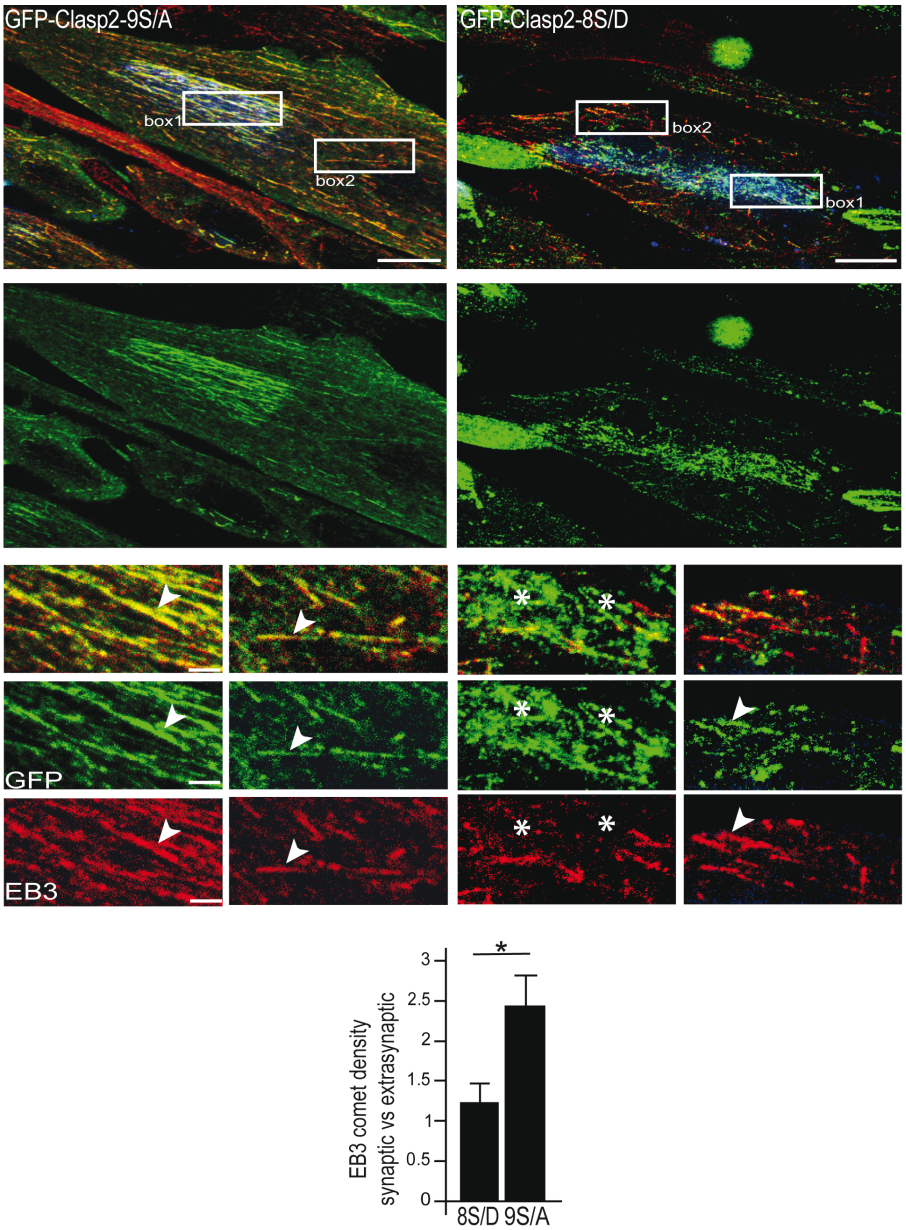

Figure 3: Expression of phospho-mimetic, but not of phosphorylation-resistant CLASP2 prevents MT capturing at agrin-induced AChR clusters.
Myotubes differentiated on neural agrin immobilized on a laminin-substrate were infected with the indicated adenoviral CLASP2 constructs; two days later, myotubes were fixed and stained for GFP-CLASP2 (green), EB3 (red) and for AChRs with fluorophore-conjugated α-BTX (blue) and examined by LSCM. Boxed areas are shown enlarged in bottom panels (box1: inside AChR cluster; box2: outside AChR cluster). Only myotubes expressing phosphorylation-resistant, but not those expressing phospho-mimetic CLASP2 display AChR cluster-specific enrichment of microtubules (as indicated by EB3 comets). Note the unstructured GFP immunoreactivity at AChR clusters of myotubes expressing phospho-mimetic CLASP2 (see text for discussion). Arrowheads indicate comets positive for EB3 and CLASP2, asterisks indicate GFP-CLASP2 staining in the absence of EB3 co-localization. Graph shows the difference in relative EB3 comets densities inside vs. outside clusters in myotubes expressing the respective CLASP2 mutants (means ± s.e.m.; n = 8 clusters examined in CLASP2-9xS/A, n = 7 clusters examined in CLASP2-8xS/D, from two independent experiments). * = $p<0.05$; two-sided t-test, scale bar = 10 µm; 2.5 µm (inset).

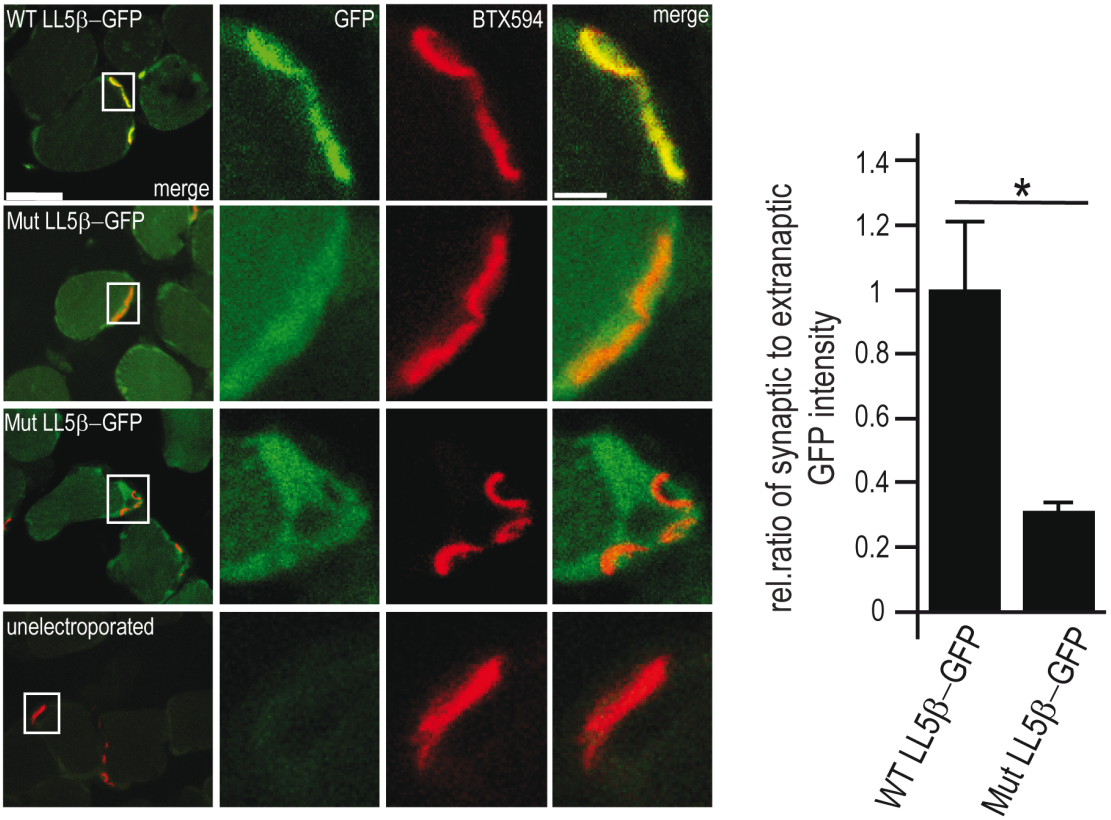

Figure 4: LL5β is recruited to the synaptic membrane via its PH domain interacting with PIP_3. Soleus muscles were electroporated with expression constructs for either wild-type GFP-LL5β or a GFP-LL5β mutant with 2 critical point mutations in its PH domain (Mut GFP-LL5β) known to abolish binding to PIP_3. Two weeks later, muscles were stained for AChRs (red), and NMJs were identified in cryosections by their α-BTX staining. GFP fluorescence at AChRs relative to that in non-synaptic membrane of the same myofiber was taken as a read-out for LL5β localization. Scale bars: 25 µm, inset: 5 µm. Graph shows ratio of GFP fluorescence at NMJs in fibers electroporated with the respective constructs. n = 8 each; * = $p<0.05$, two-sided t-test.

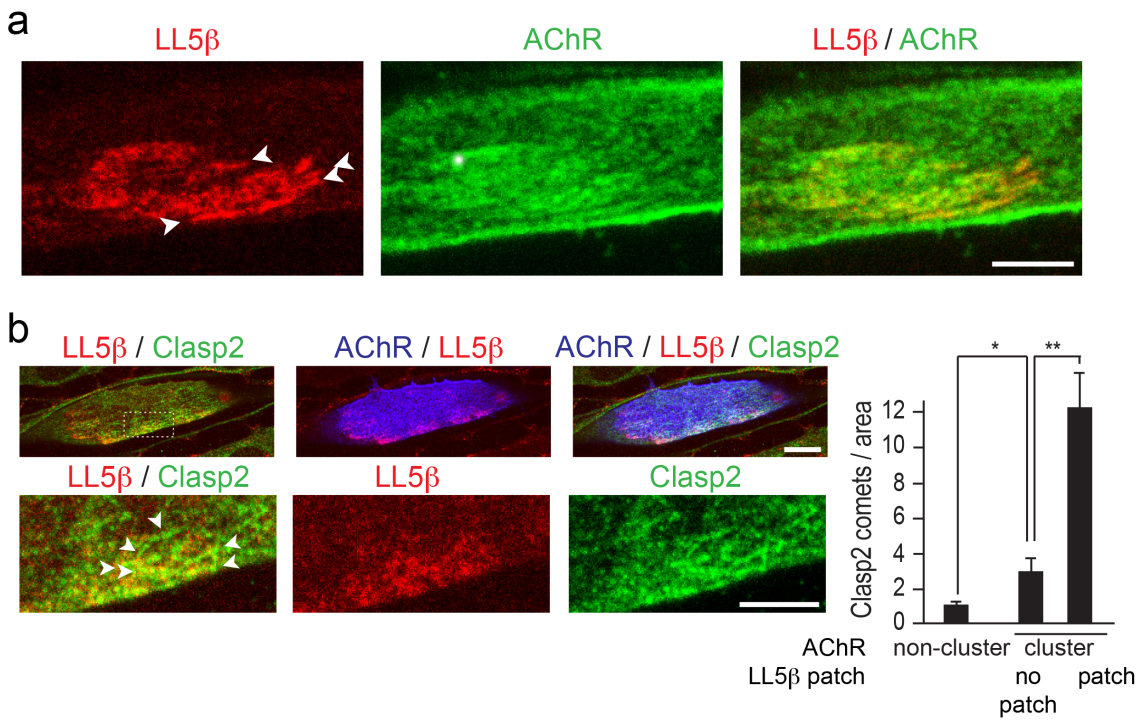

Figure 5: Patches of LL5β localize inside agrin-induced AChR clusters and are associated with CLASP2-decorated MT plus-ends.
(a) Patch of LL5β (red) within an AChR cluster (green). Note the striped appearance of the LL5b-rich area (arrowheads); scale bar: 5 µm. (b) Patches of LL5β (red) inside AChR clusters (blue) are enriched in CLASP2-decorated MT plus-ends (green), consistent with CLASP2-dependent MT capturing at synaptic membranes by LL5β. Myotubes infected with GFP-CLASP2 adenovirus were fixed in PFA 48 post infection and stained for AChR, endogenous LL5β and GFP. Lower row shows magnification of boxed area; note enrichment of CLASP2-comets (arrowheads) within LL5β patches. Scale bar: 10 µm (upper row), 5 µm (lower row). Graph showing a quantification of comets/area within the indicated regions of myotubes; mean ± s.e.m.; ** = $p<0.01$; * = $p<0.05$; n = 6 myotubes with >10 comets/cell.

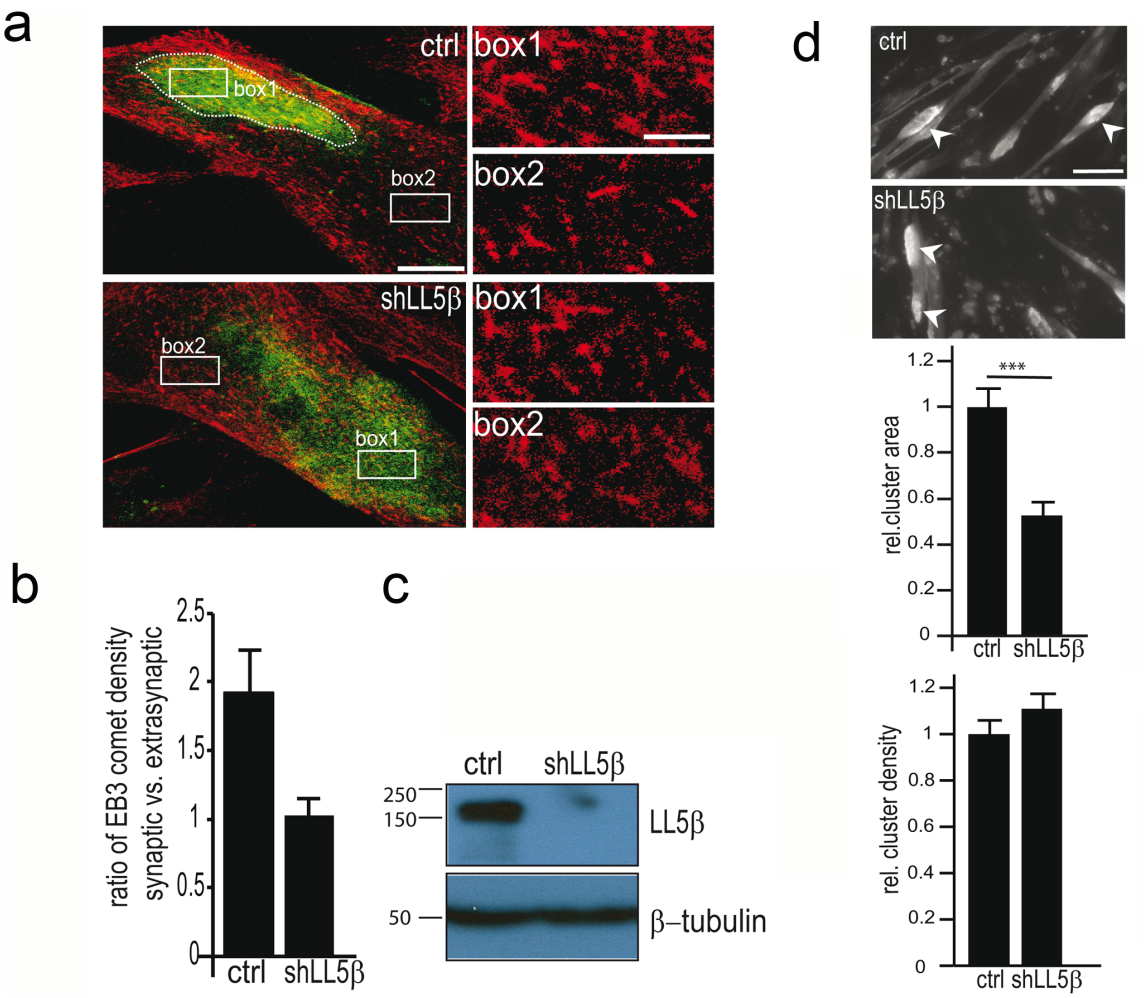

Figure 6: Knock-down of LL5β expression by RNAi abolishes capturing of MT plus-ends at agrin-induced AChR clusters.
(a) Representative images of myotubes cultured on patches of agrin and infected with lentiviral particles encoding shLL5β (hairpin 2, see methods) or scrambled shRNA. 48 hours later, myotubes were stained for EB3 (red) and AChRs (green). Densities of EB3-decorated comets inside (box1) versus outside AChR clusters (box2) were compared. Boxed areas are magnified to the right. Scale bar: 10 µm; enlarged: 2.5 µm. (b) Graph showing density of EB3 comets inside relative to that outside AChR clusters in control vs. LL5β knock-down myotubes. Graph showing mean ± s.e.m.; n = 12 for both parameters. (c) Western blot of lysates from control and LL5β knocked-down myotubes. Note almost complete abolishment of LL5β protein by hairpin 2. (d) The size of AChR cluster area is smaller in myotubes with LL5β knock-down than in control myotubes. Similar densities of AChR clusters suggest that decrease in cluster size is due to reduced AChR insertion. Graph depicts mean ± s.e.m.; n = 52 AChR clusters (ctrl); n = 58 AChR clusters (shLL5β), *** = $p<0.001$, two-sided t-test. Similar data were obtained with hairpin no. 4 (not shown).

IV. Discussion

During my thesis, I showed that agrin induces PI3K signaling and inactivation of GSK3β in muscle and cultured myotubes, which enables binding of the +TIP protein CLASP2 to microtubule plus-ends and MT capture at the subsynaptic membrane via +TIP interaction with the PIP_3-sensor LL5β. This process contributes to focal AChR transport towards and insertion into the postsynaptic muscle membrane.

MT capture in response to signals that activate PI3K and/or inactivate GSK3β is well known from the literature to occur in migratory cells and during neuronal polarization (Eng et al., 2006; Kumar et al., 2009; Ridley et al., 2003; Sun et al., 2009; Watanabe et al., 2009; Wittmann and Waterman-Storer, 2005; Wu et al., 2011; Yucel and Oro, 2011; Zumbrunn et al., 2001a). So far, analysis of MT capture was mostly performed either by showing MT capture via documentation of MT dynamics *per se*, or rather indirectly by studying cell-morphological changes as they occur during cell migration or axonal outgrowth – processes, which are known to involve MT capture. We analyzed MT behavior and capture in real-time and related it directly to a cellular function, which in the case of myotubes is the focal transport of AChR receptors towards and their insertion into the postsynaptic membrane. I thus provide – in close collaboration with my colleagues - an agrin-induced signaling pathway along with its functional role in MT capture and AChR insertion/clustering in myotubes.

To study MT behavior and its functional relevance for focal insertion and clustering of AChRs, we used a model in which we present agrin attached to a laminin-substrate, which mimics the physiologic presentation (Denzer et al., 1997). In contrast to simply adding agrin to the medium, this way of agrin presentation not only induces the clustering of AChRs, but also increases expression of AChRε and most likely other synaptic proteins (Jones et al., 1996). In addition, to follow MT dynamics in real-time, we used muscle cells derived from a GFP-CLIP-170 knock-in mouse model, which expresses

the ubiquitous +TIP CLIP-170 as GFP-tagged fusion protein at endogenous levels (Akhmanova et al., 2005). Taken together, our cell culture system allowed us to study agrin-induced MT behavior and capture under conditions, which mimic the *in vivo* situation as close as possible.

Using this cell culture system, we showed that agrin induces the capture of CLIP-170-decorated MT at the subsynaptic membrane, and moreover could demonstrate that the genetic loss of *Clasp2* – a GSK3β-regulated +TIP protein - reduces AChR clustering *in vitro* and affects the NMJ manifold *in vivo*. In *Clasp2*-deficient mice, postsynaptic MT capture is reduced and AChR accumulations are smaller and less dense. Furthermore, the number of subsynaptic myonuclei is reduced (Schmidt et al., 2012). The reduction of subsynaptic MT capture in *Clasp2*-deficient animals seems to be the main cause for the reduction in size and density of postsynaptic AChR accumulation, since we observed that the reduction of AChR cluster size in *Clasp2*$^{-/-}$ myotubes could be rescued by expression of CLASP2. Although we cannot rule out that the reduced density and size of postsynaptic AChR accumulations in myofibers is partly due to the reduced number of synaptic nuclei and thus reduced expression of AChR subunit genes, this explanation is unlikely, as NMJs of heterozygous AChR$\varepsilon^{+/-}$ display no reduced AChR density at their NMJs compared to wt animals (Missias et al., 1997).

We ascribed the synaptic phenotypes that we observed in *Clasp2*-deficient muscle and myotubes directly to the deficits in CLASP2-mediated MTs capture at the subsynaptic membrane, but additional explanations are possible: CLASP proteins can directly nucleate MTs in migrating epithelial cells at the developing Golgi, in a manner independent of centrosomes, and these Golgi-emanating MTs are preferentially oriented towards the leading edge, suggesting that they contribute to MT and cellular asymmetry and enable enhanced post-Golgi transport to the cell front (Efimov et al., 2007). Furthermore, these Golgi-nucleated MTs themselves enable full Golgi maturation, polarized vesicle transport towards the cell periphery and cell

polarization (Miller et al., 2009). Thus, the lack of CLASP2 could affect the focal insertion of AChRs not only by defects in subsynaptic MT capture, but also by suboptimal Golgi-processing of AChRs and by a reduced total number of Golgi-originating MTs available for subsynaptic capture.

In summary, CLASP proteins help to establish directional intracellular MT transport tracks by two separate, but probably interconnected mechanisms: MT nucleation at the Golgi by acting as a MT minus-end binding protein and MT capture at specific subcellular sites by its classical function as a +TIP. In muscle, Golgi and stable MTs were found to accumulate in the subsynaptic area (Jasmin et al., 1989; Jasmin et al., 1990). Given the high and constant demand for protein supply at the postsynaptic muscle membrane, establishment of enhanced and focused cargo delivery by local concentration of Golgi and stable MT transport tracks helps to ensure that this demand is met.

In addition to demonstrating agrin-induced and CLASP2-mediated MT capture at AChR clusters, we established a biochemical signal transduction pathway, where agrin induces PI3K activity and inhibition of GSK3β in myofibers and differentiated muscle cells (Schmidt et al., 2012). The agrin-induced PI3K activity promotes subsynaptic MT capture twofold: Firstly by downstream inactivation of GSK3β, which creates a pool of unphosphorylated +TIP molecules available for MT-binding and secondly by recruiting the PIP_3-sensor LL5β, which relocates to environments with high PI3K activity and acts as a cortical capture partner for CLASP2-decorated MTs (manuscript II).

LL5β is recruited to PIP_3-containing membrane domains (Paranavitane et al., 2003), but cortical recruitment via binding to those integrins, which act as receptors for laminin-5 (laminin-332 according to the new nomenclature) has been documented as well in epithelial cells (Hotta et al., 2010). Anyhow, laminin-5 is only deposited in the basement membrane of epithelia but not of muscle cells (Tsuruta et al., 2008). In turn, we demonstrated high PI3K

activity at the postsynaptic membrane (Schmidt et al., 2012), and failure to localize to the postsynaptic muscle membrane for a LL5β mutant with defective PH-domain (manuscript II), thus suggesting that PIP_3-containing membrane domains are responsible for cortical recruitment of LL5β to AChR clusters in myofibers and myotubes.

Our newer results showed that constitutively active GSK3β interferes with the agrin-induced clustering of AChRs in myotubes, likely by hyperphosphorylation of CLASP2 and thus interference with CLASP2-mediated MT capture at the subsynaptic membrane. This assumption is reinforced by the fact that the inhibitory effect of constitutively active GSK3β on AChR clustering could be partially relieved by expression of non-phosphorylatable CLASP2 (manuscript II). Our results are in agreement with the notion, that CLASP2 binding to EB1 and MTs is abolished by GSK3β phosphorylation, while non-phosphorylatable CLASP2 still binds EBs/MT plus-ends and acts as a +TIP in presence of constitutively active GSK3β (Kumar et al., 2009; Watanabe et al., 2009). Taken together, it seems that inhibition of GSK3β enables cell polarization of myotubes in similar ways as described for other cell types like fibroblasts, epithelia and skin stem cells, namely by polarizing the MT cytoskeleton via regulation of +TIP proteins such as CLASP, ACF7 or APC (Akhmanova et al., 2001; Kumar et al., 2009; Watanabe et al., 2009; Wittmann and Waterman-Storer, 2005; Wu et al., 2011; Zumbrunn et al., 2001a).

Interestingly, the +TIPs which are regulated by GSK3β (APC, ACF7 and CLASP2) are the same as those, which accumulate at MT plus-ends non-uniformly. Binding of these +TIPs is biased towards the plus-ends of MTs, which are directed to polarized structures, such as the leading edge of migratory cells or the future axon in neurons. Moreover, these non-ubiquitous +TIPs are required for polarization and/or motility, while ubiquitous +TIPs such as CLIP-170 are not (Akhmanova et al., 2001; Barth et al., 2008; Drabek et al., 2006; Wu et al., 2011).

Consistent with our view that the postsynaptic muscle membrane and AChR clusters represent a form of cell polarization in myotubes, we found GSK3β to be inactive at the postsynaptic membrane and MT plus-ends enriched at the NMJ and agrin-induced AChR clusters (Schmidt et al., 2012). In more detail, we found that CLASP2-decorated MT plus-ends are preferentially captured at LL5β deposits within AChR aggregations in myotubes (manuscript II), similar as described for motile cells (Lansbergen et al., 2006).

In line with our hypothesis, that AChR clustering is a form of MT-dependent cell polarization, others showed APC to be present at the postsynaptic muscle membrane and being involved in AChR clustering in myotubes (Wang et al., 2003). mDia has been shown to be a cortical capture partner for APC-decorated MTs in LPA-stimulated fibroblasts and to enable their polarization and migration (Wen et al., 2004), but it is unknown whether APC/mDia interaction is of relevance for MT capture and AChR clustering in myotubes.

CLASP proteins have been shown to respond to increasing levels of GSK3β activity in a bi-modal MT binding manner. While high GSK3β activity completely phosphorylates relevant residues and blocks CLASP binding to MTs, medium GSK3β activity permits CLASP to act in the classical way as +TIP, which enables axonal outgrowth. Complete lack of GSK3β activity leaves CLASP unphosphorylated and leads to CLASP binding along the MT lattice, which attenuates axon growth (Hur et al., 2011). A similar gradual binding behavior of CLASP2 as a function of phosphorylation by GSK3β was described in migrating epithel cells (Kumar et al., 2009). Taken together, these publications indicate that cell polarization as manifested by neuronal polarization/axonal outgrowth or epithelial migration, respectively, requires that GSK3 activity is tightly regulated in amplitude as well as spatially and temporally.

To study the physiologic role of GSK3 phosphorylation *in vivo*, a knock-in mouse model was created, in which both GSK3α and GSK3β were rendered

constitutive active by substituting the endogenous genes with point mutants, where the phosphorylatable serines are replaced by alanines, while retaining endogenous expression levels (McManus et al., 2005). These GSK3α-S21A/GSK3β-S9A double knock-in mice display normal development and show no sign of metabolic abnormalities or insulin resistance (McManus et al., 2005), whereas neuronal functions appear impaired: Gene-targeted mice have impaired neurogenesis (Eom and Jope, 2009), are hyperactive, and suffer from mood instability (Polter et al., 2010) and inadequate social behavior (Mines et al., 2012).

Of note, using the same double knock-in mouse model, it was demonstrated that axonal outgrowth, an important experimental paradigm for cell polarization, is unaffected by constitutively active GSK3 isoenzymes (Gärtner et al., 2006). This comes as a surprise, since localized inactivation of GSK3 specifically at the tip of the presumptive axon is thought to be crucial for the establishment of polarized MT outgrowth and MT stabilization, which precedes neuronal polarization and axonal outgrowth. Nevertheless, global inhibition of GSK3β disturbed polarization and lead to the formation of multiple axon-like processes. The unpolarized outgrowth of cell processes was accompanied by symmetric delivery of membrane components to all neuronal processes and equal distribution of the +TIP APC in all processes – which under physiologic conditions accumulates only at the tip of the future axon (Gärtner et al., 2006).

The findings by Gärtner *et al*., that axonal outgrowth can still occur in neurons expressing both GSK3 isoenzymes only in a constitutively active form (Gärtner et al., 2006), but is blocked by global GSK3 inhibition, imply that selective MT outgrowth – prerequisite for axon formation – could involve regulation of GSK3 by mechanism other than phosphorylation of Ser9 (GSK3β) and Ser21 (GSK3α), respectively. Indeed, inactivation of GSK3 by sequestration into protein complexes or change of subcellular localization are known to fine-tune its activity spatially and temporally (Medina and

Wandosell, 2011b), thus probably excluding constitutively active GSK3 from the point of future axonal outgrowth. Furthermore, additional phosphorylation sites in GSK3β are known to positively regulate its activity, such as tyrosine-phosphorylation on Tyr216 (Cole et al., 2004) – localized blockade of this tyrosine-phosphorylation event could therefore probably contribute to the GSK3β activity gradient proposed by (Hur et al., 2011) to be necessary for proper axonal outgrowth - even in presence of the activating S9A mutation. In line with this, Axin and its effector Dvl were shown to stabilize axonal MTs downstream of Wnt by inhibiting GSK3β activity without inducing GSK3β phosphorylation on Ser9 (Ciani et al., 2004), suggesting that Wnt-induced inactivation of GSK3β occurs by complex formation rather than through phosphorylation, as already described earlier (Ding et al., 2000). In the context of AChR clustering in myotubes, Dvl was also shown to positively affect AChR clusters in myotubes (Luo et al., 2002), although it is not clear whether this positive effect occurs by a potential stabilization of subsynaptic MTs.

We assume that myotubes manifest their polarity by focal insertion of AChR – and this process is indeed sensitive to GSK3β activity and can be rescued with GSK3β-insensitive point mutants of CLASP2. In addition to its binding to EBs and MTs, CLASP2 phosphorylation by GSK3β interferes with CLASP2 binding to IQGAP1 (Watanabe et al., 2009). IQGAP1 has been shown to capture MTs at the actin cytoskeleton after its activation by Rac1/Cdc42 through direct interaction with the +TIP CLIP-170 in fibroblasts (Fukata et al., 2002). Furthermore, IQGAP1 can recruit APC - which itself can act as a +TIP - but can also act as capture factor for CLIP-170-decorated MTs when bound to actin/IQGAP1 (Watanabe et al., 2004). As a final result, the F-actin and MT cytoskeletal are cross-linked, which is crucial for cell migration and other biological processes (Rodriguez et al., 2003).

Binding of MT-associated CLASP2 to IQGAP1, as described above for fibroblasts, could thus be a general additional mechanism to capture CLASP2-

decorated MTs and to connect them to the cortical actin network (Watanabe et al., 2009), although we did not study this possibility in myotubes. Of note, direct binding of CLASP proteins to actin filaments was described, thereby crosslinking F-actin and MTs (Tsvetkov et al., 2007).

CLIP-170 on the other hand, is a ubiquitous +TIP protein, which we used as a GFP-tagged fusion protein (Akhmanova et al., 2005) to study the behavior of dynamic MTs (Schmidt et al., 2012). CLIP-170 is involved in MT capture in migratory fibroblasts, although not in a manner regulated by GSK3β (Fukata et al., 2002; Watanabe et al., 2004). Interestingly, in muscle, CLIP-170 is predominantly expressed as a splice variant bearing a short, helix-breaking insert (Griparic and Keller, 1998), but the possible function of this splice insert and whether it is specific for the whole muscle or possibly has any postsynaptic functions within myofibers was never explored.

In newly formed myotubes, AChR are homogenously distributed over the whole cell surface and only with further differentiation, clusters of AChR appear, the appearance of AChRs on the cell surface and its condensation into clusters are therefore sequential events (Prives et al., 1976).
In this seminal report, chick embryo extract - which contains agrin – was added to the medium to induce AChR clusters, it is therefore not clear whether these findings can be fully transferred to our system, in which agrin is immobilized and focally presented to myotubes. Initial homologous distribution of AChRs in the muscle membrane is observed *in vivo* (Sanes and Lichtman, 2001), suggesting that lateral movement of initially evenly distributed AChRs also contributes to AChR clustering in cultured myotubes, especially in early stages. Nevertheless, we focused in our studies on the MT-mediated focal insertion of AChRs and did not address the contribution of lateral movement of AChRs that are initially evenly distributed in the myofiber membrane to the formation of AChR clusters.

Consistent with the reasonable assumption that the polar cytoskeletal systems are involved in AChR trafficking and clustering, the involvement of both F-actin and MTs in this process has been well documented, but reports are partially conflicting. When myotubes were treated with chicken brain extract (CBE), the observed increase of AChRs transported to the membrane could be blocked with MT-depolymerizing drugs, but not by depolymerizing actin, implying that AChR forward transport towards the whole myofiber membrane occurs on MTs rather than on F-actin (Connolly, 1985). This is consistent with our finding that MT depolymerization affects the size of AChR by interfering with targeted forward transport and probably lateral movement of AChRs (Schmidt et al., 2012). Earlier reports described movement of AChRs within the plane of the membrane as being mediated by MTs (Connolly, 1984), while in contrast, others found a significant role for actin filaments by propelling membranous AChRs together, thereby clustering them (Dai et al., 2000; Geng et al., 2009).

On the other hand, when MTs were stabilized by taxol, increased overall transport of AChRs to the cell surface was not observed, which implies that not the number of MTs, but rather the synthesis of mature AChRs or the number of available molecular motors or +TIPs available for subsynaptic MT capture are the limiting factors for AChR membrane insertion. Nevertheless, AChR clustering was increased upon taxol treatment (Connolly and Oldfin, 1985), suggesting that stabilized MTs elevate the aggregation of ACh receptors already present at the myotube cell surface.

Depolymerization of F-actin disperses pre-existing surface AChR clusters in myotubes, while depolymerization of MTs has no or only a slight effect on AChR cluster maintenance; both treatments leave the total number of surface AChRs unchanged (Connolly, 1984; Connolly, 1985; Connolly and Graham, 1985). These findings are consistent with the role of the actin cytoskeleton to anchor aggregated AChRs via interaction with rapsyn – therefore F-actin being important for the maintenance of surface AChRs

clusters (Apel et al., 1997; Moransard et al., 2003). Our own data also showed no effect of MT depolymerization on the size of pre-existing AChR clusters, thus loss of MTs does not destabilize AChR clusters or induce AChR their removal (Schmidt et al., 2012). Previous reports even described complete blockade of AChR removal upon MT depolymerization - thereby increasing AChR half-life at the cell surface – but found no effect of F-actin depolymerization on AChR removal or AChR surface half-life (Connolly, 1984; Connolly, 1985).

Although the detailed contributions of F-actin and MTs to the process of AChR transport, insertion, lateral movement, clustering, stabilization, anchoring and removal are not completely clear, the published data together establish that MTs are necessary for transport of AChR-loaded vesicles towards the whole myotube membrane and also for directed focal transport to AChR clusters. F-actin in turn anchors AChRs at clusters by interaction with rapsyn. Both F-actin and MTs can mediate propelling of AChRs in the plane of the membrane, while MTs are responsible for AChR removal from both cluster sites as well as from the extra-synaptic membrane.

Besides important contributions of the F-actin and MT cytoskeletal systems to postsynaptic maturation when studied as isolated entities, a complex physical and regulatory interplay between F-actin and MTs as described for other cell types and for basic biologic processes such as cell division, polarization, differentiation and migration (Basu and Chang, 2007; de Forges et al., 2012; Gundersen et al., 2004; Li and Gundersen, 2008; Rodriguez et al., 2003) most likely also contributes to postsynaptic muscle differentiation. Such complex F-actin/MT interactions were not specifically explored in muscle, but are well documented in neurons (Neukirchen and Bradke, 2011) and migratory cells (Ridley et al., 2003; Welf and Haugh, 2011). In both neurons and migrating cells, cytoskeletal organization and interaction is controlled by GTPases of the Rho and Ras family, which receive dozens of upstream inputs (with - in regard to our work - PI3K signaling being a major input) and

influence numerous downstream effectors (Hall, 2005; Hall and Lalli, 2010; Watanabe et al., 2005).

Intracellular MT plus-end directed transport of vesicles and organelles towards the cell periphery is mediated by kinesin 1, 2 & 3. This directed cargo transport helps to establish and maintain polarity, to satisfy elevated subcellular protein demand and to ensure cargo transport over long distances as observed in axons. (Verhey and Hammond, 2009). Moreover, in axons, many MTs are stabilized by post-translational modifications, which increases not only their lifetime (Janke and Bulinski, 2011), but also their kinesin-mediated transport properties (Cai et al., 2009; Reed et al., 2006), consistent with cellular efforts to provide an environment in axons for reliable cargo transport towards the axonal growth cone. In line with this, we (Schmidt et al., 2012) and others (Jasmin et al., 1990) found subsynaptic MTs in muscle being stabilized by detyrosination and acetylation respectively. These stable MT could thus not only confer mechanic stability to the postsynaptic specialization, but would also ensure elevated protein supply along synapse-directed MTs.

Furthermore, we found GSK3β to be strongly inactivated at the postsynaptic muscle membrane (Schmidt et al., 2012), and this inactivation of GSK3β was previously associated with enhanced kinesin-mediated transport. Phosphorylation of kinesin light chain - which is a constituent of kinesin 1, the major kinesin motor for vesicle transport (Verhey and Hammond, 2009) – by GSK3 specifically inhibits anterograde transport towards MT plus-ends (Morfini et al., 2002). Therefore, our observations that GSK3β is inactivated at the postsynaptic muscle membrane and that pharmacological inhibition of GSK3 increases agrin-induced AChR clustering (Schmidt et al., 2012), would be in agreement with enhanced kinesin-mediated transport of AChRs and other synaptic molecules towards the postsynaptic membrane upon inactivation of GSK3.

The presence of MTs that are stabilized by post-translational modifications occurs already early during myogenic differentiation (Gundersen et al., 1989) in cultured muscle cells and could be induced for example by Myc-nick, the calpain-digestion product of c-Myc, which is enriched in muscle and upregulated during myotube differentiation. Myc-nick not only promotes MT acetylation by recruitment of acetyltransferases, but also accelerates MT differentiation (Conacci-Sorrell et al., 2010). If these acetylated and therefore stabilized MTs are the same MTs that are later used for the transport of AChR towards the postsynaptic region is not known.

Despite the lack of a centrosome or MTOC, differentiated myotubes display steady-state perinuclear nucleation of MT (Zaal et al., 2011), although this MT nucleation can seemingly occur independently of the Golgi – in contrast to migrating cells, where non-centrosomal MT nucleation occurred mostly on the Golgi and in a manner dependent on CLASP2 recruitment (Efimov et al., 2007).

Besides the direct structural and trafficking benefits, which the establishment of stable MTs offers to the postsynaptic specialization, MTs are also involved in nuclear movement and tethering in myotubes. The +TIPs CLIP-190 - the fly homologue of CLIP-170 - and $p150^{Glued}$ regulate MT interactions with the cortex and thereby influence myonuclear positioning in Drosophila (Folker et al., 2012). Once MT tracks are established, nuclei are loaded onto KHC (Kinesin Heavy Chain, Kif5b), which then binds to MT via MAP7 and organizes nuclear positioning in myotubes. Mouse and fly myotubes mutant for *MAP7* display incorrect nuclear positioning, and affected flies display muscle dysfunction and locomotion defects. In general, proper subcellular nuclei positioning and differential gene expression from nuclei in syncytia are a source of cellular polarization/differentiation (Ruegg, 2005).

The functional importance of correct positioning of myonuclei and in particular of synaptic nuclei is explained by the fact that synaptic genes are

specifically expressed in subsynaptic nuclei (Brenner et al., 1990; Merlie and Sanes, 1985) and that gene products do not freely diffuse in myotubes and muscle, but rather stay in vicinity of the nucleus, which expressed the gene (Pavlath et al., 1989). Besides the drosophila +TIP CLIP-190, ACF-7 was also demonstrated to be involved in nuclear positioning and anchoring in the Balbiani body of zebrafish (Gupta et al., 2010), while we demonstrated reduced number of subsynaptic myonuclei in *Clasp2* knock-out mice (Schmidt et al., 2012). At the present stage, however, it is not clear whether +TIPs are generally involved in nuclear positioning and/or subcellular tethering. Although we did not address why *Clasp2*-deficient myofibers have less subsynaptic myonuclei beyond the descriptive level (Schmidt et al., 2012), it might be possible that CLASP2 is implicated in correct position of synaptic nuclei in mouse myofibers.

After correct positioning, synaptic myonuclei are anchored underneath AChR clusters in myotubes (Englander and Rubin, 1987), likely by Syne proteins (Grady et al., 2005) and SUN proteins (Lei et al., 2009), which all bind to the nuclear envelope and tether nuclei to the cytoskeleton. Surprisingly, loss of Syne-1 abolishes subsynaptic nuclear aggregates in myofibers, but this loss did not interfere with NMJ maturation (Grady et al., 2005). In contrast *Syne1/2* double-knock-out mice died perinatally due to respiratory failure caused by improper diaphragm innervation, suggesting that proper position of subsynaptic myonuclei might be dispensable for cell-autonomous postsynaptic differentiation, but be crucial for correct motor innervation (Zhang et al., 2007).

V. References

Akhmanova, A., and J.A. Hammer Iii. 2010. Linking molecular motors to membrane cargo. *Current Opinion in Cell Biology*. 22:479-487.

Akhmanova, A., C.C. Hoogenraad, K. Drabek, T. Stepanova, B. Dortland, T. Verkerk, W. Vermeulen, B.M. Burgering, C.I. De Zeeuw, F. Grosveld, and N. Galjart. 2001. CLASPs Are CLIP-115 and -170 Associating Proteins Involved in the Regional Regulation of Microtubule Dynamics in Motile Fibroblasts. *Cell*. 104:923-935.

Akhmanova, A., A.L. Mausset-Bonnefont, W. van Cappellen, N. Keijzer, C.C. Hoogenraad, T. Stepanova, K. Drabek, J. van der Wees, M. Mommaas, J. Onderwater, H. van der Meulen, M.E. Tanenbaum, R.H. Medema, J. Hoogerbrugge, J. Vreeburg, E.J. Uringa, J.A. Grootegoed, F. Grosveld, and N. Galjart. 2005. The microtubule plus-end-tracking protein CLIP-170 associates with the spermatid manchette and is essential for spermatogenesis. *Genes Dev*. 19:2501-2515.

Akhmanova, A., and M.O. Steinmetz. 2008a. Tracking the ends: a dynamic protein network controls the fate of microtubule tips. *Nature Rev. Mol. Cell Biol.* 9:309-322.

Akhmanova, A., and M.O. Steinmetz. 2008b. Tracking the ends: a dynamic protein network controls the fate of microtubule tips. *Nat Rev Mol Cell Biol*. 9:309-322.

Akhmanova, A., and M.O. Steinmetz. 2010. Microtubule +TIPs at a glance. *Journal of Cell Science*. 123:3415-3419.

Al-Bassam, J., N.A. Larsen, A.A. Hyman, and S.C. Harrison. 2007. Crystal Structure of a TOG Domain: Conserved Features of XMAP215/Dis1-Family TOG Domains and Implications for Tubulin Binding. *Structure*. 15:355-362.

Alberts, B., A. Johnson, J. Lewis, M. Raff, K. Roberts, and P. Walter. 2002. Molecular biology of the cell. Garland Science Taylor & Francis Group.

Ali, A., K.P. Hoeflich, and J.R. Woodgett. 2001. Glycogen synthase kinase-3: properties, functions, and regulation. *Chemical reviews*. 101:2527-2540.

Allen, C., and G.G. Borisy. 1974. Structural polarity and directional growth of microtubules of Chlamydomonas flagella. *Journal of molecular biology*. 90:381-402.

Amos, L.A., and A. Klug. 1974. Arrangement of Subunits in Flagellar Microtubules. *Journal of Cell Science*. 14:523-549.

An, M.C., W. Lin, J. Yang, B. Dominguez, D. Padgett, Y. Sugiura, P. Aryal, T.W. Gould, R.W. Oppenheim, M.E. Hester, B.K. Kaspar, C.-P. Ko, and K.-F. Lee. 2010. Acetylcholine negatively regulates development of the neuromuscular junction through distinct cellular mechanisms. *Proceedings of the National Academy of Sciences*. 107:10702-10707.

Antin, P.B., S. Forry-Schaudies, T.M. Friedman, S.J. Tapscott, and H. Holtzer. 1981. Taxol induces postmitotic myoblasts to assemble interdigitating microtubule-myosin arrays that exclude actin filaments. *J Cell Biol*. 90:300-308.

Antolik, C., D.H. Catino, A.M. O'Neill, W.G. Resneck, J.A. Ursitti, and R.J. Bloch. 2007. The actin binding domain of ACF7 binds directly to the tetratricopeptide repeat domains of rapsyn. *Neuroscience*. 145:56-65.

Apel, E.D., D.J. Glass, L.M. Moscoso, G.D. Yancopoulos, and J.R. Sanes. 1997. Rapsyn is required for MuSK signaling and recruits synaptic components to a MuSK-containing scaffold. *Neuron*. 18:623-635.

Applewhite, D.A., K.D. Grode, D. Keller, A.D. Zadeh, K.C. Slep, and S.L. Rogers. 2010. The spectraplakin Short stop is an actin-microtubule cross-linker that contributes to organization of the microtubule network. *Mol Biol Cell*. 21:1714-1724.

Banks, G.B., C. Fuhrer, M.E. Adams, and S.C. Froehner. 2003. The postsynaptic submembrane machinery at the neuromuscular junction: requirement for rapsyn and the utrophin/dystrophin-associated complex. *J Neurocytol*. 32:709-726.

Barth, A.I., H.Y. Caro-Gonzalez, and W.J. Nelson. 2008. Role of adenomatous polyposis coli (APC) and microtubules in directional cell migration and neuronal polarization. *Seminars in cell & developmental biology*. 19:245-251.

Bartolini, F., and G.G. Gundersen. 2006. Generation of noncentrosomal microtubule arrays. *Journal of Cell Science*. 119:4155-4163.

Basu, R., and F. Chang. 2007. Shaping the actin cytoskeleton using microtubule tips. *Curr Opin Cell Biol*. 19:88-94.

Beffert, U., G.M. Dillon, J.M. Sullivan, C.E. Stuart, J.P. Gilbert, J.A. Kambouris, and A. Ho. 2012. Microtubule Plus-End Tracking Protein CLASP2 Regulates Neuronal Polarity and Synaptic Function. *The Journal of neuroscience : the official journal of the Society for Neuroscience*. 32:13906-13916.

Bergamin, E., P.T. Hallock, S.J. Burden, and S.R. Hubbard. 2010. The Cytoplasmic Adaptor Protein Dok7 Activates the Receptor Tyrosine Kinase MuSK via Dimerization. *Molecular Cell*. 39:100-109.

Beronja, S., G. Livshits, S. Williams, and E. Fuchs. 2010. Rapid functional dissection of genetic networks via tissue-specific transduction and RNAi in mouse embryos. *Nature medicine*. 16:821-827.

Bezakova, G., and M.A. Ruegg. 2003. New insights into the roles of agrin. *Nat Rev Mol Cell Biol*. 4:295-309.

Bieling, P., S. Kandels-Lewis, I.A. Telley, J. van Dijk, C. Janke, and T. Surrey. 2008. CLIP-170 tracks growing microtubule ends by dynamically recognizing composite EB1/tubulin-binding sites. *The Journal of Cell Biology*. 183:1223-1233.

Bienz, M. 2002. The subcellular destinations of APC proteins. *Nat Rev Mol Cell Biol*. 3:328-338.

Blanco-Bose, W.E., C.C. Yao, R.H. Kramer, and H.M. Blau. 2001. Purification of mouse primary myoblasts based on alpha 7 integrin expression. *Experimental cell research*. 265:212-220.

Bloch, R.J. 1986. Actin at receptor-rich domains of isolated acetylcholine receptor clusters. *J Cell Biol*. 102:1447-1458.

Borges, L.S., and M. Ferns. 2001. Agrin-induced phosphorylation of the acetylcholine receptor regulates cytoskeletal anchoring and clustering. *J Cell Biol*. 153:1-12.

Borges, L.S., S. Yechikhov, Y.I. Lee, J.B. Rudell, M.B. Friese, S.J. Burden, and M.J. Ferns. 2008. Identification of a motif in the acetylcholine receptor beta subunit whose phosphorylation regulates rapsyn association and postsynaptic receptor localization. *The Journal of neuroscience : the official journal of the Society for Neuroscience*. 28:11468-11476.

Borisy, G.G., and E.W. Taylor. 1967a. The mechanism of action of colchicine. Binding of colchincine-3H to cellular protein. *J Cell Biol*. 34:525-533.

Borisy, G.G., and E.W. Taylor. 1967b. The mechanism of action of colchicine. Colchicine binding to sea urchin eggs and the mitotic apparatus. *J Cell Biol*. 34:535-548.

Brandon, E.P., W. Lin, K.A. D'Amour, D.P. Pizzo, B. Dominguez, Y. Sugiura, S. Thode, C.-P. Ko, L.J. Thal, F.H. Gage, and K.-F. Lee. 2003. Aberrant Patterning of Neuromuscular Synapses in Choline Acetyltransferase-Deficient Mice. *The Journal of Neuroscience*. 23:539-549.

Brenner, H.R., V. Witzemann, and B. Sakmann. 1990. Imprinting of acetylcholine receptor messenger RNA accumulation in mammalian neuromuscular synapses. *Nature*. 344:544-547.

Bu, W., and L.K. Su. 2003. Characterization of functional domains of human EB1 family proteins. *The Journal of biological chemistry*. 278:49721-49731.

Burden, S.J. 1998. The formation of neuromuscular synapses. *Genes & Development*. 12:133-148.

Burden, S.J. 2002. Building the vertebrate neuromuscular synapse. *Journal of Neurobiology*. 53:501-511.

Burgess, R.W., Q.T. Nguyen, Y.J. Son, J.W. Lichtman, and J.R. Sanes. 1999. Alternatively spliced isoforms of nerve- and muscle-derived agrin: their roles at the neuromuscular junction. *Neuron*. 23:33-44.

Burgess, R.W., W.C. Skarnes, and J.R. Sanes. 2000. Agrin isoforms with distinct amino termini: differential expression, localization, and function. *J Cell Biol*. 151:41-52.

Cai, D., D.P. McEwen, J.R. Martens, E. Meyhofer, and K.J. Verhey. 2009. Single molecule imaging reveals differences in microtubule track selection between Kinesin motors. *PLoS Biol.* 7:e1000216.

Cantley, L.C. 2002. The phosphoinositide 3-kinase pathway. *Science*. 296:1655-1657.

Caroni, P., S. Rotzler, J.C. Britt, and H.R. Brenner. 1993. Calcium influx and protein phosphorylation mediate the metabolic stabilization of synaptic acetylcholine receptors in muscle. *The Journal of neuroscience : the official journal of the Society for Neuroscience*. 13:1315-1325.

Cassimeris, L., and C. Spittle. 2001. Regulation of microtubule-associated proteins. *International review of cytology*. 210:163-226.

Chan, P.M., and E. Manser. 2012. PAKs in human disease. *Progress in molecular biology and translational science*. 106:171-187.

Chapin, S.J., J.C. Bulinski, and G. Gundersen. 1991. Microtubule bundling in cells. *Nature*. 349:24-24.

Chen, F., L. Qian, Z.H. Yang, Y. Huang, S.T. Ngo, N.J. Ruan, J. Wang, C. Schneider, P.G. Noakes, Y.Q. Ding, L. Mei, and Z.G. Luo. 2007. Rapsyn interaction with calpain stabilizes AChR clusters at the neuromuscular junction. *Neuron*. 55:247-260.

Ciani, L., O. Krylova, M.J. Smalley, T.C. Dale, and P.C. Salinas. 2004. A divergent canonical WNT-signaling pathway regulates microtubule dynamics: dishevelled signals locally to stabilize microtubules. *J Cell Biol*. 164:243-253.

Cohen, P., and M. Goedert. 2004. GSK3 inhibitors: development and therapeutic potential. *Nature reviews. Drug discovery*. 3:479-487.

Cole, A., S. Frame, and P. Cohen. 2004. Further evidence that the tyrosine phosphorylation of glycogen synthase kinase-3 (GSK3) in mammalian cells is an autophosphorylation event. *The Biochemical journal*. 377:249-255.

Conacci-Sorrell, M., C. Ngouenet, and R.N. Eisenman. 2010. Myc-nick: a cytoplasmic cleavage product of Myc that promotes alpha-tubulin acetylation and cell differentiation. *Cell*. 142:480-493.

Connolly, J.A. 1984. Role of the cytoskeleton in the formation, stabilization, and removal of acetylcholine receptor clusters in cultured muscle cells. *J Cell Biol*. 99:148-154.

Connolly, J.A. 1985. Microtubules, microfilaments and the transport of acetylcholine receptors in embryonic myotubes. *Experimental cell research*. 159:430-440.

Connolly, J.A., and A.J. Graham. 1985. Actin filaments and acetylcholine receptor clusters in embryonic chick myotubes. *European journal of cell biology*. 37:191-195.

Connolly, J.A., and B.V. Oldfin. 1985. Microtubules and the formation of acetylcholine receptor clusters in chick embryonic muscle cells. *European journal of cell biology*. 39:173-178.

Dai, Z., X. Luo, H. Xie, and H.B. Peng. 2000. The actin-driven movement and formation of acetylcholine receptor clusters. *J Cell Biol*. 150:1321-1334.

de Forges, H., A. Bouissou, and F. Perez. 2012. Interplay between microtubule dynamics and intracellular organization. *The international journal of biochemistry & cell biology*. 44:266-274.

De Zeeuw, C.I., C.C. Hoogenraad, E. Goedknegt, E. Hertzberg, A. Neubauer, F. Grosveld, and N. Galjart. 1997. CLIP-115, a Novel Brain-Specific Cytoplasmic Linker Protein, Mediates the Localization of Dendritic Lamellar Bodies. *Neuron*. 19:1187-1199.

DeChiara, T.M., D.C. Bowen, D.M. Valenzuela, M.V. Simmons, W.T. Poueymirou, S. Thomas, E. Kinetz, D.L. Compton, E. Rojas, J.S. Park, C. Smith, P.S. DiStefano, D.J. Glass, S.J. Burden, and G.D. Yancopoulos. 1996. The Receptor Tyrosine Kinase MuSK Is Required for Neuromuscular Junction Formation In Vivo. *Cell*. 85:501-512.

Denzer, A.J., R. Brandenberger, M. Gesemann, M. Chiquet, and M.A. Ruegg. 1997. Agrin binds to the nerve-muscle basal lamina via laminin. *J Cell Biol*. 137:671-683.

Denzer, A.J., M. Gesemann, B. Schumacher, and M.A. Ruegg. 1995. An amino-terminal extension is required for the secretion of chick agrin and its binding to extracellular matrix. *J Cell Biol*. 131:1547-1560.

Desai, A., and T.J. Mitchison. 1997. Microtubule polymerization dynamics. *Annual review of cell and developmental biology*. 13:83-117.

Ding, V.W., R.H. Chen, and F. McCormick. 2000. Differential regulation of glycogen synthase kinase 3beta by insulin and Wnt signaling. *The Journal of biological chemistry*. 275:32475-32481.

DiNitto, J.P., T.C. Cronin, and D.G. Lambright. 2003. Membrane recognition and targeting by lipid-binding domains. *Science's STKE : signal transduction knowledge environment*. 2003:re16.

DiNitto, J.P., and D.G. Lambright. 2006. Membrane and juxtamembrane targeting by PH and PTB domains. *Biochimica et biophysica acta*. 1761:850-867.

Drabek, K., M. van Ham, T. Stepanova, K. Draegestein, R. van Horssen, C.L. Sayas, A. Akhmanova, T. ten Hagen, R. Smits, R. Fodde, F. Grosveld, and N. Galjart. 2006. Role of CLASP2 in Microtubule Stabilization and the Regulation of Persistent Motility. *Current Biology*. 16:2259-2264.

Efimov, A., A. Kharitonov, N. Efimova, J. Loncarek, P.M. Miller, N. Andreyeva, P. Gleeson, N. Galjart, A.R. Maia, I.X. McLeod, J.R. Yates, 3rd, H. Maiato, A. Khodjakov, A. Akhmanova, and I. Kaverina. 2007. Asymmetric CLASP-dependent nucleation of noncentrosomal microtubules at the trans-Golgi network. *Dev Cell*. 12:917-930.

Elhanany-Tamir, H., Y.V. Yu, M. Shnayder, A. Jain, M. Welte, and T. Volk. 2012. Organelle positioning in muscles requires cooperation between two KASH proteins and microtubules. *J Cell Biol*. 198:833-846.

Eng, C.H., T.M. Huckaba, and G.G. Gundersen. 2006. The Formin mDia Regulates GSK3β through Novel PKCs to Promote Microtubule Stabilization but Not MTOC Reorientation in Migrating Fibroblasts. *Molecular Biology of the Cell*. 17:5004-5016.

Engel, A.G. 2008. The neuromuscular junction. *Handbook of clinical neurology / edited by P.J. Vinken and G.W. Bruyn*. 91:103-148.

Engelman, J.A., J. Luo, and L.C. Cantley. 2006. The evolution of phosphatidylinositol 3-kinases as regulators of growth and metabolism. *Nature reviews. Genetics*. 7:606-619.

Englander, L.L., and L.L. Rubin. 1987. Acetylcholine receptor clustering and nuclear movement in muscle fibers in culture. *J Cell Biol*. 104:87-95.

Eom, T.Y., and R.S. Jope. 2009. Blocked inhibitory serine-phosphorylation of glycogen synthase kinase-3alpha/beta impairs in vivo neural precursor cell proliferation. *Biological psychiatry*. 66:494-502.

Escher, P., E. Lacazette, M. Courtet, A. Blindenbacher, L. Landmann, G. Bezakova, K.C. Lloyd, U. Mueller, and H.R. Brenner. 2005. Synapses form in skeletal muscles lacking neuregulin receptors. *Science*. 308:1920-1923.

Etienne-Manneville, S., and A. Hall. 2003. Cdc42 regulates GSK-3beta and adenomatous polyposis coli to control cell polarity. *Nature*. 421:753-756.

Evans, L., T. Mitchison, and M. Kirschner. 1985. Influence of the centrosome on the structure of nucleated microtubules. *The Journal of Cell Biology*. 100:1185-1191.

Finn, A.J., G. Feng, and A.M. Pendergast. 2003. Postsynaptic requirement for Abl kinases in assembly of the neuromuscular junction. *Nature neuroscience*. 6:717-723.

Folker, E.S., V.K. Schulman, and M.K. Baylies. 2012. Muscle length and myonuclear position are independently regulated by distinct Dynein pathways. *Development*. 139:3827-3837.

Force, T., and J.R. Woodgett. 2009. Unique and overlapping functions of GSK-3 isoforms in cell differentiation and proliferation and cardiovascular development. *The Journal of biological chemistry*. 284:9643-9647.

Fukata, M., T. Watanabe, J. Noritake, M. Nakagawa, M. Yamaga, S. Kuroda, Y. Matsuura, A. Iwamatsu, F. Perez, and K. Kaibuchi. 2002. Rac1 and Cdc42 capture microtubules through IQGAP1 and CLIP-170. *Cell*. 109:873-885.

Fumagalli, G., S. Balbi, A. Cangiano, and T. Lomo. 1990. Regulation of turnover and number of acetylcholine receptors at neuromuscular junctions. *Neuron*. 4:563-569.

Fumoto, K., C.C. Hoogenraad, and A. Kikuchi. 2006. GSK-3beta-regulated interaction of BICD with dynein is involved in microtubule anchorage at centrosome. *EMBO J*. 25:5670-5682.

Galjart, N. 2005. CLIPs and CLASPs and cellular dynamics. *Nat Rev Mol Cell Biol*. 6:487-498.

Galjart, N. 2010. Plus-end-tracking proteins and their interactions at microtubule ends. *Current biology : CB*. 20:R528-537.

Gard, D.L., B.E. Becker, and S. Josh Romney. 2004. MAPping the eukaryotic tree of life: structure, function, and evolution of the MAP215/Dis1 family of microtubule-associated proteins. *International review of cytology*. 239:179-272.

Gärtner, A., X. Huang, and A. Hall. 2006. Neuronal polarity is regulated by glycogen synthase kinase-3 (GSK-3β) independently of Akt/PKB serine phosphorylation. *Journal of Cell Science*. 119:3927-3934.

Gautam, M., P.G. Noakes, L. Moscoso, F. Rupp, R.H. Scheller, J.P. Merlie, and J.R. Sanes. 1996. Defective Neuromuscular Synaptogenesis in Agrin-Deficient Mutant Mice. *Cell*. 85:525-535.

Geng, L., H.L. Zhang, and H.B. Peng. 2009. The formation of acetylcholine receptor clusters visualized with quantum dots. *BMC neuroscience*. 10:80.

Gesemann, M., V. Cavalli, A.J. Denzer, A. Brancaccio, B. Schumacher, and M.A. Ruegg. 1996. Alternative splicing of agrin alters its binding to heparin, dystroglycan, and the putative agrin receptor. *Neuron*. 16:755-767.

Gesemann, M., A.J. Denzer, and M.A. Ruegg. 1995. Acetylcholine receptor-aggregating activity of agrin isoforms and mapping of the active site. *The Journal of Cell Biology*. 128:625-636.

Gillespie, J.R., V. Ulici, H. Dupuis, A. Higgs, A. Dimattia, S. Patel, J.R. Woodgett, and F. Beier. 2011. Deletion of glycogen synthase kinase-3beta in cartilage

results in up-regulation of glycogen synthase kinase-3alpha protein expression. *Endocrinology*. 152:1755-1766.

Glass, D.J., D.C. Bowen, T.N. Stitt, C. Radziejewski, J. Bruno, T.E. Ryan, D.R. Gies, S. Shah, K. Mattsson, S.J. Burden, P.S. DiStefano, D.M. Valenzuela, T.M. DeChiara, and G.D. Yancopoulos. 1996. Agrin Acts via a MuSK Receptor Complex. *Cell*. 85:513-523.

Goodson, H.V., S.B. Skube, R. Stalder, C. Valetti, T.E. Kreis, E.E. Morrison, and T.A. Schroer. 2003. CLIP-170 interacts with dynactin complex and the APC-binding protein EB1 by different mechanisms. *Cell Motility and the Cytoskeleton*. 55:156-173.

Gordon, L.R., K.D. Gribble, C.M. Syrett, and M. Granato. 2012. Initiation of synapse formation by Wnt-induced MuSK endocytosis. *Development*. 139:1023-1033.

Grady, R.M., D.A. Starr, G.L. Ackerman, J.R. Sanes, and M. Han. 2005. Syne proteins anchor muscle nuclei at the neuromuscular junction. *Proceedings of the National Academy of Sciences of the United States of America*. 102:4359-4364.

Griparic, L., and T.C. Keller. 1998. Identification and expression of two novel CLIP-170/Restin isoforms expressed predominantly in muscle. *Biochimica et biophysica acta*. 1405:35-46.

Gundersen, G.G. 2002. Evolutionary conservation of microtubule-capture mechanisms. *Nat Rev Mol Cell Biol*. 3:296-304.

Gundersen, G.G., and J.C. Bulinski. 1986. Microtubule arrays in differentiated cells contain elevated levels of a post-translationally modified form of tubulin. *European journal of cell biology*. 42:288-294.

Gundersen, G.G., E.R. Gomes, and Y. Wen. 2004. Cortical control of microtubule stability and polarization. *Current Opinion in Cell Biology*. 16:106-112.

Gundersen, G.G., S. Khawaja, and J.C. Bulinski. 1989. Generation of a stable, posttranslationally modified microtubule array is an early event in myogenic differentiation. *The Journal of Cell Biology*. 109:2275-2288.

Gupta, T., F.L. Marlow, D. Ferriola, K. Mackiewicz, J. Dapprich, D. Monos, and M.C. Mullins. 2010. Microtubule actin crosslinking factor 1 regulates the Balbiani body and animal-vegetal polarity of the zebrafish oocyte. *PLoS Genet*. 6.

Hall, A. 2005. Rho GTPases and the control of cell behaviour. *Biochemical Society transactions*. 33:891-895.

Hall, A., and G. Lalli. 2010. Rho and Ras GTPases in axon growth, guidance, and branching. *Cold Spring Harb Perspect Biol*. 2:a001818.

Hammond, J.W., D. Cai, and K.J. Verhey. 2008. Tubulin modifications and their cellular functions. *Curr Opin Cell Biol*. 20:71-76.

Handschin, C., Y.M. Kobayashi, S. Chin, P. Seale, K.P. Campbell, and B.M. Spiegelman. 2007. PGC-1alpha regulates the neuromuscular junction program and ameliorates Duchenne muscular dystrophy. *Genes Dev*. 21:770-783.

Hayashi, I., and M. Ikura. 2003. Crystal Structure of the Amino-terminal Microtubule-binding Domain of End-binding Protein 1 (EB1). *Journal of Biological Chemistry*. 278:36430-36434.

Henriquez, J.P., and P.C. Salinas. 2012. Dual roles for Wnt signalling during the formation of the vertebrate neuromuscular junction. *Acta physiologica (Oxford, England)*. 204:128-136.

Henriquez, J.P., A. Webb, M. Bence, H. Bildsoe, M. Sahores, S.M. Hughes, and P.C. Salinas. 2008. Wnt signaling promotes AChR aggregation at the neuromuscular synapse in collaboration with agrin. *Proceedings of the National Academy of Sciences of the United States of America*. 105:18812-18817.

Hoeflich, K.P., J. Luo, E.A. Rubie, M.S. Tsao, O. Jin, and J.R. Woodgett. 2000. Requirement for glycogen synthase kinase-3beta in cell survival and NF-kappaB activation. *Nature*. 406:86-90.

Honnappa, S., S.M. Gouveia, A. Weisbrich, F.F. Damberger, N.S. Bhavesh, H. Jawhari, I. Grigoriev, F.J.A. van Rijssel, R.M. Buey, A. Lawera, I. Jelesarov, F.K. Winkler, K. Wüthrich, A. Akhmanova, and M.O. Steinmetz. 2009. An EB1-Binding Motif Acts as a Microtubule Tip Localization Signal. *Cell*. 138:366-376.

Honnappa, S., C.M. John, D. Kostrewa, F.K. Winkler, and M.O. Steinmetz. 2005. Structural insights into the EB1-APC interaction. *EMBO J*. 24:261-269.

Hotta, A., T. Kawakatsu, T. Nakatani, T. Sato, C. Matsui, T. Sukezane, T. Akagi, T. Hamaji, I. Grigoriev, A. Akhmanova, Y. Takai, and Y. Mimori-Kiyosue. 2010. Laminin-based cell adhesion anchors microtubule plus ends to the epithelial cell basal cortex through LL5α/β. *The Journal of Cell Biology*. 189:901-917.

Howard, J., and A.A. Hyman. 2007. Microtubule polymerases and depolymerases. *Curr. Opin. Cell Biol.* 19:31-35.

Hur, E.-M., Saijilafu, B.D. Lee, S.-J. Kim, W.-L. Xu, and F.-Q. Zhou. 2011. GSK3 controls axon growth via CLASP-mediated regulation of growth cone microtubules. *Genes & Development*. 25:1968-1981.

Inoue, A., K. Setoguchi, Y. Matsubara, K. Okada, N. Sato, Y. Iwakura, O. Higuchi, and Y. Yamanashi. 2009. Dok-7 Activates the Muscle Receptor Kinase MuSK and Shapes Synapse Formation. *Sci. Signal.* 2:ra7-.

Janke, C., and J. Bulinski. 2011. Post-translational regulation of the microtubule cytoskeleton: mechanisms and functions. *Nat Rev Mol Cell Biol*. 12:773-786.

Jasmin, B.J., J. Cartaud, M. Bornens, and J.P. Changeux. 1989. Golgi apparatus in chick skeletal muscle: changes in its distribution during end plate development and after denervation. *Proceedings of the National Academy of Sciences of the United States of America*. 86:7218-7222.

Jasmin, B.J., J.P. Changeux, and J. Cartaud. 1990. Compartmentalization of cold-stable and acetylated microtubules in the subsynaptic domain of chick skeletal muscle fibre. *Nature*. 344:673-675.

Jaworski, J., C.C. Hoogenraad, and A. Akhmanova. 2008. Microtubule plus-end tracking proteins in differentiated mammalian cells. *The International Journal of Biochemistry & Cell Biology*. 40:619-637.

Jennings, C.G., S.M. Dyer, and S.J. Burden. 1993. Muscle-specific trk-related receptor with a kringle domain defines a distinct class of receptor tyrosine kinases. *Proceedings of the National Academy of Sciences*. 90:2895-2899.

Jiang, H., W. Guo, X. Liang, and Y. Rao. 2005. Both the establishment and the maintenance of neuronal polarity require active mechanisms: critical roles of GSK-3beta and its upstream regulators. *Cell*. 120:123-135.

Jimbo, T., Y. Kawasaki, R. Koyama, R. Sato, S. Takada, K. Haraguchi, and T. Akiyama. 2002. Identification of a link between the tumour suppressor APC and the kinesin superfamily. *Nature cell biology*. 4:323-327.

Jing, L., L.R. Gordon, E. Shtibin, and M. Granato. 2010. Temporal and spatial requirements of unplugged/MuSK function during zebrafish neuromuscular development. *PLoS ONE*. 5:e8843.

Jing, L., J.L. Lefebvre, L.R. Gordon, and M. Granato. 2009. Wnt signals organize synaptic prepattern and axon guidance through the zebrafish unplugged/MuSK receptor. *Neuron*. 61:721-733.

Jones, G., A. Herczeg, M.A. Ruegg, M. Lichtsteiner, S. Kroger, and H.R. Brenner. 1996. Substrate-bound agrin induces expression of acetylcholine receptor epsilon-subunit gene in cultured mammalian muscle cells. *Proceedings of the National Academy of Sciences of the United States of America*. 93:5985-5990.

Jones, G., T. Meier, M. Lichtsteiner, V. Witzemann, B. Sakmann, and H.R. Brenner. 1997. Induction by agrin of ectopic and functional postsynaptic-like membrane in innervated muscle. *Proceedings of the National Academy of Sciences of the United States of America*. 94:2654-2659.

Kaidanovich-Beilin, O., J.-M. Beaulieu, R.S. Jope, and J.R. Woodgett. 2012. Neurological functions of the masterswitch protein kinase – GSK-3. *Frontiers in Molecular Neuroscience*. 5.

Kaidanovich-Beilin, O., and J.R. Woodgett. 2011. GSK-3: functional insights from cell biology and animal models. *Frontiers in Molecular Neuroscience*. 4.

Kapitein, L.C., and C.C. Hoogenraad. 2011. Which way to go? Cytoskeletal organization and polarized transport in neurons. *Molecular and Cellular Neuroscience*. 46:9-20.

Karsenti, E., F. Nedelec, and T. Surrey. 2006. Modelling microtubule patterns. *Nature cell biology*. 8:1204-1211.

Kawasaki, Y., T. Senda, T. Ishidate, R. Koyama, T. Morishita, Y. Iwayama, O. Higuchi, and T. Akiyama. 2000. Asef, a link between the tumor suppressor APC and G-protein signaling. *Science*. 289:1194-1197.

Kim, N., and S.J. Burden. 2008. MuSK controls where motor axons grow and form synapses. *Nature neuroscience*. 11:19-27.

Kim, N., A.L. Stiegler, T.O. Cameron, P.T. Hallock, A.M. Gomez, J.H. Huang, S.R. Hubbard, M.L. Dustin, and S.J. Burden. 2008. Lrp4 Is a Receptor for Agrin and Forms a Complex with MuSK. *Cell*. 135:334-342.

Kim, W.Y., X. Wang, Y. Wu, B.W. Doble, S. Patel, J.R. Woodgett, and W.D. Snider. 2009. GSK-3 is a master regulator of neural progenitor homeostasis. *Nature neuroscience*. 12:1390-1397.

Kim, W.Y., F.Q. Zhou, J. Zhou, Y. Yokota, Y.M. Wang, T. Yoshimura, K. Kaibuchi, J.R. Woodgett, E.S. Anton, and W.D. Snider. 2006. Essential roles

for GSK-3s and GSK-3-primed substrates in neurotrophin-induced and hippocampal axon growth. *Neuron*. 52:981-996.

Kim, Y.T., E.M. Hur, W.D. Snider, and F.Q. Zhou. 2011. Role of GSK3 Signaling in Neuronal Morphogenesis. *Front Mol Neurosci.* 4:48.

Kirschner, M., and T. Mitchison. 1986. Beyond self-assembly: From microtubules to morphogenesis. *Cell*. 45:329-342.

Kishi, M., T.T. Kummer, S.J. Eglen, and J.R. Sanes. 2005. LL5beta: a regulator of postsynaptic differentiation identified in a screen for synaptically enriched transcripts at the neuromuscular junction. *J Cell Biol*. 169:355-366.

Kita, K., T. Wittmann, I.S. Nathke, and C.M. Waterman-Storer. 2006. Adenomatous polyposis coli on microtubule plus ends in cell extensions can promote microtubule net growth with or without EB1. *Mol Biol Cell*. 17:2331-2345.

Kodama, A., I. Karakesisoglou, E. Wong, A. Vaezi, and E. Fuchs. 2003. ACF7: an essential integrator of microtubule dynamics. *Cell*. 115:343-354.

Kroboth, K., I.P. Newton, K. Kita, D. Dikovskaya, J. Zumbrunn, C.M. Waterman-Storer, and I.S. Nathke. 2007. Lack of adenomatous polyposis coli protein correlates with a decrease in cell migration and overall changes in microtubule stability. *Mol Biol Cell*. 18:910-918.

Kumar, P., M.S. Chimenti, H. Pemble, A. Schönichen, O. Thompson, M.P. Jacobson, and T. Wittmann. 2012. Multisite Phosphorylation Disrupts Arginine-Glutamate Salt Bridge Networks Required for Binding of Cytoplasmic Linker-associated Protein 2 (CLASP2) to End-binding Protein 1 (EB1). *Journal of Biological Chemistry*. 287:17050-17064.

Kumar, P., K.S. Lyle, S. Gierke, A. Matov, G. Danuser, and T. Wittmann. 2009. GSK3β phosphorylation modulates CLASP–microtubule association and lamella microtubule attachment. *The Journal of Cell Biology*. 184:895-908.

Kumar, P., and T. Wittmann. 2012. +TIPs: SxIPping along microtubule ends. *Trends in Cell Biology*. 22:418-428.

Kummer, T.T., T. Misgeld, and J.R. Sanes. 2006. Assembly of the postsynaptic membrane at the neuromuscular junction: paradigm lost. *Current Opinion in Neurobiology*. 16:74-82.

Lansbergen, G., I. Grigoriev, Y. Mimori-Kiyosue, T. Ohtsuka, S. Higa, I. Kitajima, J. Demmers, N. Galjart, A.B. Houtsmuller, F. Grosveld, and A. Akhmanova. 2006. CLASPs Attach Microtubule Plus Ends to the Cell Cortex through a Complex with LL5β. *Developmental Cell*. 11:21-32.

Lansbergen, G., Y. Komarova, M. Modesti, C. Wyman, C.C. Hoogenraad, H.V. Goodson, R.P. Lemaitre, D.N. Drechsel, E. van Munster, T.W. Gadella, Jr., F. Grosveld, N. Galjart, G.G. Borisy, and A. Akhmanova. 2004. Conformational changes in CLIP-170 regulate its binding to microtubules and dynactin localization. *J Cell Biol*. 166:1003-1014.

Ledbetter, M.C., and K.R. Porter. 1964. Morphology of Microtubules of Plant Cell. *Science*. 144:872-874.

Lei, K., X. Zhang, X. Ding, X. Guo, M. Chen, B. Zhu, T. Xu, Y. Zhuang, R. Xu, and M. Han. 2009. SUN1 and SUN2 play critical but partially redundant roles in

anchoring nuclei in skeletal muscle cells in mice. *Proceedings of the National Academy of Sciences of the United States of America*. 106:10207-10212.

Li, R., and G.G. Gundersen. 2008. Beyond polymer polarity: how the cytoskeleton builds a polarized cell. *Nat Rev Mol Cell Biol*. 9:860-873.

Li, X.M., X.P. Dong, S.W. Luo, B. Zhang, D.H. Lee, A.K. Ting, H. Neiswender, C.H. Kim, E. Carpenter-Hyland, T.M. Gao, W.C. Xiong, and L. Mei. 2008. Retrograde regulation of motoneuron differentiation by muscle beta-catenin. *Nature neuroscience*. 11:262-268.

Lichtman, J.W., and J.R. Sanes. 2003. Watching the neuromuscular junction. *Journal of Neurocytology*. 32:767-775.

Lin, W., B. Dominguez, J. Yang, P. Aryal, E.P. Brandon, F.H. Gage, and K.F. Lee. 2005. Neurotransmitter acetylcholine negatively regulates neuromuscular synapse formation by a Cdk5-dependent mechanism. *Neuron*. 46:569-579.

Linnoila, J., Y. Wang, Y. Yao, and Z.-Z. Wang. 2008. A Mammalian Homolog of Drosophila Tumorous Imaginal Discs, Tid1, Mediates Agrin Signaling at the Neuromuscular Junction. *Neuron*. 60:625-641.

Liu, Y., D. Padgett, M. Takahashi, H. Li, A. Sayeed, R.W. Teichert, B.M. Olivera, J.J. McArdle, W.N. Green, and W. Lin. 2008. Essential roles of the acetylcholine receptor γ-subunit in neuromuscular synaptic patterning. *Development*. 135:1957-1967.

Luders, J., and T. Stearns. 2007. Microtubule-organizing centres: a re-evaluation. *Nat Rev Mol Cell Biol*. 8:161-167.

Ludueńa, R.F., E.M. Shooter, and L. Wilson. 1977. Structure of the tubulin dimer. *Journal of Biological Chemistry*. 252:7006-7014.

Luo, S., B. Zhang, X.P. Dong, Y. Tao, A. Ting, Z. Zhou, J. Meixiong, J. Luo, F.C. Chiu, W.C. Xiong, and L. Mei. 2008. HSP90 beta regulates rapsyn turnover and subsequent AChR cluster formation and maintenance. *Neuron*. 60:97-110.

Luo, Z.G., H.S. Je, Q. Wang, F. Yang, G.C. Dobbins, Z.H. Yang, W.C. Xiong, B. Lu, and L. Mei. 2003. Implication of geranylgeranyltransferase I in synapse formation. *Neuron*. 40:703-717.

Luo, Z.G., Q. Wang, J.Z. Zhou, J. Wang, Z. Luo, M. Liu, X. He, A. Wynshaw-Boris, W.C. Xiong, B. Lu, and L. Mei. 2002. Regulation of AChR clustering by Dishevelled interacting with MuSK and PAK1. *Neuron*. 35:489-505.

MacAulay, K., B.W. Doble, S. Patel, T. Hansotia, E.M. Sinclair, D.J. Drucker, A. Nagy, and J.R. Woodgett. 2007. Glycogen synthase kinase 3alpha-specific regulation of murine hepatic glycogen metabolism. *Cell metabolism*. 6:329-337.

Mandelkow, E.M., R. Schultheiss, R. Rapp, M. Müller, and E. Mandelkow. 1986. On the surface lattice of microtubules: helix starts, protofilament number, seam, and handedness. *The Journal of Cell Biology*. 102:1067-1073.

Marangi, P.A., J.R. Forsayeth, P. Mittaud, S. Erb-Vogtli, D.J. Blake, M. Moransard, A. Sander, and C. Fuhrer. 2001. Acetylcholine receptors are required for agrin-induced clustering of postsynaptic proteins. *EMBO J*. 20:7060-7073.

Maurer, Sebastian P., Franck J. Fourniol, G. Bohner, Carolyn A. Moores, and T. Surrey. 2012. EBs Recognize a Nucleotide-Dependent Structural Cap at Growing Microtubule Ends. *Cell*. 149:371-382.

McMahan, U.J., S.E. Horton, M.J. Werle, L.S. Honig, S. Kroger, M.A. Ruegg, and G. Escher. 1992. Agrin isoforms and their role in synaptogenesis. *Curr Opin Cell Biol*. 4:869-874.

McManus, E.J., K. Sakamoto, L.J. Armit, L. Ronaldson, N. Shpiro, R. Marquez, and D.R. Alessi. 2005. Role that phosphorylation of GSK3 plays in insulin and Wnt signalling defined by knockin analysis. *EMBO J*. 24:1571-1583.

Medina, M., and F. Wandosell. 2011a. Deconstructing GSK-3: The Fine Regulation of Its Activity. *International journal of Alzheimer's disease*. 2011:479249.

Medina, M., and F. Wandosell. 2011b. Deconstructing GSK-3: The Fine Regulation of Its Activity. *International Journal of Alzheimer's Disease*. 2011.

Megeath, L.J., M.T. Kirber, C. Hopf, W. Hoch, and J.R. Fallon. 2003. Calcium-dependent maintenance of agrin-induced postsynaptic specializations. *Neuroscience*. 122:659-668.

Merlie, J.P., and J.R. Sanes. 1985. Concentration of acetylcholine receptor mRNA in synaptic regions of adult muscle fibres. *Nature*. 317:66-68.

Metzger, T., V. Gache, M. Xu, B. Cadot, E.S. Folker, B.E. Richardson, E.R. Gomes, and M.K. Baylies. 2012. MAP and kinesin-dependent nuclear positioning is required for skeletal muscle function. *Nature*. 484:120-124.

Miller, P.M., A.W. Folkmann, A.R. Maia, N. Efimova, A. Efimov, and I. Kaverina. 2009. Golgi-derived CLASP-dependent microtubules control Golgi organization and polarized trafficking in motile cells. *Nature cell biology*. 11:1069-1080.

Mimori-Kiyosue, Y., I. Grigoriev, G. Lansbergen, H. Sasaki, C. Matsui, F. Severin, N. Galjart, F. Grosveld, I. Vorobjev, S. Tsukita, and A. Akhmanova. 2005. CLASP1 and CLASP2 bind to EB1 and regulate microtubule plus-end dynamics at the cell cortex. *The Journal of Cell Biology*. 168:141-153.

Mines, M.A., E. Beurel, and R.S. Jope. 2012. Examination of methylphenidate-mediated behavior regulation by glycogen synthase kinase-3 in mice. *European journal of pharmacology*.

Misgeld, T., R.W. Burgess, R.M. Lewis, J.M. Cunningham, J.W. Lichtman, and J.R. Sanes. 2002. Roles of Neurotransmitter in Synapse Formation: Development of Neuromuscular Junctions Lacking Choline Acetyltransferase. *Neuron*. 36:635-648.

Missias, A.C., J. Mudd, J.M. Cunningham, J.H. Steinbach, J.P. Merlie, and J.R. Sanes. 1997. Deficient development and maintenance of postsynaptic specializations in mutant mice lacking an 'adult' acetylcholine receptor subunit. *Development*. 124:5075-5086.

Mitchison, T., and M. Kirschner. 1984. Dynamic instability of microtubule growth. *Nature*. 312:237-242.

Mittaud, P., P.A. Marangi, S. Erb-Vogtli, and C. Fuhrer. 2001. Agrin-induced activation of acetylcholine receptor-bound Src family kinases requires Rapsyn and correlates with acetylcholine receptor clustering. *The Journal of biological chemistry*. 276:14505-14513.

Mohamed, A.S., K.A. Rivas-Plata, J.R. Kraas, S.M. Saleh, and S.L. Swope. 2001. Src-class kinases act within the agrin/MuSK pathway to regulate acetylcholine receptor phosphorylation, cytoskeletal anchoring, and clustering. *The Journal of neuroscience : the official journal of the Society for Neuroscience*. 21:3806-3818.

Mohri, H. 1968. Amino-acid composition of "Tubulin" constituting microtubules of sperm flagella. *Nature*. 217:1053-1054.

Moransard, M., L.S. Borges, R. Willmann, P.A. Marangi, H.R. Brenner, M.J. Ferns, and C. Fuhrer. 2003. Agrin Regulates Rapsyn Interaction with Surface Acetylcholine Receptors, and This Underlies Cytoskeletal Anchoring and Clustering. *Journal of Biological Chemistry*. 278:7350-7359.

Morfini, G., G. Szebenyi, R. Elluru, N. Ratner, and S.T. Brady. 2002. Glycogen synthase kinase 3 phosphorylates kinesin light chains and negatively regulates kinesin-based motility. *EMBO J*. 21:281-293.

Moseley, J.B., F. Bartolini, K. Okada, Y. Wen, G.G. Gundersen, and B.L. Goode. 2007. Regulated binding of adenomatous polyposis coli protein to actin. *The Journal of biological chemistry*. 282:12661-12668.

Näthke, I. 2004. APC at a glance. *Journal of Cell Science*. 117:4873-4875.

Nathke, I.S., C.L. Adams, P. Polakis, J.H. Sellin, and W.J. Nelson. 1996. The adenomatous polyposis coli tumor suppressor protein localizes to plasma membrane sites involved in active cell migration. *J Cell Biol*. 134:165-179.

Neukirchen, D., and F. Bradke. 2011. Neuronal polarization and the cytoskeleton. *Seminars in Cell & Developmental Biology*. 22:825-833.

Ngo, S.T., P.G. Noakes, and W.D. Phillips. 2007. Neural agrin: a synaptic stabiliser. *The international journal of biochemistry & cell biology*. 39:863-867.

Nizhynska, V., R. Neumueller, and R. Herbst. 2007. Phosphoinositide 3-kinase acts through RAC and Cdc42 during agrin-induced acetylcholine receptor clustering. *Dev Neurobiol*. 67:1047-1058.

Nogales, E., and H.W. Wang. 2006. Structural intermediates in microtubule assembly and disassembly: how and why? *Curr Opin Cell Biol*. 18:179-184.

Oakley, C.E., and B.R. Oakley. 1989. Identification of γ-tubulin, a new member of the tubulin superfamily encoded by MipA gene of Aspergillus nidulans. *Nature*. 338:662-664.

Okada, K., A. Inoue, M. Okada, Y. Murata, S. Kakuta, T. Jigami, S. Kubo, H. Shiraishi, K. Eguchi, M. Motomura, T. Akiyama, Y. Iwakura, O. Higuchi, and Y. Yamanashi. 2006. The Muscle Protein Dok-7 Is Essential for Neuromuscular Synaptogenesis. *Science*. 312:1802-1805.

Ono, F., S.-i. Higashijima, A. Shcherbatko, J.R. Fetcho, and P. Brehm. 2001. Paralytic Zebrafish Lacking Acetylcholine Receptors Fail to Localize Rapsyn Clusters to the Synapse. *The Journal of Neuroscience*. 21:5439-5448.

Paranavitane, V., W.J. Coadwell, A. Eguinoa, P.T. Hawkins, and L. Stephens. 2003. LL5beta is a phosphatidylinositol (3,4,5)-trisphosphate sensor that can bind the cytoskeletal adaptor, gamma-filamin. *The Journal of biological chemistry*. 278:1328-1335.

Patel, S., B.W. Doble, K. MacAulay, E.M. Sinclair, D.J. Drucker, and J.R. Woodgett. 2008. Tissue-Specific Role of Glycogen Synthase Kinase 3β in

Glucose Homeostasis and Insulin Action. *Molecular and Cellular Biology*. 28:6314-6328.

Pavlath, G.K., K. Rich, S.G. Webster, and H.M. Blau. 1989. Localization of muscle gene products in nuclear domains. *Nature*. 337:570-573.

Pease, D.C. 1963. THE ULTRASTRUCTURE OF FLAGELLAR FIBRILS. *The Journal of Cell Biology*. 18:313-326.

Perez, F., G.S. Diamantopoulos, R. Stalder, and T.E. Kreis. 1999. CLIP-170 Highlights Growing Microtubule Ends In Vivo. *Cell*. 96:517-527.

Peris, L., M. Thery, J. Fauré, Y. Saoudi, L. Lafanechère, J.K. Chilton, P. Gordon-Weeks, N. Galjart, M. Bornens, L. Wordeman, J. Wehland, A. Andrieux, and D. Job. 2006. Tubulin tyrosination is a major factor affecting the recruitment of CAP-Gly proteins at microtubule plus ends. *The Journal of Cell Biology*. 174:839-849.

Pizon, V., F. Gerbal, C.C. Diaz, and E. Karsenti. 2005. Microtubule-dependent transport and organization of sarcomeric myosin during skeletal muscle differentiation. *EMBO J*. 24:3781-3792.

Polter, A., E. Beurel, S. Yang, R. Garner, L. Song, C.A. Miller, J.D. Sweatt, L. McMahon, A.A. Bartolucci, X. Li, and R.S. Jope. 2010. Deficiency in the inhibitory serine-phosphorylation of glycogen synthase kinase-3 increases sensitivity to mood disturbances. *Neuropsychopharmacology : official publication of the American College of Neuropsychopharmacology*. 35:1761-1774.

Prives, J., I. Silman, and A. Amsterdam. 1976. Appearance and disappearance of acetycholine receptor during differentiation of chick skeletal muscle in vitro. *Cell*. 7:543-550.

Raynaud-Messina, B., and A. Merdes. 2007. γ-tubulin complexes and microtubule organization. *Current Opinion in Cell Biology*. 19:24-30.

Reed, N.A., D. Cai, T.L. Blasius, G.T. Jih, E. Meyhofer, J. Gaertig, and K.J. Verhey. 2006. Microtubule acetylation promotes kinesin-1 binding and transport. *Current biology : CB*. 16:2166-2172.

Reist, N.E., M.J. Werle, and U.J. McMahan. 1992. Agrin released by motor neurons induces the aggregation of acetylcholine receptors at neuromuscular junctions. *Neuron*. 8:865-868.

Ridley, A.J., M.A. Schwartz, K. Burridge, R.A. Firtel, M.H. Ginsberg, G. Borisy, J.T. Parsons, and A.R. Horwitz. 2003. Cell Migration: Integrating Signals from Front to Back. *Science*. 302:1704-1709.

Rodriguez, O.C., A.W. Schaefer, C.A. Mandato, P. Forscher, W.M. Bement, and C.M. Waterman-Storer. 2003. Conserved microtubule-actin interactions in cell movement and morphogenesis. *Nature cell biology*. 5:599-609.

Rotzler, S., and H.R. Brenner. 1990. Metabolic stabilization of acetylcholine receptors in vertebrate neuromuscular junction by muscle activity. *J Cell Biol*. 111:655-661.

Ruegg, M.A. 2005. Organization of synaptic myonuclei by Syne proteins and their role during the formation of the nerve-muscle synapse. *Proceedings of the National Academy of Sciences of the United States of America*. 102:5643-5644.

Ruegg, M.A., K.W. Tsim, S.E. Horton, S. Kroger, G. Escher, E.M. Gensch, and U.J. McMahan. 1992. The agrin gene codes for a family of basal lamina proteins that differ in function and distribution. *Neuron*. 8:691-699.

Sakakibara, H., and K. Oiwa. 2011. Molecular organization and force-generating mechanism of dynein. *FEBS Journal*. 278:2964-2979.

Samuel, M.A., G. Valdez, J.C. Tapia, J.W. Lichtman, and J.R. Sanes. 2012. Agrin and Synaptic Laminin Are Required to Maintain Adult Neuromuscular Junctions. *PLoS ONE*. 7:e46663.

Sanchez-Soriano, N., M. Travis, F. Dajas-Bailador, C. Goncalves-Pimentel, A.J. Whitmarsh, and A. Prokop. 2009. Mouse ACF7 and drosophila short stop modulate filopodia formation and microtubule organisation during neuronal growth. *J Cell Sci*. 122:2534-2542.

Sandow, A. 1952. Excitation-contraction coupling in muscular response. *The Yale journal of biology and medicine*. 25:176-201.

Sanes, J.R. 2003. The Basement Membrane/Basal Lamina of Skeletal Muscle. *Journal of Biological Chemistry*. 278:12601-12604.

Sanes, J.R., and J.W. Lichtman. 1999. Development of the vertebrate neuromuscular junction. *Annual review of neuroscience*. 22:389-442.

Sanes, J.R., and J.W. Lichtman. 2001. Induction, assembly, maturation and maintenance of a postsynaptic apparatus. *Nat Rev Neurosci*. 2:791-805.

Schaeffer, L., A. de Kerchove d'Exaerde, and J.P. Changeux. 2001. Targeting transcription to the neuromuscular synapse. *Neuron*. 31:15-22.

Schmidt, N., M. Akaaboune, N. Gajendran, I. Martinez-Pena y Valenzuela, S. Wakefield, R. Thurnheer, and H.R. Brenner. 2011. Neuregulin/ErbB regulate neuromuscular junction development by phosphorylation of alpha-dystrobrevin. *J Cell Biol*. 195:1171-1184.

Schmidt, N., S. Basu, S. Sladecek, S. Gatti, J. van Haren, S. Treves, J. Pielage, N. Galjart, and H.R. Brenner. 2012. Agrin regulates CLASP2-mediated capture of microtubules at the neuromuscular junction synaptic membrane. *J Cell Biol*. 198:421-437.

Schroer, T.A. 2004. Dynactin. *Annual review of cell and developmental biology*. 20:759-779.

Sharp, D.J., and J.L. Ross. 2012. Microtubule-severing enzymes at the cutting edge. *J Cell Sci*. 125:2561-2569.

Shi, L., A.K.Y. Fu, and N.Y. Ip. 2012. Molecular mechanisms underlying maturation and maintenance of the vertebrate neuromuscular junction. *Trends in Neurosciences*. 35:441-453.

Sine, S.M. 2012. End-plate acetylcholine receptor: structure, mechanism, pharmacology, and disease. *Physiological reviews*. 92:1189-1234.

Slep, K.C. 2010. Structural and mechanistic insights into microtubule end-binding proteins. *Current Opinion in Cell Biology*. 22:88-95.

Slep, K.C., and R.D. Vale. 2007. Structural Basis of Microtubule Plus End Tracking by XMAP215, CLIP-170, and EB1. *Molecular Cell*. 27:976-991.

Sonnenberg, A., and R.K. Liem. 2007. Plakins in development and disease. *Experimental cell research*. 313:2189-2203.

Steinmetz, M.O., and A. Akhmanova. 2008. Capturing protein tails by CAP-Gly domains. *Trends in biochemical sciences*. 33:535-545.

Straube, A., and A. Merdes. 2007. EB3 regulates microtubule dynamics at the cell cortex and is required for myoblast elongation and fusion. *Current biology : CB*. 17:1318-1325.

Subramanian, A., A. Prokop, M. Yamamoto, K. Sugimura, T. Uemura, J. Betschinger, J.A. Knoblich, and T. Volk. 2003. Shortstop recruits EB1/APC1 and promotes microtubule assembly at the muscle-tendon junction. *Current biology : CB*. 13:1086-1095.

Sun, T., M. Rodriguez, and L. Kim. 2009. Glycogen synthase kinase 3 in the world of cell migration. *Development, growth & differentiation*. 51:735-742.

Suozzi, K.C., X. Wu, and E. Fuchs. 2012. Spectraplakins: Master orchestrators of cytoskeletal dynamics. *The Journal of Cell Biology*. 197:465-475.

Sutherland, C. 2011. What Are the bona fide GSK3 Substrates? *International journal of Alzheimer's disease*. 2011:505607.

Taelman, V.F., R. Dobrowolski, J.L. Plouhinec, L.C. Fuentealba, P.P. Vorwald, I. Gumper, D.D. Sabatini, and E.M. De Robertis. 2010. Wnt signaling requires sequestration of glycogen synthase kinase 3 inside multivesicular endosomes. *Cell*. 143:1136-1148.

Tai, C.Y., D.L. Dujardin, N.E. Faulkner, and R.B. Vallee. 2002. Role of dynein, dynactin, and CLIP-170 interactions in LIS1 kinetochore function. *J Cell Biol*. 156:959-968.

Takahashi, M., T. Kubo, A. Mizoguchi, C.G. Carlson, K. Endo, and K. Ohnishi. 2002. Spontaneous muscle action potentials fail to develop without fetal-type acetylcholine receptors. *EMBO reports*. 3:674-681.

Tassin, A.M., B. Maro, and M. Bornens. 1985. Fate of microtubule-organizing centers during myogenesis in vitro. *J Cell Biol*. 100:35-46.

Treves, S., M. Vukcevic, J. Griesser, C.F. Armstrong, M.X. Zhu, and F. Zorzato. 2010. Agonist-activated Ca2+ influx occurs at stable plasma membrane and endoplasmic reticulum junctions. *J Cell Sci*. 123:4170-4181.

Tsuruta, D., H. Kobayashi, H. Imanishi, K. Sugawara, M. Ishii, and J.C. Jones. 2008. Laminin-332-integrin interaction: a target for cancer therapy? *Current medicinal chemistry*. 15:1968-1975.

Tsvetkov, A.S., A. Samsonov, A. Akhmanova, N. Galjart, and S.V. Popov. 2007. Microtubule-binding proteins CLASP1 and CLASP2 interact with actin filaments. *Cell Motil Cytoskeleton*. 64:519-530.

Valenzuela, D.M., T.N. Stitt, P.S. DiStefano, E. Rojas, K. Mattsson, D.L. Compton, L. Nunez, J.S. Park, J.L. Stark, D.R. Gies, S. Thomas, M.M. Le Beau, A.A. Fernald, N.G. Copeland, N.A. Jenkins, S.J. Burden, D.J. Glass, and G.D. Yancopoulos. 1995. Receptor tyrosine kinase specific for the skeletal muscle lineage: Expression in embryonic muscle, at the neuromuscular junction, and after injury. *Neuron*. 15:573-584.

Vallee, R.B., J.C. Williams, D. Varma, and L.E. Barnhart. 2004. Dynein: An ancient motor protein involved in multiple modes of transport. *J Neurobiol*. 58:189-200.

Verhey, K.J., and J.W. Hammond. 2009. Traffic control: regulation of kinesin motors. *Nature Rev. Mol. Cell Biol.* 10:765-777.

Verhey, K.J., N. Kaul, and V. Soppina. 2011. Kinesin assembly and movement in cells. *Annual review of biophysics*. 40:267-288.

Walker, R.A., E.T. O'Brien, N.K. Pryer, M.F. Soboeiro, W.A. Voter, H.P. Erickson, and E.D. Salmon. 1988. Dynamic instability of individual microtubules analyzed by video light microscopy: rate constants and transition frequencies. *The Journal of Cell Biology*. 107:1437-1448.

Wang, J., X.Q. Fu, W.L. Lei, T. Wang, A.L. Sheng, and Z.G. Luo. 2010. Nuclear factor kappaB controls acetylcholine receptor clustering at the neuromuscular junction. *The Journal of neuroscience : the official journal of the Society for Neuroscience*. 30:11104-11113.

Wang, J., Z. Jing, L. Zhang, G. Zhou, J. Braun, Y. Yao, and Z.Z. Wang. 2003. Regulation of acetylcholine receptor clustering by the tumor suppressor APC. *Nature neuroscience*. 6:1017-1018.

Wang, Q., B. Zhang, W.C. Xiong, and L. Mei. 2006. MuSK signaling at the neuromuscular junction. *Journal of molecular neuroscience : MN*. 30:223-226.

Watanabe, T., J. Noritake, and K. Kaibuchi. 2005. Regulation of microtubules in cell migration. *Trends Cell Biol*. 15:76-83.

Watanabe, T., J. Noritake, M. Kakeno, T. Matsui, T. Harada, S. Wang, N. Itoh, K. Sato, K. Matsuzawa, A. Iwamatsu, N. Galjart, and K. Kaibuchi. 2009. Phosphorylation of CLASP2 by GSK-3β regulates its interaction with IQGAP1, EB1 and microtubules. *Journal of Cell Science*. 122:2969-2979.

Watanabe, T., S. Wang, J. Noritake, K. Sato, M. Fukata, M. Takefuji, M. Nakagawa, N. Izumi, T. Akiyama, and K. Kaibuchi. 2004. Interaction with IQGAP1 links APC to Rac1, Cdc42, and actin filaments during cell polarization and migration. *Dev Cell*. 7:871-883.

Weatherbee, S.D., K.V. Anderson, and L.A. Niswander. 2006. LDL-receptor-related protein 4 is crucial for formation of the neuromuscular junction. *Development*. 133:4993-5000.

Webster, D.R., G.G. Gundersen, J.C. Bulinski, and G.G. Borisy. 1987. Differential turnover of tyrosinated and detyrosinated microtubules. *Proceedings of the National Academy of Sciences*. 84:9040-9044.

Weisenberg, R.C., G.G. Borisy, and E.W. Taylor. 1968. The colchicine-binding protein of mammalian brain and its relation to microtubules. *Biochemistry*. 7:4466-4479.

Welf, E.S., and J.M. Haugh. 2011. Signaling pathways that control cell migration: models and analysis. *Wiley interdisciplinary reviews. Systems biology and medicine*. 3:231-240.

Wen, Y., C.H. Eng, J. Schmoranzer, N. Cabrera-Poch, E.J.S. Morris, M. Chen, B.J. Wallar, A.S. Alberts, and G.G. Gundersen. 2004. EB1 and APC bind to mDia to stabilize microtubules downstream of Rho and promote cell migration. *Nature cell biology*. 6:820-830.

Weston, C., C. Gordon, G. Teressa, E. Hod, X.D. Ren, and J. Prives. 2003. Cooperative regulation by Rac and Rho of agrin-induced acetylcholine

receptor clustering in muscle cells. *The Journal of biological chemistry*. 278:6450-6455.

Weston, C., B. Yee, E. Hod, and J. Prives. 2000. Agrin-induced acetylcholine receptor clustering is mediated by the small guanosine triphosphatases Rac and Cdc42. *J Cell Biol*. 150:205-212.

Weston, C.A., G. Teressa, B.S. Weeks, and J. Prives. 2007. Agrin and laminin induce acetylcholine receptor clustering by convergent, Rho GTPase-dependent signaling pathways. *J Cell Sci*. 120:868-875.

Wilson, M.H., and E.L.F. Holzbaur. 2012. Opposing microtubule motors drive robust nuclear dynamics in developing muscle cells. *Journal of Cell Science*. 125:4158-4169.

Wittmann, T., and C.M. Waterman-Storer. 2005. Spatial regulation of CLASP affinity for microtubules by Rac1 and GSK3β in migrating epithelial cells. *The Journal of Cell Biology*. 169:929-939.

Witzemann, V. 2006. Development of the neuromuscular junction. *Cell and Tissue Research*. 326:263-271.

Witzemann, V., H. Schwarz, M. Koenen, C. Berberich, A. Villarroel, A. Wernig, H.R. Brenner, and B. Sakmann. 1996. Acetylcholine receptor ε-subunit deletion causes muscle weakness and atrophy in juvenile and adult mice. *Proceedings of the National Academy of Sciences*. 93:13286-13291.

Woodgett, J.R. 1990. Molecular cloning and expression of glycogen synthase kinase-3/factor A. *EMBO J*. 9:2431-2438.

Wu, H., Y. Lu, A. Barik, A. Joseph, M.M. Taketo, W.C. Xiong, and L. Mei. 2012. beta-Catenin gain of function in muscles impairs neuromuscular junction formation. *Development*. 139:2392-2404.

Wu, H., W.C. Xiong, and L. Mei. 2010. To build a synapse: signaling pathways in neuromuscular junction assembly. *Development*. 137:1017-1033.

Wu, X., A. Kodama, and E. Fuchs. 2008. ACF7 Regulates Cytoskeletal-Focal Adhesion Dynamics and Migration and Has ATPase Activity. *Cell*. 135:137-148.

Wu, X., Q.-T. Shen, D.S. Oristian, C.P. Lu, Q. Zheng, H.-W. Wang, and E. Fuchs. 2011. Skin Stem Cells Orchestrate Directional Migration by Regulating Microtubule-ACF7 Connections through GSK3[beta]. *Cell*. 144:341-352.

Yoshimura, T., Y. Kawano, N. Arimura, S. Kawabata, A. Kikuchi, and K. Kaibuchi. 2005. GSK-3beta regulates phosphorylation of CRMP-2 and neuronal polarity. *Cell*. 120:137-149.

Yuan, B., R. Latek, M. Hossbach, T. Tuschl, and F. Lewitter. 2004. siRNA Selection Server: an automated siRNA oligonucleotide prediction server. *Nucleic acids research*. 32:W130-134.

Yucel, G., and A.E. Oro. 2011. Cell Migration: GSK3β Steers the Cytoskeleton's Tip. *Cell*. 144:319-321.

Yumoto, N., N. Kim, and S.J. Burden. 2012. Lrp4 is a retrograde signal for presynaptic differentiation at neuromuscular synapses. *Nature*. 489:438-442.

Zaal, K.J., E. Reid, K. Mousavi, T. Zhang, A. Mehta, E. Bugnard, V. Sartorelli, and E. Ralston. 2011. Who needs microtubules? Myogenic reorganization of

MTOC, Golgi complex and ER exit sites persists despite lack of normal microtubule tracks. *PLoS One*. 6:e29057.

Zaoui, K., K. Benseddik, P. Daou, D. Salaün, and A. Badache. 2010. ErbB2 receptor controls microtubule capture by recruiting ACF7 to the plasma membrane of migrating cells. *Proceedings of the National Academy of Sciences*. 107:18517-18522.

Zhang, B., C. Liang, R. Bates, Y. Yin, W.C. Xiong, and L. Mei. 2012. Wnt proteins regulate acetylcholine receptor clustering in muscle cells. *Mol Brain*. 5:1756-6606.

Zhang, B., S. Luo, Q. Wang, T. Suzuki, W.C. Xiong, and L. Mei. 2008. LRP4 Serves as a Coreceptor of Agrin. *Neuron*. 60:285-297.

Zhang, X., R. Xu, B. Zhu, X. Yang, X. Ding, S. Duan, T. Xu, Y. Zhuang, and M. Han. 2007. Syne-1 and Syne-2 play crucial roles in myonuclear anchorage and motor neuron innervation. *Development*. 134:901-908.

Zong, Y., B. Zhang, S. Gu, K. Lee, J. Zhou, G. Yao, D. Figueiredo, K. Perry, L. Mei, and R. Jin. 2012. Structural basis of agrin-LRP4-MuSK signaling. *Genes Dev*. 26:247-258.

Zumbrunn, J., K. Kinoshita, A.A. Hyman, and I.S. Nathke. 2001a. Binding of the adenomatous polyposis coli protein to microtubules increases microtubule stability and is regulated by GSK3 beta phosphorylation. *Current biology : CB*. 11:44-49.

Zumbrunn, J., K. Kinoshita, A.A. Hyman, and I.S. Näthke. 2001b. Binding of the adenomatous polyposis coli protein to microtubules increases microtubule stability and is regulated by GSK3[beta] phosphorylation. *Current Biology*. 11:44-49.

Zumbrunn, J., K. Kinoshita, A.A. Hyman, and I.S. Näthke. 2001c. Binding of the adenomatous polyposis coli protein to microtubules increases microtubule stability and is regulated by GSK3β phosphorylation. *Current Biology*. 11:44-49.

VI. List of Abbreviations

+TIP	Plus end tracking protein
ACh	Acetylcholine
AChR	Acetylcholine receptor
ACF7 / MACF1	Actin cross-linking factor-7 / MT actin cross-linking factor 1
ADP	Adenosine-diphosphate
APC	Adenomatous polyposis coli protein
ATP	Adenosine-triphosphate
c.a.	constitutively active
CAP-Gly	Cytoskeleton-associated protein Gly-rich domains
CBE	Chicken brain extract
Cdc42	Cell division cycle 42
CLASP	Cytoplasmic linker protein associated protein
CLIP-170	Cytoplasmic linker protein of 170 kD
DAPI	4',6'-Diamidin-2'-phenylindol- dihydrochlorid
d.n.	dominant negative
D-MEM	Dulbecco's Modified Eagle Medium
E. coli	Escherichia coli
EB	End binding protein
EDTA	Ethylendiamin-tetraacetate
EGTA	Ethylenglykol-bis(aminoethylether)-N,N'-tetraacetate
GAP	GTPase-activating proteins
GDP	Guanine-diphosphate
GEF	Guanine Nucleotide Exchange Factors
GF	Growth Factor
GFP	Green Fluorescent Protein
GSK3β	Glycogen Synthase Kinase 3b
GTP	Guanine-triphosphate
HEPES	2-(4-(2-Hydroxyethyl)- 1-piperazinyl)-ethansulfonic acid
IQGAP1	IQ motif containing GTPase Activating Protein 1
LPA	Lysophosphatidic Acid
MACF	Microtubule Actin Cross-linking Factor
MAP	Microtubule-associated protein
MBD	Microtubule-binding domain
MgCl2	Magnesium chloride
MT	Microtubule
MTOC	Microtubule Organizing Center
NMJ	Neuromuscular Junction
o/n	overnight
PI3K	Phosphatidylinositol-3-Kinase
PBS	Phosphate-buffered Saline
PFA	Paraformaldehyde
PTM	Post-translational modification
PIPES	Piperazin-N,N'-bis(2-ethansulfonsäure)
RT	Room temperature

SDS	Sodium dodecyl Sulfate
shRNA	Short hairpin RNA
siRNA	Small interfering RNA
TEMED	N,N,N',N'-Tetramethylethylenediamine

VII. Curriculum Vitae

Personal Details

Name	Sladeček
Surname	Stefan
Nationality	Austrian
Date & place of birth	May 9, 1978 in Vienna, Austria
Marital status	unmarried

Education

2007 - 2012	PhD Student in Biochemistry at the Univ. of Basel, CH
2001 - 2007	Study of Molecular Biology at the Univ. of Vienna, AT (Graduation with first class honors in January 2007)
2004/09 - 2005/02	Studies at the Charles Univ., Prague, CZ (ERASMUS – Scholar)
1997 - 2000	Pre-degree in Human Biology & Psychology, Univ. of Vienna, AT
1988 - 1996	Amerling-Gymnasium, Vienna, AT

Civil Service

1999/10 - 2000/09	Ambulance Man at the Austrian Red Cross